# BEHIND THE IRON CURTAIN: DEXRAS1 MEDIATES GLUTAMATE-NMDA INDUCED NEURONAL IRON UPTAKE

by

Jaime H. Cheah

A dissertation submitted to Johns Hopkins University in conformity with the requirements of the degree of the Doctor of Philosophy

Baltimore, Maryland

March, 2006

# ABSTRACT

Iron is an enigmatic molecule – a divalent metal absolutely required for life, but toxic in excess. Because of this dual nature, iron trafficking within the cell is tightly regulated, with little free iron available in the cytosol. Iron entry into the cell is mediated through two distinct pathways, both of which utilize the Divalent Metal Transporter (DMT1), a twelve-transmembrane protein which is the only known iron importer in the cell. Dexras1 is a small G-protein regulated by glucocorticoids and neuronal nitric oxide synthase (nNOS). Using yeast-two-hybrid analysis, we have discovered that Dexras1 interacts with DMT1 via an adaptor protein, the Peripheral Benzodiazepine Receptor Associated Protein (PAP7). We have identified a novel signaling cascade in neurons whereby stimulation of glutamate-NMDA receptors activates nNOS, leading to *S*-nitrosylation of Dexras1, which by its interaction with PAP7 and DMT1, physiologically induces iron uptake. We have also investigated whether misregulation of this pathway participates in NMDA-mediated neuronal excitoxicity.

**Thesis Advisor: Dr. Solomon H. Snyder**

**Thesis Reader: Dr. Michael Caterina**

# ACKNOWLEDGEMENTS

First and foremost, I would like to express my deepest gratitude to my thesis advisor, Dr. Solomon H. Snyder. He taught me to work with confidence in myself and has always maintained faith in me. He is a wonderful mentor, a great advisor and has contributed greatly not only in my development as a scientist, but also as a person.

I would also like to thank the members of my thesis committee, Drs. Peter Devreotes, Michael Caterina and Jay Baraban for their support and enthusiasm in my research, for insightful discussions and for always steering me in the right direction.

I could not have done this work without the help of Dr. Sangwon Kim whose knowledge of iron metabolism got me started and whose wisdom saw me through my thesis research. I also want to thank my terrific undergrads- Stanley Patterson, Kate Clancy and Andrea Brem - all of whom have been a joy to teach and have contributed greatly to my work.

I am grateful to the members of the Snyder lab for providing me with such a wonderful work environment. I am especially thankful to Dr. Darren Boehning, Byoung-Il Bae, Adam Resnick, Alex Huang, Makoto Hara and our research associates, Lynda Hester, Adele Snowman and Roxanne Barrow for their helpful discussions and for being there through the ups and downs of a graduate career.

I thank my parents, Sin Hock Cheah and Yoke Ngoh Lim, my brother, Isaac, my in-laws, Reinard and Hilda Kohls, my best friend, Lisa Persaud and all my other friends for their unfailing love and support. Finally, I am eternally grateful to my fiancé, Darcy Kohls, who has stood by me through nine years together. After seven years of graduate school, four years apart, all the late night phone calls and flights from Boston to Baltimore, he has helped me find my way to the light at the end of the tunnel. This chapter of our journey together now ends and a new one begins.

# TABLE OF CONTENTS

# List of Figures

# CHAPTER 1:

# Introduction

## PART 1: IRON

### ***Part 1.1: Iron Absorption***

Iron is the most abundant metal in the body and is an essential cofactor for cytochromes, oxygen binding molecules, such as heme, and many other enzymes, including those involved in DNA and neurotransmitter synthesis (reviewed in [(Andrews, 1999; Donovan and Andrews, 2004; Hentze et al., 2004)]). As iron has a dual nature – necessary for life, but toxic in excess- it is tightly regulated within the cell and also in its uptake into the cell. Iron absorption is the sole mechanism by which iron stores in the body are regulated, as there is no known physiological mechanism for iron excretion (McCance and Widdowson, 1938).

Iron is taken up from the diet in two forms: inorganic non-heme iron or heme. 1-3 grams of iron is stored in the adult body, balanced between dietary uptake and loss (Muir and Hopfer, 1985). Non-heme iron is absorbed in the duodenum and upper jejunum (Donovan and Andrews, 2004), which is regulated by the levels of iron stores. At low levels, absorption is increased, while at high levels,

absorption is decreased. The physical state of iron itself influences its absorption: at pH 7, ferrous ($Fe^{2+}$) is converted into the insoluble ferric ($Fe^{3+}$) state. Gastric acid lowers pH, thus enhancing solubility and uptake of $Fe^{2+}$ by intestinal mucosal cells. Other factors which enhance absorption are ascorbate and citrate (Conrad and Umbreit, 1993), while phytates, tannins and antacids inhibit absorption and other divalent metals, such as lead, cobalt, manganese and zinc are competitors for absorption.

Iron passes from the gut lumen through the apical and basolateral membrane of the enterocytes to reach the plasma membrane (Figure 1) (reviewed in [(Andrews, 1999; Hentze et al., 2004). Low pH dissolves ingested iron and facilitates the enzymatic reduction of ferric iron to ferrous iron at the apical surface via a brush border ferrireductase, Dcytb (Riedel et al., 1995). $Fe^{2+}$ is transported across the apical membrane into the enterocyte via the Divalent Metal Transporter (DMT-1, discussed later) (Cellier et al., 1995; Fleming et al., 1997) in a proton-coupled process. Once inside the enterocyte, the iron has two fates: it can either be stored in ferritin if body iron stores are high, or it can be transported across the basolateral membrane to reach the plasma (Andrews, 1999). Iron efflux requires two proteins: the transporter itself called Ireg1, also known

as Metal Transporter 1 (MTP1) or Ferroportin (Abboud and Haile, 2000; Andrews, 1999; Donovan et al., 2000; McKie et al., 2000), and a multicopper ferroxidase called hephaestin (Andrews, 1999; Vulpe et al., 1999). $Fe^{2+}$ is converted to $Fe^{3+}$ by hephaestin, which is then immediately bound to transferrin (Tf). The mechanism of iron loading onto Tf is unknown, though it may involve a copper oxidase known as ceruloplasmin (Harris et al., 1999). Two molecules of $Fe^{3+}$ can bind to Tf, which renders the iron insoluble under physiological conditions, preventing iron-mediated free radical toxicity and facilitating transport into cells. Most cells in the body are believed to acquire iron from plasma Tf via transferrin receptors (TfR) and receptor-mediated endocytosis (discussed later) (Klausner et al., 1983). 80% of iron bound to circulating Tf is delivered to the bone marrow and incorporated into newly formed erythrocytes (Finch et al., 1982; JANDL and KATZ, 1963).

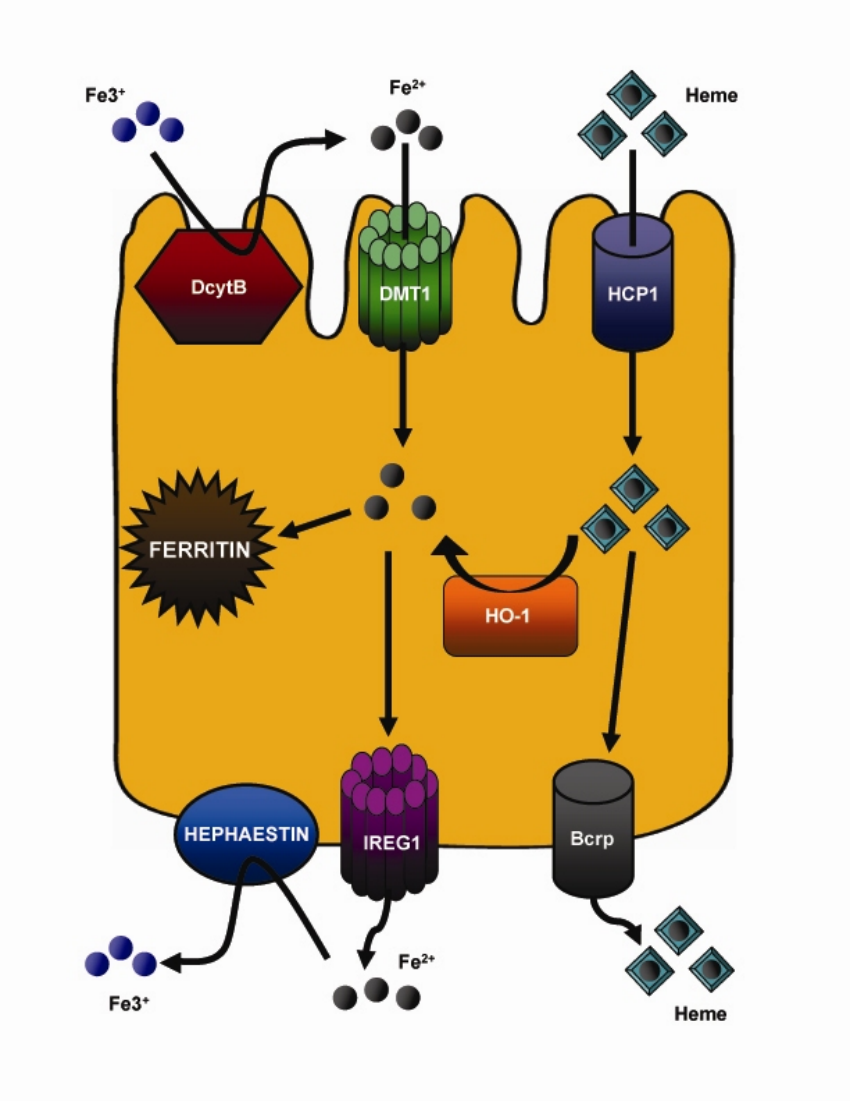


**Figure 1:** Schematic Illustration of Iron Absorption

Iron can be absorbed from the diet into the gut in two different forms: either as ferric iron ($Fe^{3+}$) or as heme. At low pH in the gut, most of the free iron is converted to the ferrous ($Fe^{2+}$) form, with some help from the ferrireductase, DcytB. The $Fe^{2+}$ is transported across the apical membrane of the enterocyte via DMT1, where it can either be stored in ferritin or be transported across the basolateral membrane to reach the plasma. Iron efflux is mediated by Ireg1, an iron transporter, and hephaestin, a multicopper ferroxidase that converts $Fe^{2+}$ back to $Fe^{3+}$, where it is bound by Tf.
Heme is transported across the apical membrane by the recently identified heme transporter, HCP1. Within the cell, iron can be freed from the protoporphyrin ring by HO1 and join the inorganic iron pool, or the heme can transit through the cell intact and be exported by the heme transporter Bcrp.

Several factors can regulate iron absorption (reviewed in [(Andrews, 1999; Donovan and Andrews, 2004)]):

1) MUCOSAL BLOCK or DIETARY REGULATOR – Iron absorption is affected by recent dietary iron uptake. In the event of a large recent iron uptake, the enterocyte is rendered refractory to absorption for several days.
2) STORES REGULATOR – Iron absorption is affected by levels of total body iron, which is sensed by iron saturation in circulating Tf. This iron sufficiency information modulates the expression of hepcidin, a 20-25 amino acid peptide produced in and secreted by the liver, which acts as a negative regulator of iron absorption (Nicolas et al., 2002; Weinstein et al., 2002). Hepcidin levels increase in the presence of iron overload, and decreases during iron deficiency. This regulation potentially acts at the level of the duodenal crypt cells (pre-mature enterocytes) and may involve the alteration of levels of DMT1 at the apical membrane.
3) ERYTHROPOIETIC REGULATOR – Iron absorption responds to the demands of erythropoiesis, independent of total body iron levels. When erythroid cells require

iron, hepcidin expression levels decrease and lead to increase in iron absorption. The erythropoietic regulator has a greater capacity for influencing iron absorption than does the stores regulator.

4) ACUTE HYPOXIA – Iron absorption is stimulated through some unknown mechanism.

Iron can also be absorbed as heme, which can also enter the enterocyte via a recently identified heme transporter called Heme Carrier Protein 1 (HCP1) (Shayeghi et al., 2005), which localizes to the apical membrane of duodenal enterocytes. Dietary heme attaches to the brush border and is transported into the cells intact. Within the cell, iron can be freed from the protoporphyrin ring, likely by heme oxygenase 1 (Raffin et al., 1974), an enzyme that breaks down heme to liberate iron. This iron can then presumable join the inorganic iron pool which can then enter the serum via Ireg1, though some heme transits through the enterocyte intact and can be exported by two heme exporters, Bcrp or FLVCR (Krishnamurthy et al., 2004; Quigley et al., 2004).

Table 1 shows the distribution and usage of iron. It is important to note that only 1-3 mg of iron enters the body each day, however, the requirement by various organelles, such as red blood cells, is much higher. To

achieve these high levels, iron is supplied via recycling of senescent red cells and catabolism of hemoglobin by macrophages. The liver is a primary depot for iron storage as hepatocytes can do iron uptake, storage and export, and although the major players have not been identified, it is believed that ceruloplasmin may play a role in iron export through some unknown mechanism (Andrews, 1999; Donovan and Andrews, 2004; Hentze et al., 2004).

| **DISTRIBUTION OF IRON** | |
|---|---|
| Dietary Iron Uptake | 1-2 mg/day |
| Plasma Transferrin | 3 mg |
| Utilization: | |
| Myoglobin (muscle) | 300 mg |
| Bone Marrow | 300 mg |
| Erythrocytes (hemoglobin) | 1800 mg |
| Storage: | |
| Reticuloendothelial macrophages | 600 mg |
| Liver Parenchyma | 1000 mg |
| Iron Loss | 1-2 mg/day |

**Table 1:** Distribution of iron in the body (adapted from (Andrews, 1999))

*Part 1.2: Iron Trafficking in the Cell*

Iron is taken up into the cell via two methods: the classical Tf-mediated iron uptake pathway and the Non-Transferrin Bound Iron (NTBI) uptake. Iron required for physiological processes is taken up through Tf-mediated iron uptake (Figure 2) (Iacopetta and Morgan, 1983; Karin and Mintz, 1981; Klausner et al., 1983). Tf binds to two molecules of $Fe^{3+}$ released from the enterocyte. The Fe-Tf then binds to the TfR and, via receptor mediated endocytosis, leads to internalization of TfR and DMT1 within an endocytic vesicle containing holo-Tf. Acidification of the endosome to pH 5.5 – 6.0 via an ATP-dependent proton pump leading Tf to release iron and bind tighter to TfR (Dautry-Varsat et al., 1983; Paterson et al., 1984; Van et al., 1982; Yamashiro et al., 1984). Iron then exits the endosome via DMT1 and enters the intracellular labile iron pool, which is then delivered to the mitochondria for heme biosythesis and formation of iron-sulfur clusters or to ferritin for storage. The iron is so tightly regulated in the cell by binding to protein that the labile iron pool cannot be measured. The intact apoTf-TfR complex recycles to the cell surface, where the neutral pH promotes the detachment of Tf from TfR and back into circulation (Donovan and Andrews, 2004).

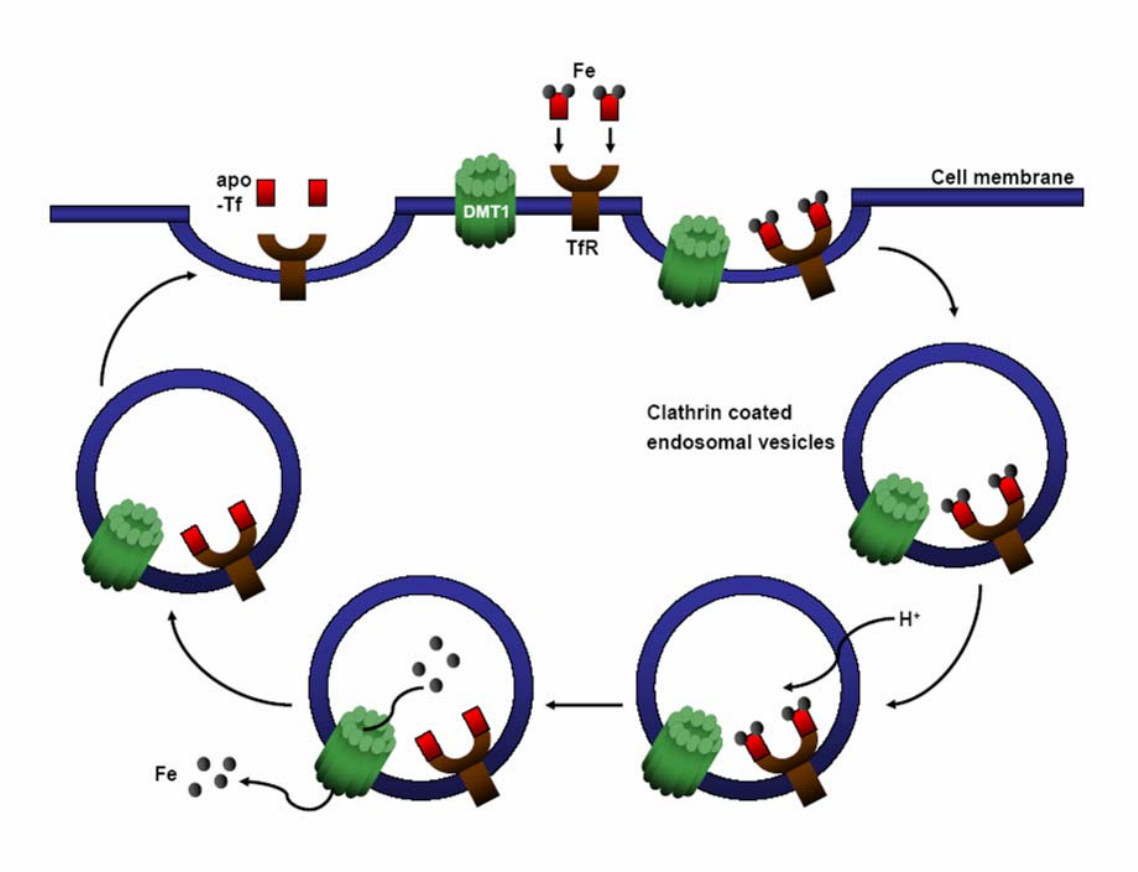


**Figure 2:** The Transferrin Cycle

Iron required for physiological processes is taken up through the transferrin (Tf) cycle. Tf binds to two molecules of $Fe^{3+}$ released from the enterocyte, which then binds to the Tf receptor (TfR) and, via receptor mediated endocytosis, leads to the internalization of TfR and DMT1 within an endosome. Acidification of the endosome to pH 5.5 allows Tf to release the iron, which then exits the endosome via DMT1 into the labile iron pool. The intact Tf-TfR complex then recycles to the cell surface, where the neutral pH promotes the detachment of Tf from TfR and back into circulation.

For NTBI uptake, DMT1 in the plasma membrane directly mediates iron transport, though this iron is not used for physiological purposes(Fleming et al., 1997; Gunshin et al., 1997). It's been postulated that this iron may act in a pathophysiological manner. NTBI uptake can occur when iron overload produces fully saturated Tf. This NTB iron circulating is in a chelatable, low molecular weight form and is weakly associated with albumin, citrate, amino acids and sugars (Farcich and Morgan, 1992; Fleming et al., 1997; Garrick et al., 1999; Richardson and Ponka, 1997). Non-hematopoietic tissues, such as the liver, endocrine organs, kidneys and heart, can preferentially take up this iron. In the brain, the free iron levels exceed that of Tf, so NTBI uptake is also used (Moos and Morgan, 1998; Rouault, 2001).

***Transferrin***

Plasma Tf is a 80 kDa glycoprotein synthesized in and secreted by the liver. It contains N-terminal and C-terminal iron binding domains (reviewed in [(Huebers et al., 1984)]). These domains are globular structures of 330 amino acids divided into subunits with iron binding and anion binding sites in the intersubdomain cleft. This cleft opens with release of iron and closes with binding (reviewed in [(Baker and Lindley, 1992)]). Tf has six

coordination sites for binding to iron, with a Kd of $10^{-22}$ M, and only in the presence of an anion, predominantly carbonate. The anion serves as a bridge between metal and protein, excluding water from two coordination sites (Aisen and Listowsky, 1980; Shongwe et al., 1992). The remaining four coordination sites on Tf consist of a histidine nitrogen, an aspartate carboxyl oxygen and two tyrosine phenolate oxygen (Anderson et al., 1989; Bailey et al., 1988). Anion binding must take place before iron binding; iron release from Tf involves protonation of the carbonate, during the acidification of the endosome, thus loosening the metal-protein bond. Each molecule of Tf can bind to two molecules of diferric iron. The average Tf molecule has a half-life of eight days and may be used up to 100 times for iron delivery (Harford et al., 1994). Tf is not universally required for efficient iron transport, but it is the major physiological source for iron in the body.

***Transferrin Receptor***

The TfR is a single transmembrane, disulfide-linked homodimer of two glycoproteins of 760 amino acids each (Cheng et al., 2004b). Each monomer has four glycosylation sites, three are N-linked while one is O-linked, leading to a 90 kDa protein (Hayes et al., 1992). Mutations that

abolish N-linked glycosylation lead to the receptor having decreased Tf-binding and surface expression (Williams and Enns, 1991; Williams and Enns, 1993). The transmembrane domain resides between amino acids 62-89 and functions as an internal signal peptide (Zerial et al., 1986). TfR has the ability to bind to both monoferric (Kd = $10^{-6}$/mole) and diferric (Kd = $10^{-7}$ – $10^{-9}$M) iron (Sawyer and Krantz, 1986; Stein and Sussman, 1986); as the concentration of circulating Tf is 25μM, the TfRs are normally fully saturated. Binding of Tf to Tfr is mediated by its C-terminus (Zak et al., 1994); once bound, the Tf-TfR complex is rapidly internalized into clathrin-coated pits to form endocytic vesicles. This process requires the 61 amino acid intracellular tail of TfR (Girones et al., 1991; McGraw and Maxfield, 1990; Rothenberger et al., 1987), specifically the conserved Tyr-Thr-Arf-Phe (YTRF) sequence which functions as a signal for endocytic internalization (Collawn et al., 1993).

The expression level of TfR is regulated by the intracellular levels of iron. At low iron levels, the expression is increased to bring more iron into the cell, while conversely, at high iron levels, the expression level of TfR is decreased. This regulation is mediated by Iron Regulatory Proteins (IRPs) binding to Iron Response

Elements (IREs) on the mRNA of TfR (details discussed below) (reviewed in [(Hentze et al., 2004)]).

***Ferritin***

Ferritin is the cellular iron storage protein (Torti and Torti, 2002). A complex 24 subunit heteropolymer made up of heavy (H) and L (light) chains. The H-chains are 21 kDa while the L-chains are 19.7 kDa. These form a sphere with a hollow interior that is capable of binding up to 4500 atoms of crystalline iron (Harrison, 1977; Theil, 1987) in a soluble, non-toxic but bioavailable form, such as ferrihydrite. The H-chain has ferroxidase activity, able to convert $Fe^{2+}$ to $Fe^{3+}$, promoting incorporation into ferritin (Lawson et al., 1991; Levi et al., 1988). The L-chain is associated with nucleation of the mineral core within the protein shell. Different combinations of each of the subunits lead to different isoforms of ferritin, which show tissue specific variation (Drysdale, 1988). Ferritins that are heavy in L-chains correlate to increased iron storage while ferritins that are predominantly H-chains correlate with increased iron utilization and response to stress (Drysdale, 1988; Theil, 1987). The H:L ratio increases with activation of heme synthesis or cellular proliferation (McClarty et al., 1990; Pattanapanyasat et

al., 1987). Over time, ferritin molecules aggregate to form clusters with are engulfed by lysosomes and degraded (Bridges, 1987), resulting in an end product known as hemosiderin. In the case of iron overload, there is an increase in hemosiderin that can be visualized by Prussian blue staining.

The expression level of ferritin is regulated in a pattern opposite that of TfR. At low iron levels, the expression is decreased so that storage is minimized and more iron can be brought into the cell, while at high iron levels, the expression level is increased. The expression is regulated by the same IRP/IRE system as that which regulates TfR (reviewed in [(Hentze et al., 2004)]).

***Divalent Metal Transporter (DMT1)***

DMT1 is a ubiquitously expressed twelve trans-membrane channel localized to the plasma membrane and is the only known mammalian iron importer in the cell. Originally identified as Natural Resistance Associated Macrophage Protein-2 (NRAMP2) and Divalent Cation Transporter (DCT1) (Cellier et al., 1995; Fleming et al., 1997; Gunshin et al., 1997), it channels iron preferentially in the ferrous form, but can also channel cobalt, manganese, copper, cadmium, lead and zinc, but not calcium or magnesium. There

are two different splice forms of DMT1, encoding different C-termini and different 3’ untranslated regions (UTRs). In one form, the 3’UTR can contain an IRE, though whether DMT1 expression is regulated by IRPs is still unknown (Gunshin et al., 2001; Hubert and Hentze, 2002). Different DMT1 isoforms are present in different tissues: the +IRE form is found in enterocytes, while in the brain, the –IRE form is dominant.

DMT1 is known to transport iron across the apical membrane of the enterocyte and also to transport iron out of the endosome after Tf-TfR mediated iron uptake. The function of DMT1 is pH dependent, working optimally at low pH and has been reported to co-transport protons. Rodents that have a naturally occurring mutation in DMT1, known as microcytic anemia (*mk*) mice or Belgrade (*b*) rats, where glycine 185 is mutated to arginine (G185R) have defects in iron import and are anemic (Fleming et al., 1997; Fleming et al., 1998). In this case, DMT1 can no longer channel iron, but instead, channels calcium through the pore (Xu et al., 2004).

***IRPs/IREs***

IRPs and IREs are involved in the post-transcriptional control of the expression of many molecules involved in

iron homeostasis: TfR, ferritin, DMT1, Ireg1, etc. (reviewed in [(Eisenstein, 2000)]) and act as the sensor for the intracellar levels of iron. IREs are short untranslated 30 nucleotide sequences that form stable stem loop structures which are docking sites for IRPs (Andrews, 2000). There are two IRPs: IRP1 and IRP2, which are cytoplasmic proteins that bind to IREs in 5’ or 3’UTRs of mRNAs (Hentze and Kuhn, 1996). IRP1 is functions normally as an aconitase, however, in the presence of low iron levels, it switches and binds to IREs in TfR and ferritin mRNAs. This switch in activity is dictated by the iron-sulfur clusters within IRP1, which is how it senses iron levels. At normal iron levels, the iron-sulfur clusters are intact and IRP1 acts as an aconitase. At low levels, the iron-sulfur clusters can no longer form, and IRP1 binds to IREs. IRP1 is modulated by nitric oxide, as well as oxygen – during hypoxia, IRP1 binding to IREs is decreased (Haile et al., 1992; Kaptain et al., 1991).

IRP2’s regulation is different from that of IRP1. IRP2 binds to IREs in low iron conditions and is degraded at high iron concentrations. This is dependent on a cysteine-rich 73 amino acid sequence that is unique to IRP2, which leads to an iron dependent oxidation event. Under high iron conditions, this oxidized form is a target for

ubiquitination and proteosomal degradation (Kang et al., 2003; Yamanaka et al., 2003). In the brain, there is more IRP2 than IRP1, which is reversed in the heart and liver, and IRP2 knockout mice have iron overload in the central nervous system (CNS) and neurodegenerative disease (LaVaute et al., 2001; Rouault, 2001).

In the case of TfR, IRP1 binds to multiple IREs at the 3'UTR, thus stabilizing the message and allowing translation of TfR to bring more iron into the cell (Hentze and Kuhn, 1996). In the case of ferritin, IRP1 binds to the 5'UTR and blocks translation, thus decreasing the levels of the storage protein (Gray and Hentze, 1994).For DMT1, the IRPs bind to the 3' IRE while for Ireg1, the IRPs bind to the 5' IRE, but it is unknown if this really contributes to their regulation (Gunshin et al., 2001).

***Other proteins involved in iron homeostasis***

Table 2 shows a brief overview of other proteins involved in iron homeostasis. All of these proteins work together to tightly regulate the entry of iron into cell, starting with dietary iron entry in the gut to iron uptake in individual cells. Mutations in many of these proteins leads to either iron overload or iron deficiency.

| PROTEIN | Function | Disease | Iron Status |
|---|---|---|---|
| Transferrin | Ferric iron transporter in plasma | Hypotransferrinemia | Severe hypochromic, microcytic anemia but massive iron loading |
| TfR | Membrane Receptor for Tf | | |
| HFE | unknown function, but binds to TfR in enterocytes | Hereditary Hemochromatosis | Iron overload |
| Ferritin | Iron Storage in the Cell | Neuroferritinopathy | Iron overload |
| IRP1 | Iron sensor, binds to IREs | | |
| IRP2 | Iron sensor, binds to IREs | IRP2 -/- mice | Iron overload in CNS and neurodegeneration |
| DMT1 | Iron transporter in enterocytes and endosomes | mk mice Belgrade rat | Iron deficiency |
| Dcytb | Cytochrome b-like ferric reductase at apical membrane | | |
| Ireg1 | Iron export from the enterocyte | | |
| Ceruloplasmin | Copper ferroxidase | Aceruloplasnemia | Iron overload in the brain but decrease in serum iron |
| Hephaestin | Copper ferroxidase at basal membrane | | |
| Frataxin | Regulation of iron export from the mitochondria | Friedrich's ataxia | Iron overload |
| Huntingtin | Trafficking of TfR | Huntington's Disease | Iron overload |
| Heme Oxygenase 1 | Breakdown of heme to release iron | | |
| Pantothenate Kinase 2 | Regulation of co-enzyme A and turnover of cysteine | Halloverden-Spatz | Iron overload |

**Table 2:** A brief overview of proteins involved in iron homeostasis, and where known, diseases associated with mutations in the gene and the iron disposition in the cell/body.

*Part 1.3: Iron homeostasis in the brain*

Iron homeostasis in the brain is similar to that of the rest of the body in that all of the major proteins associated with regulating iron in the systemic circulation are also expressed in the central nervous system (CNS). However, iron acquisition by the CNS is problematic as the CNS is functionally separate from the systemic circulation by the blood-brain barrier and the blood-cerebrospinal barrier, and thus, cannot acquire iron from circulating serum Tf (reviewed in [(Rouault, 2001)]). Nutrients must be taken up by the barrier cells and specifically exported into the distal compartment. Little is known about the mechanism of iron release into the brain or the regulation of transport mechanisms. It is postulated that cells in the brain must send a signal that iron is required to the endothelial cells lining the blood vessels in the brain and that these cells release iron into the brain extracellular fluid (Burdo and Connor, 2003).

Iron is abundant in the brain and has distinct regional and cellular pattern of distribution, highest in the basal ganglia at a concentration equivalent to that of the liver (Thomas and Jankovic, 2004). Within the basal ganglia, iron is highest in the globus pallidus, followed

by the zona reticulata of the substantia nigra, the red nucleus and the putamen (Sorond and Ratan, 2000). Iron is predominantly stored in the oligodendrocytes, cells that produce and maintain myelin (Sorond and Ratan, 2000). They regulate iron availability to neurons and are found associated with blood vessels where they monitor transport of iron across the BBB. The oligodendrocytes are also a source for brain Tf, as is the choroid plexus and epithelial cells, but the amount of Tf made is about 100-fold lower than that of serum Tf (Burdo and Connor, 2003; Sorond and Ratan, 2000). In fact, unlike the systemic circulation, iron is often found to be as much as a molar excess relative to that of Tf iron binding capacity and thus, brain Tf is often saturated. Under normal conditions, there may be significant NTBI uptake into cells. This NTB iron may be associated with low molecular weight molecules, such as citrate and ascorbate, which aid in its transport around the brain (Burdo and Connor, 2003; Rouault, 2001).

Similar to systemic iron homeostasis, the following proteins are involved, with some proteins being found specifically in the brain (reviewed in [(Thomas and Jankovic, 2004)]):

1) UPTAKE - Tf/TfR, melanotransferrin, lactotransferrin, DMT1, MTP1/Ireg1 and Stimulator of Iron Transport (SFT)
2) STORAGE – Ferritin, neuromelanin
3) RELEASE – Ceruloplasmin/ferroxidase, HO1
4) METABOLISM – HO1, Tf, ferroreductase
5) POST-TRANSCRIPTIONAL CONTROL: IRP1, IRP2, IREs, DMT1, changes in redox state of the cell

*Part 1.4: Iron and Neurodegeneration*

Most of the studies of iron in the brain have centered around its pathophysiological properties and participation in various neurodegenerative diseases (reviewed in [(Ponka, 2004; Rouault, 2001; Shoham and Youdim, 2000; Zecca et al., 2004)]). Iron accumulates normally as a result of ageing, however, when iron is present in excess, it has the ability to produce reactive oxygen species, such as hydroxyl radicals, via Fenton Chemistry, which can augment neuronal injury (Gutteridge et al., 1981). These hydroxyl radicals are highly reactive and can attack proteins, lipids and DNA, forming cross-links and inhibiting function (Bacon and Britton, 1990).

**Fenton Reaction:** $Fe^{2+} + H_2O_2 \rightarrow OH\bullet + OH^- + Fe^{3+}$

There are two classes of iron related neurodegenerative disorders: 1) those that result from defects in iron metabolism and/or homeostasis and present with neurological defects, such as aceruloplasminemia and Friedrich's ataxia and 2) those neurological diseases that present with iron accumulation in specific brain regions, such as Huntington's disease and Alzheimer's disease. For example, in Parkinson's disease, there is an increased iron content in neuromelanin-containing cells, particularly in the substantia nigra (Zecca et al., 2004). In both cases, this involves protein modification, misfolding and aggregation, and formation of intracellular inclusion bodies, all of which are hallmarks of many neurodegenerative diseases. In the second class of neurodegenerative diseases, it is unknown whether the iron accumulation seen is just a by-product of degenerating neurons or whether the high iron concentration contributes to the pathology of the disease.

## PART 2: DEXRAS1 AND RHES

### *Part 2.1: Dexras1*

Dexras1 is a small G-protein belonging to a subfamily of Ras proteins. It was originally revealed by differential display as an upregulated mRNA after treatment with dexamethasone, a synthetic glucocorticoid (Kemppainen and Behrend, 1998). Dexras1's mRNA was shown to be upregulated in as little as 30 minutes, peaking at 2 hours. Northern blotting results have shown that Dexras1 is enriched in the brain, but is also localized to the heart, liver and kidneys. The cDNA encoding the protein was found to be about 900 bases or about 30 kDa. While Dexras1 contains all of the conserved G-protein regions, such as the P-loop at the N-terminus, which binds to GDP/GTP, the magnesium binding loop and a C-terminal CAAX box, a prenylation site, it differs from the typical small GTPases as it has an extended C-terminal tail of about 7 kDa (Kemppainen and Behrend, 1998). Like all G-proteins, Dexras1 is inactive when bound to GDP. Upon binding to GTP, it undergoes a confirmational switch, at which point it can bind to downstream effector molecules. The functions for Dexras1 have been fairly diverse; so far it has been found

to inhibit cyclic AMP-dependent ACTH secretion (Graham et al., 2001; Kemppainen and Behrend, 1998), bind to and act as a guanine nucleotide exchange factor (GEF) for the heterotrimeric G-protein (Gαi2) leading to inhibition of adenylate cylase (Cismowski et al., 2001; Cismowski et al., 2000; Graham et al., 2002; Graham et al., 2004; Kemppainen and Behrend, 1998), and is localized to the suprachiasmatic nucleus where it is involved in the entrainment of the circadian clock (Cheng et al., 2004a; Takahashi et al., 2003).

In order for a G-protein to be activated, it must release GDP and bind to GTP. This is the rate-limiting step in the activation of G-proteins, thus, these small G-proteins usually require some kind of GEF to catalyze the exchange of GDP for GTP. Thus far, no protein GEF has yet been identified for Dexras1.

Nitric oxide (NO) is a well-established neurotransmitter in the brain and in the nerves of the autonomic nervous system throughout the body. Its primary functions are muscle relaxation, penile erection and movement of food through the digestive tract (Furchgott and Zawadzki, 1980; Ignarro et al., 1987; Palmer et al., 1987). NO is a produced by nitric oxide sythase (nNOS) (Bredt and

Snyder, 1990), which converts arginine to citrulline, producing NO. The enzymatic reaction is outlined below:

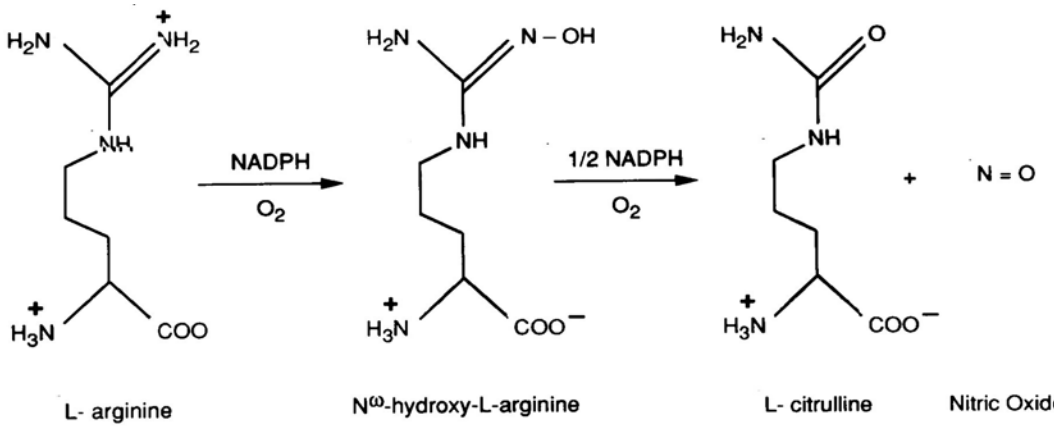


There are several forms of NOS. Neuronal NOS (nNOS) has a molecular weight of 160 kDa, while endothelial NOS (eNOS) and macrophage NOS (mNOS or iNOS) are about 130 kDa. nNOS and eNOS are constitutively expressed, while iNOS is inducible (Hibbs, Jr. et al., 1987; Stuehr and Nathan, 1989). All isoforms occur as dimmers.

nNOS is stimulated to produce NO via the NMDA receptor. Glutamate binds to the NMDA receptor, causing calcium channels to open, such that the intracellular calcium concentration is increased. The calcium binds to calmodulin, which binds and activates NOS, in turn, leading to NO production and diffusion of NO from the neuron. NO release from the neuron leads to activation of guanyl cyclase, leading to the production of cGMP as a secondary messenger (Bredt et al., 1990; Bredt and Snyder, 1989).

A second role for NO is protein *S*-nitrosylation (Hess et al., 2005). The nitric oxide moiety is usually attached at a cysteine residue side chain. Because NO is highly reactive and is easily inactivated by oxygen, superoxide and glutathione, it is increasingly appreciated that NO may not simply diffuse freely to reach its physiological target but may be conveyed to these sites by interactions of nNOS with other proteins. We have previously identified CAPON, a 55 kDa protein that contains a C-terminal domain that binds to the PDZ domain of nNOS as well as an N-terminal phosphotyrosine binding (PTB) domain (Jaffrey et al., 1998). CAPON interacts with Dexras1, creating a tertiary complex between nNOS, CAPON and Dexras1 (Fang et al., 2000). This leads to the nitrosylation of Dexras1 on cysteine-11, thus activating Dexras1, by causing the protein to bind to GTP in the absence of a protein GEF (Figure 3) ((Fang et al., 2000; Jaffrey et al., 2002). The selective lessening of Dexras1 activation in the brains of mice with targeted deletion of nNOS and the existence of a ternary complex of nNOS, CAPON and Dexras1, establish that neuronally derived NO physiologically serves as a guanine nucleotide exchange factor to activate Dexras1 by *S*-nitrosylation (Fang et al., 2000).

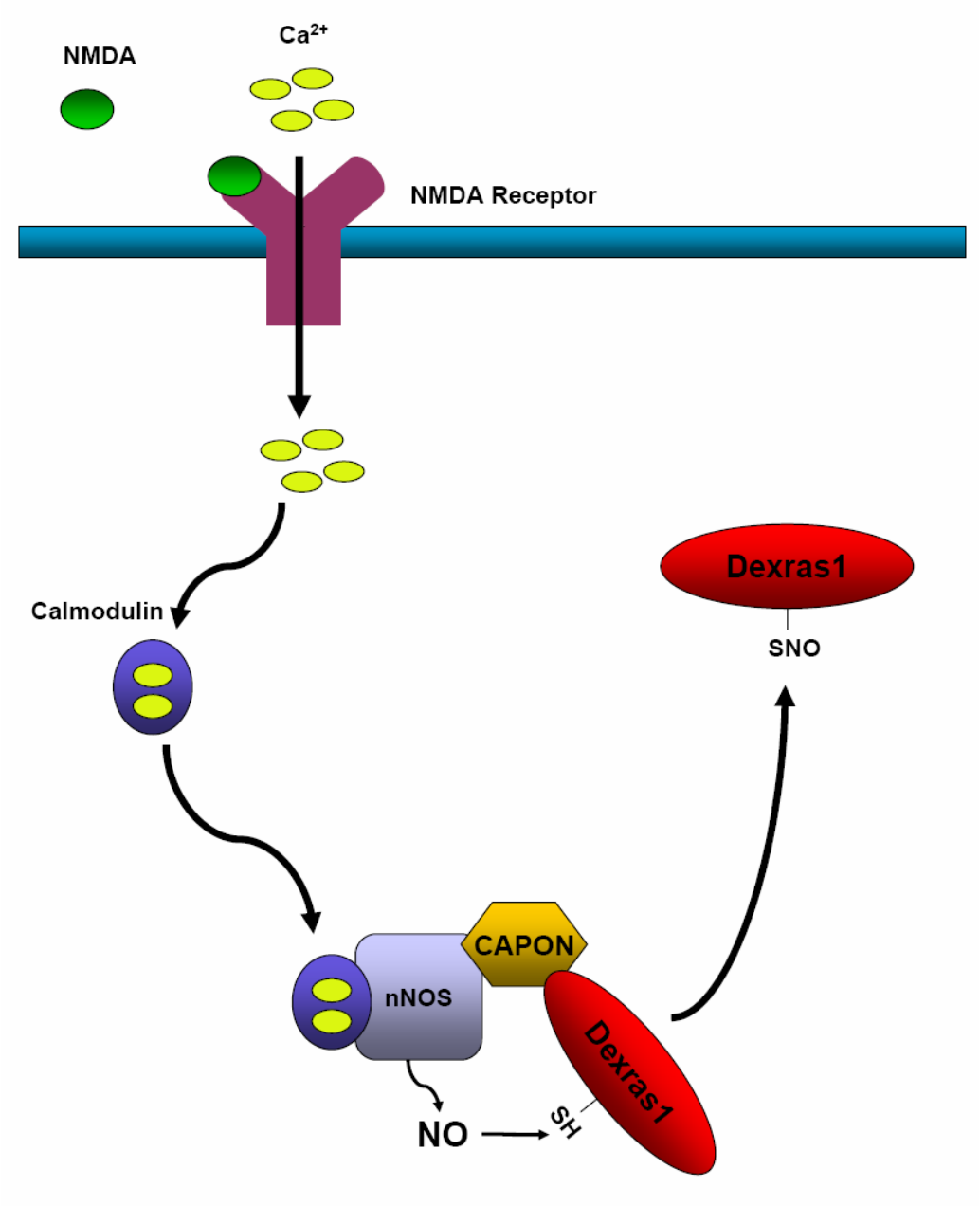


**Figure 3:** Dexras1 is regulated by NMDA and nNOS

Glutamate-NMDA binds to the NMDA receptor at the plasma membrane, allowing calcium ($Ca^{2+}$) to flux through the receptor and enter the cytoplasm, where it binds to calmodulin. This $Ca^{2+}$-calmodulin complex activates nNOS to produce nitric oxide (NO). nNOS interacts with Dexras1 via the adaptor protein CAPON, leading to *S*-nitrosylation and activation of Dexras1.

*Part 2.2: Rhes*

Rhes (Ras homolog enriched in striatum) is the closest homolog to Dexras1, sharing 62% identity (Figure 4). Though it shares homology with Dexras1, it is not transcriptionally regulated by dexamethasone, but rather, thyroid hormone (Falk et al., 1999; Vargiu et al., 2001). Rhes contains all of the conserved domains of the classical GTPases, but like Dexras1, it also contains that extended C-terminal tail of unknown function. Due to its selective expression in the striatum, it has been shown to be involved in striatal function, where Rhes knockout mice had impaired locomotor function and increase in anxiety (Spano et al., 2004). Rhes has also been shown to regulate signal transduction from G-protein coupled receptors. Rhes is post-translationally farnesylated and targeted to the membrane. Rhes is able to bind to and activate phosphoinositide 3-kinase (PI3K). Rhes also interferes with the cyclic AMP (cAMP)/ Protein Kinase A (PKA) pathway mediated by the thyroid stimulating hormone (TSH) receptor (Vargiu et al., 2004).

Though Rhes and Dexras1 are highly homologous, no study has yet been performed to determine whether Rhes is also regulated by nNOS/NMDA and *S*-nitrosylation.

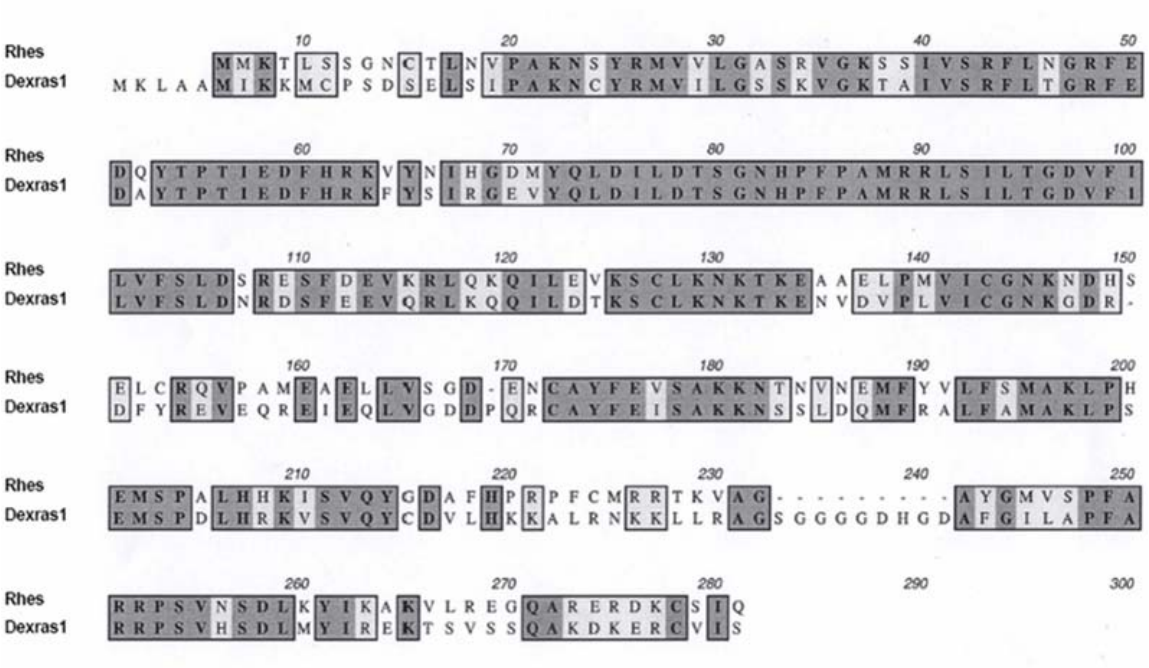


**Figure 4:** Sequence alignment of Dexras1 and Rhes

Dexras1 and Rhes share 68% homology at the amino acid level, with the typical conserved regions found in all GTP binding proteins sharing the highest homology. Rhes also contains the extended 7kDa C-terminal tail that Dexras1 has, but that is absent in other small G-proteins.

# CHAPTER 2:
# Materials and Methods

## Cells and Reagents

HEK 293T cells were maintained in DMEM with 10% fetal bovine serum (FBS), 2 mM L-Glutamine and 100U/ml penicillin-streptomycin (PS) at 37°C with 5% $CO_2$ atmosphere in a humidified incubator. PC12 cells were maintained in DMEM with 10% FBS, 5% horse serum, 2 mM L-glutamine and 100U/ml PS in the same environment. All chemicals were purchased from Sigma, unless otherwise indicated.

## Generation of constructs

Rat PAP7 was cloned from EST #5621578 (Open Biosystems) into either pCMV-GST or pCMV-HA (Clontech). Rat Dexras1, wild-type and A178V or C11S mutants, were all cloned into pCMV-Myc (Clontech).

## Characterization of PAP7

To examine the expression pattern of PAP7 throughout the body, a male C57/B6 mouse was dissected and each organ was homogenized in Buffer A (100 mM Tris pH 7.4, 150 mM NaCl, 1% Triton X-100, 15% Glycerol, 1 mM PMSF, 25 μg/ml antipain,

50 μg/ml leupeptin, 50 μg/ml aprotinin, 25 μg/ml chymostatin and 25 μg/ml pepstatin). Total protein (100 μg) was loaded onto a Western blot and immunoblotted with a rabbit anti-nNOS antibody (previously generated in our laboratory), rabbit anti-PAP7 (V. Papadopolous) antibody and rabbit anti-Dexras1 antibody (Calbiochem).

To examine the expression pattern of PAP7 in the brain, a male Sprague-Dawley rat brain was dissected into several parts, lysed in Buffer A, and total protein (100 μg) loaded and a Western blot performed.

To examine the expression pattern of PAP7 and Dexras1 in different cell lines, 100 μg of total protein from each cell line lysed in Buffer A was loaded onto a Western blot.

**GST pull-down assay**

GST or GST-tagged PAP7 constructs were co-transfected with Dexras1-Myc constructs into HEK 293T cells using PolyFect (Qiagen), with a transfection efficiency of greater than 90%. Cells were lysed 48h after transfection in Buffer A. Lysates were pre-cleared with pansorbin cells (Calbiochem), then 1 mg of total protein was incubated with glutathione-Sepharose beads overnight at 4°C. Beads were washed with Wash Buffer A (50 mM Tris pH 7.4, 500 mM NaCl, 10 mM β-

glycerophosphate) twice, then once with Buffer A. Beads were quenched in sample buffer (100 mM Tris, pH 6.8, 10% glycerol, 250 mM β-mercaptoethanol, 2% sodium dodecyl sulfate and bromophenol blue). Total protein (50 μg) was loaded as input. Dexras1-Myc binding was examined using an anti-myc antibody (Roche) followed by incubation with anti-mouse secondary conjugated to horseradish peroxidase(HRP) (Jackson Immunoresearch); blots were then stripped and probed with an anti-GST antibody conjugated to HRP to detect PAP7. Chemiluminescence (Pierce) was used to detect bands on the Western blot.

**Co-immunoprecipitation**

Undifferentiated PC12 cells were lysed in Buffer A and lysates were pre-cleared with protein A Sepharose. 1 mg of total protein was incubated with 2 μg of either goat anti-Dexras1 antibody (Abcam) or rabbit anti-NRAMP2 antibody (Alpha Diagnostics) overnight at 4°C, then protein A Sepharose beads were added for 1h. Beads were washed in Buffer A three times and quenched in sample buffer. Total PC12 lysate (100 μg) was loaded as input. PAP7 binding was detected using a rabbit anti-PAP7 antibody, followed by anti-rabbit Ig conjugated to HRP.

For the ternary complex interaction, a male C57/B6 mouse was sacrificed and the whole brain was dissected and homogenized in Buffer A. Lysates were pre-cleared with protein A Sepharose. 1 mg of total protein was incubated with 2 μg of rabbit anti-PAP7 antibody overnight at 4°C, then protein A Sepharose beads were added for 1h. Beads were washed in Buffer A three times and quenched in sample buffer. Total brain lysate (100 μg) was loaded as input. Dexras1 and DMT1 binding was detected using a rabbit anti-Dexras1 or anti-NRAMP2 antibody, followed by anti-rabbit Ig conjugated to HRP.

**Immunofluorescence Staining**

Undifferentiated PC12 cells were plated on poly-D-lysine coated glass coverslip dishes. For PAP7 localization to the Golgi, these cells were transfected with a plasmid containing a Golgi marker conjugated to YFP (pEYFP-Golgi, Clonetech) using Lipofectamine 2000 (Invitrogen). After 48 hours, cells were stained as below.

Cells were fixed in 4% paraformaldehyde in PBS, permeabilized in 1% Triton X-100 in PBS and blocked in PBS with 1% normal goat serum and 2% normal horse serum. Endogenous Dexras1 was detected using a goat anti-Dexras1 antibody; endogenous PAP7 was detected using a rabbit anti-

PAP7 antibody. Anti-goat Ig conjugated to FITC and anti-rabbit Ig conjugated to rhodamine was obtained from Molecular Probes. Confocal microscropy images were obtained using a PerkinElmer UltraView LCI (Live Cell Imaging) System.

**_S_-nitrosylation of Dexras1**

PC12 cells were treated with various concentrations of GSNO (Alexis Biochemicals) for 3h. Cells were washed in PBS and harvested. *S*-nitrosylation of Dexras1 was monitored using the biotin-switch assay previously described (Jaffrey and Snyder, 2001). Dexras1 was detected on the immunoblot using a rabbit anti-Dexras1 antibody (Calbiochem).

**Iron Uptake Assays**

*In HEK 293T Cells* - NTBI uptake assays were performed as previously described (Picard et al., 2000). In brief, HEK 293T cells were transfected (greater than 90% efficiency) with PAP7-HA and Dexras1-Myc (or mutants) using Lipofectamine and PLUS Reagent (Invitrogen) for 3h in DMEM only, then supplemented with full media After 48h, the cells were washed with phosphate buffered saline (PBS) then resuspended into Iron Uptake Buffer (25 mM Tris, 25 mM MES, 140 mM NaCl, 5.4 mM KCl, 5 mM glucose, 1.8 mM $CaCl_2$, pH 5.5)

and transferred to glass test tubes. Ascorbic acid was added to 1 mM $FeSO_4$ at a 44:1 ratio. $^{55}FeCl_3$ (PerkinElmer Life Science) was added to the iron/ascorbic acid mixture, which was then added to the cells in Iron Uptake Buffer to a final concentration of 20 μM. Cells were incubated at 37°C with shaking for 30 minutes. The cells were washed twice with cold PBS + 0.5 mM EDTA and harvested. An aliquot of resuspended cells was taken for protein assay using the Bio-Rad Protein Assay Reagent; the protein concentrations of individual samples were used to quantitate $^{55}Fe$ incorporation (cpm/μg protein). Samples were normalized to control.

*In primary cortical neurons* - Cells were dissected out of E16-E18 wild-type or nNOS knockout mice and plated in 6 well plates at 3 X $10^6$ cells per well. Cells were maintained in Primary Neuron Media (Neurobasal media supplemented with B27 serum, 2 mM L-glutamine and 100U/ml PS) at 37°C with 5% $CO_2$ atmosphere in a humidified incubator. Using this media, the growth of the glia is suppressed and the amount of glia is less than 0.5% of the total culture, giving us an essentially pure neuronal culture.

Neurons were aged 14-20 days after plating before being used for iron uptake assays. Cells were treated as follows:

100μM NMDA for 30 min, 300μM NMDA for 10 minutes or 5 μM ionomycin for 10 min. For samples with MK801, cells were pre-treated with 10 μM MK801 for 10 min, then 100 μM NMDA was added for 30 min. Cells were then washed once with warm PBS. For samples with MK801, the drug was added back after NMDA treatment.

For NTBI uptake assays, 1 ml of warm Iron Uptake Buffer containing 20 μM iron prepared as above was added to each well and incubated at 37°C with 5% $CO_2$ atmosphere in a humidified incubator for 30 min. Cells were harvested, washed twice in cold PBS + 0.5 mM EDTA and processed as above.

For Tf-iron uptake pathway, assays were performed as previously described (Kim and Ponka, 2002). In brief, apo-transferrin was loaded with $^{55}Fe^{2+}$ and the concentration measured. After treatment, cells were incubated in a final concentration of 10 μM transferrin (1 μM $^{55}$Fe-transferrin and 9 μM holo-transferrin) in 1 ml of Primary Neuron Media for 2h. Cells were harvested, washed twice in cold PBS + 0.5 mM EDTA and processed as above.

**RNA Interference in PC12 cells**

The Dexras1 RNA interference (RNAi) insert was designed using the Genescript siRNA design center and cloned into pRNAT-U6.1/Neo (Genescript). To obtain knockdown in PC12 cells, 24 μg of Dexras1 RNAi were transfected into cells using Lipofectamine 2000 (Invitrogen) in Optimem overnight. Control transfection used the pRNAT-U6.1/Neo empty vector. The next morning, cells were fed with full media and allowed to recover for 24h. They were transfected again overnight, and then allowed to recover for 2 days before treatment with GSNO for 3h. The transfection efficiency after the double transfection was greater than 90%. To monitor knockdown, lysate (100 μg) was run on a Western blot (mock transfected cells had no DNA), and Dexras1 protein levels were monitored using a rabbit anti-Dexras1 antibody.

**Heme Incorporation Assay**

Primary rat cortical neurons were treated with 100 μM NMDA, then incubated in $^{55}$Fe-transferrin as described above. Cells were washed in PBS + 0.5 mM EDTA, then resuspended in 1 ml of 0.2N HCl. Using an aliquot of cell lysate, the protein concentration of individual samples was determined using the Biorad Protein Assay. The resuspended cells were heated

at 100°C for 10 minutes, cooled on ice, and then transferred to glass test tubes. 10% TCA (3 ml) was added to each sample, vortexed, and incubated on ice for 15 minutes. Protein precipitate was pelleted by centrifugation, and the pellet was washed in 3 ml of 10% TCA, and resuspended in 500 μL of 0.2N HCl. Scintillation fluid was added and $^{55}Fe^{2+}$ incorporated into heme counted in a scintillation counter. Samples were normalized to control.

**HemoQuant Assay**

To measure heme content in whole brains, the HemoQuant assay was performed as previously described (Schwartz et al., 1983). Whole brains from age-matched wild-type and nNOS knockout mice were lysed in 4 ml of Buffer A. 50 μg of lysate was added to 1 ml of saturated 2M oxalic acid in a glass test-tube. Two sets of triplicates were set up for each sample – one set are blanks, while the other set are samples. The sample set was boiled at 100°C for 30 minutes, then cooled to room temperature. The blank set was left at room temperature. Boiling samples in 2M oxalic acid converts heme to prophyrin, the fluorescence of which was read in a spectrofluorometer using 400 nm excitation and 662 nm emission. The blank values were subtracted from the

sample values. nNOS knockout porphyrin readings were normalized to the age matched wild-type controls (100%).

**Measurement of Reactive Oxygen Species**

To measure highly reactive oxygen species (hROS), such as hydroxyl free radicals generated by the Fenton reaction, we employed 2-[6-(4'-hydroxy)phenoxy-3*H*-xanthen-3-on-9-yl]benzoic acid (HPF) (Cell Technology, Inc, Mountain View, CA) (Setsukinai et al., 2003). This scarcely fluorescent compound binds specifically to hydroxyl free radicals, and less specifically to peroxynitrate, and converts to a highly fluorescent molecule.

Rat primary cortical neurons were prepared as above and aged for 14 days after plating. Measurement of hROS was conducted according to the manufacturer's protocol. Briefly, neurons were pretreated with either 0 μM or 100 μM SIH for 3 hours in full media, which was then removed, and the cells were washed once with Hanks Balanced Salt Solution (HBSS). 5 μM HPF in HBSS was added to the cells and incubated at 37°C with 5% $CO_2$ atmosphere in a humidified incubator for 30 min. 0 μM or 300 μM NMDA was then added to the cells and incubated for another 30 minutes. Cells were harvested in HBSS and fluorescence was measured in a

fluorimeter utilizing excitation 488 nm and emission 515 nm.

**Phosphorylation Studies**

To examine *in vivo* phosphorylation of PAP7, we transfected HEK 293T cells with a myc-tagged construct using Polyfect. 48 hours after transfections, we replaced the media on the cells with DMEM (Invitrogen) containing no sodium phosphate and supplemented with $^{32}$P-orthophosphate (Perkin Elmer) and incubated for 4 hours. All inhibitors were made up in DMSO and added at this time at the following final concentrations: 1 μM staurosporine, 1 μM H-89, 1 μM GFX, 25 μM TBB, 50 μM DRB, 100 μM Olomoucine, 10 μM SB-216763 and 1 μM Indirubin-3-monoxime (Biomol). Cells were rinsed twice in PBS and lysed in Buffer A. Cell lysates were precleared using Pansorbin cells for 30 minutes and a protein assay performed. Immunoprecipitations were performed using 1 mg of total lysate and 2 μg of anti-myc antibody, pulled down with Protein A Sepharose. Beads were washed with Buffer A three times, quenched in sample buffer and loaded on a 4-12% Bis-Tris gel. The gel was then either stained with Commassie stain or transferred to nitrocellulose. After autoradiography, blots were probed with anti-myc antibody for sample input.

To examine *in vitro* phosphorylation of PAP7, Dexras1 and Rhes, we transfected HEK 293T cells with myc-tagged constructs using Polyfect. After 48 hours, cells were harvested and immunoprecipitations were performed as above using an anti-myc antibody. After washing the samples twice in Wash Buffer A, once in Buffer A and then twice in PBS, samples were either untreated or treated with lambda-phosphatase at 30C for 2 – 4 hours, then washed again three times with PBS. The samples were then treated with different kinases and $^{32}$P-gamma-ATP (Perkin Elmer) for 30 minutes at 30C. The samples were quenched in SDS-PAGE buffer, loaded on a 4-12% Bis-Tris gel and transferred to nitrocellulose. The blot was exposed to film, then probed with an anti-myc antibody for input samples.

**Generation and purification of the Rhes antibody**

Rat Rhes was cloned into pGEX-4T2 and transformed into BL21-Codon Plus RIL cells (Stratagene). Bacterial cells were grown to an OD600 nm of 0.4 and protein production was stimulated with 1 mM IPTG overnight at room temperature. Cells were lysed in Buffer B (50 mM Tris pH 7.4, 150 mM NaCl, 2% Sarkosyl, 10% Glycerol, 2 mM EDTA, 5 mM DTT, 1 mM PMSF, 25 μg/ml antipain, 50 μg/ml leupeptin, 50 μg/ml aprotinin, 25 μg/ml chymostatin and 25 μg/ml pepstatin ) and

sonicated for 10 minutes. The supernatant was obtained after spinning at 20,000 x g for 20 minutes and Triton X-100 was added to a final concentration of 1%. The protein was allowed to bind to glutathione sepharose overnight at 4C and the beads were washed two times in Wash Buffer B (PBS, 10% Glycerol and 1% Triton) and then twice in Wash Buffer C (PBS and 10% Glycerol). Protein was eluted in 1 ml fractions in Elution Buffer (50 mM Tris pH 8.0, 150 mM NaCl, 10% Glycerol, 2 mM EDTA, 5 mM DTT, 20 mM reduced glutathione, 1 mM PMSF, 25 μg/ml antipain, 50 μg/ml leupeptin, 50 μg/ml aprotinin, 25 μg/ml chymostatin and 25 μg/ml pepstatin) and sent to Cocalico Biologicals for antibody production.

Polyclonal antibodies were generated in two rabbits and bleeds were obtained. The antibodies to GST in the serum were purified out using the protocol from the Flemington lab (www.flemingtonlab.com). The antibody was tested against GST or myc-tagged over-expressed proteins in HEK 293T cells to show specificity to Rhes. Whole body tissue samples were obtained from C57/B6 mice, while brain region samples were obtained from Sprague-Dawley rats. In all cases, 100 μg of total protein was loaded onto 4-12% Bis-

Tris gels, transferred and probed with the anti-Rhes antibody.

**Measurement of Cell Death**

To quantitatively measure cell death after stimulation with various agonists, we employed the MTT assay. A 5 mg/ml stock of MTT (Thiazolyl Blue Tetrazolium Bromide, Sigma, St. Louis) was diluted to a final concentration of 0.25 mg/ml in HBSS buffer and added to cells after various treatments. Cells were incubated at 37C for 2 – 4 hours, then the MTT reagent was removed and the cells washed one time in HBSS. Healthy cells with intact mitochondria convert the yellow colored MTT reagent to purple crystals within the cells, which can then be dissolved in 0.1N HCl in isopropanol. The samples, measured in triplicate, were read in a spectrophotometer at OD 580 nm and OD 630 nm. The OD 580 nm – OD 630 nm reading was normalized to control and expressed as a percentage of cell viability.

# CHAPTER 3:

# Results and Discussion

## ***Part 1: Dexras1 interacts with Peripheral Benzodiazepine Receptor Associated Protein (PAP7)***

Though it is known that Dexras1 interacts with nNOS and is activated by NO via S-nitrosylation, the function for this activated Dexras1 has not yet been determined. To elucidate physiological roles for Dexras1, we conducted yeast-two-hybrid analysis utilizing full length Dexras1 fused to the GAL4 DNA binding domain, and a rat whole brain cDNA library fused to the GAL4 DNA activation domain. A single colony identified PAP7 as a potential interactor. PAP7 is a 62 kDa protein including several domains: an acyl-coenzyme A-binding protein signature, a bipartite nuclear localization signal at the N-terminus, a Golgi dynamics (GOLD) domain at the C-terminus and glutamate (E)-, glutamine (Q)- and an asparagine (N)-rich domains (Figure 5). PAP7 was identified as an interacting protein of the peripheral benzodiazepine receptor (PBR) and may be involved in steroidogenesis in the mitochrondria. It also interacts with the regulatory subunit of PKA, though its effect on or by PKA is unknown (Li et al., 2001).

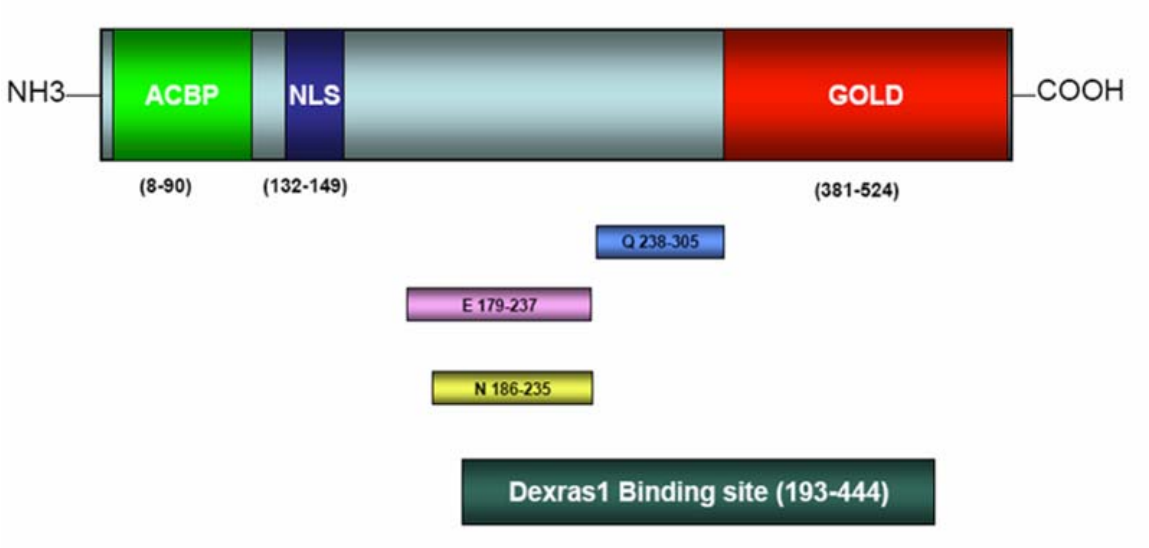


**Figure 5:** Schematic diagram of PAP7

An Acyl-CoA Binding Protein Domain (ACBP) and bipartite nuclear localization signal (NLS) are located at the N-terminus, while a Golgi Dynamics (GOLD) Domain resides at the C-terminus. The middle of the protein contains asparagine (N), glutamate (E) and glutamine (Q)-rich domains. The Dexras1 binding domain is located between amino acids 193-444 as determined by yeast two-hybrid analysis.

*Part 1.1: Characterization of PAP7*

As little is known about PAP7 and its functions, we began by characterizing PAP7 proteins expression levels in tissues and in the brain. Western blot analysis reveals that PAP7 is expressed at substantial levels in multiple mouse tissues including brain, adrenal, heart, lunch, liver, spleen and testes, but no detectable levels in the kidney, while Dexras1 is brain-selective with modest levels in the heart and testes and nNOS is expressed only in the brain (Figure 6A). PAP7 is expressed ubiquitously in all regions of the brain (Figure 6B) and occurs in high levels in many different cell lines, with very low levels in HEK 293T and HeLa cells (Figure 7). Immunohistochemical staining of PAP7 in undifferentiated PC12 cells shows that PAP7 is localized to the Golgi and to the cytosol (Figure 8). Localization of PAP7 in Golgi, where it interacts with gigantin and was designated GCP60, has been previously reported (Sohda et al., 2001).

As PAP7 interacts with PKA (Li et al., 2001), we wondered if PAP7 is phosphorylated. *In vivo* and *in vitro* phosphorylation experiments show that PAP7 is phosphorylated by CK2, not PKA, and is attenuated with treatment with TBB, a CK2 inhibitor (Figure 9A – 9D). Using different fragments of PAP7, we have shown that PAP7 is

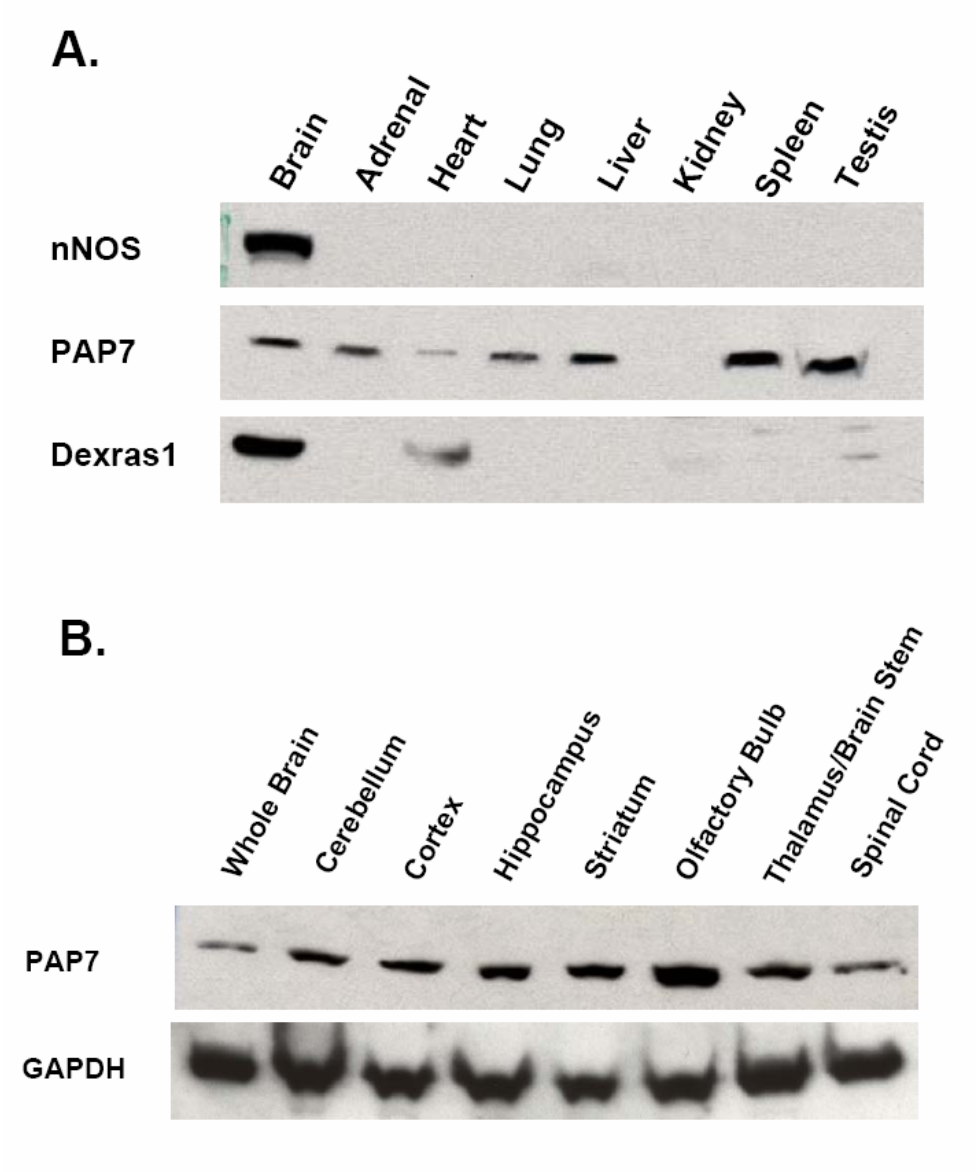


**Figure 6:** Localization of PAP7

(A) Western blot analysis shows that PAP7 is expressed at substantial levels in multiple mouse tissues, including the brain, adrenal, heart, lung, liver, spleen and testis but not in the kidney. Dexras1 is brain-specific with modest levels in the heart and testis, while nNOS is expressed only in the brain.
(B) PAP7 is expressed ubiquitously in all regions of the brain, with the highest level in the olfactory bulb.

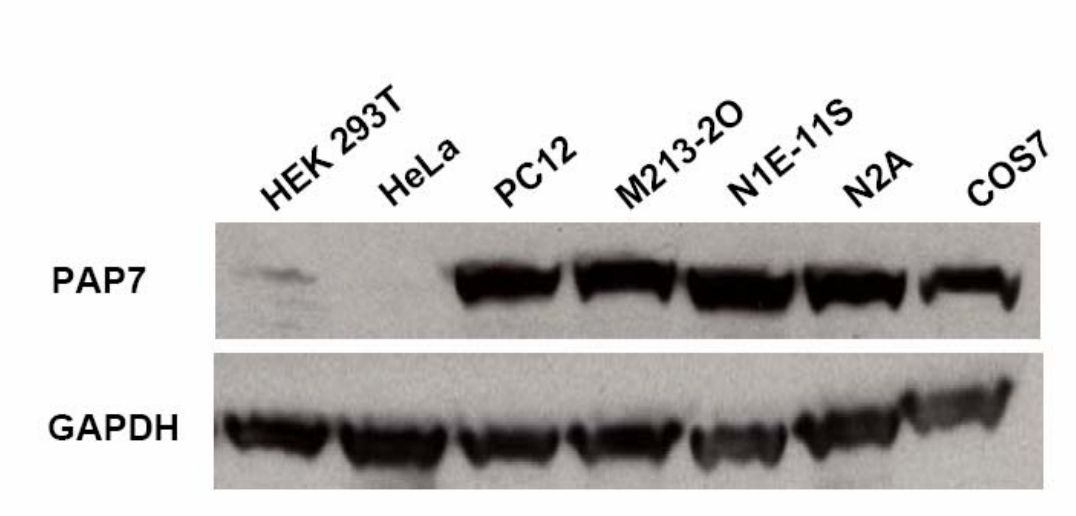


**Figure 7:** PAP7 expression in various cell lines
PAP7 is expressed in many commonly used cell lines, including PC12 cells, the two neuroblastoma cell lines, N2a and N1E-11, the striatal cell line, M213-2O and COS7 cells but not in HEK 293T or HeLa cells.

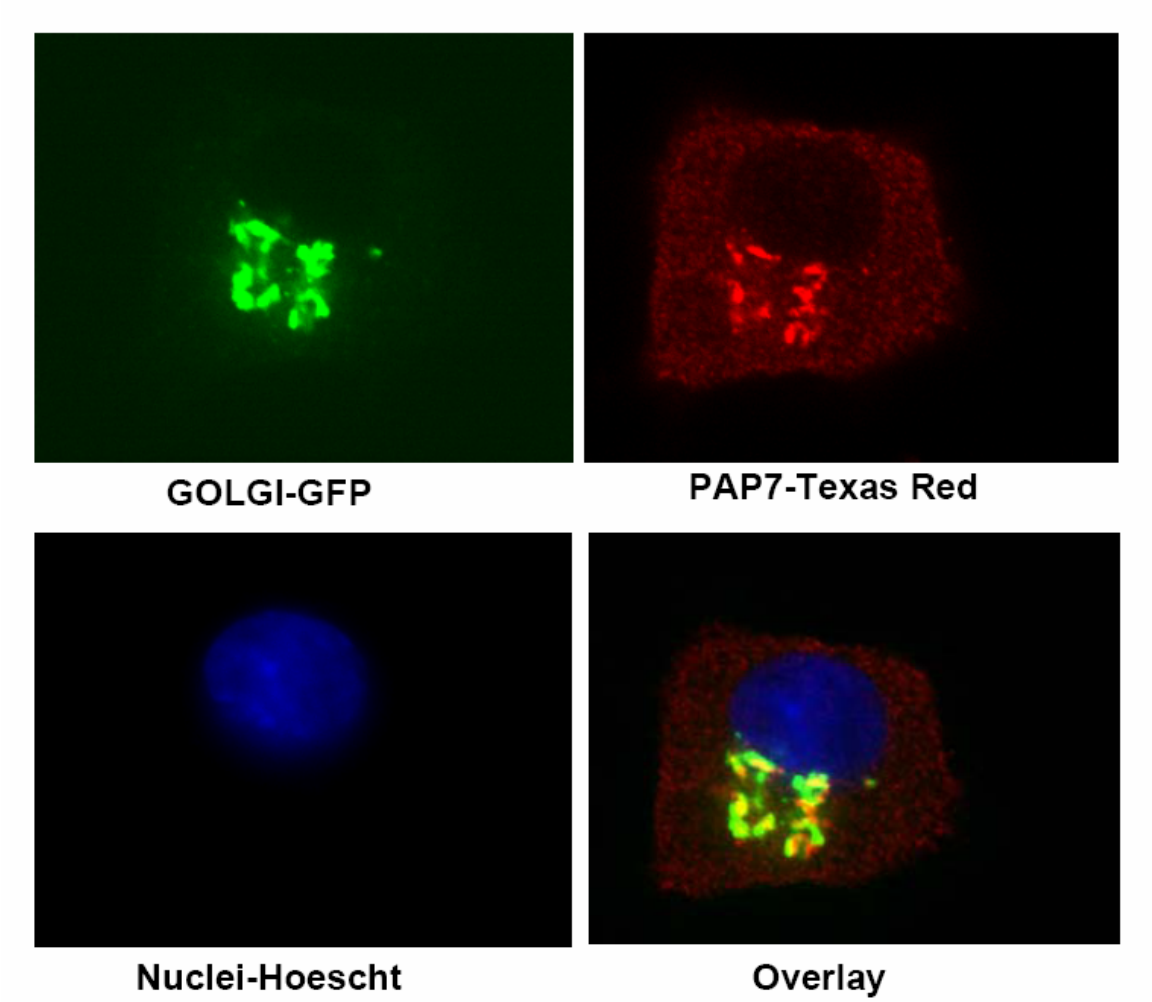


**Figure 8:** Immunohistochemical localization of PAP7

Undifferentiated PC12 cells were transfected with a Golgi marker and stained for endogenous PAP7, revealing that PAP7 is localized to both the Golgi apparatus and the cytosol.

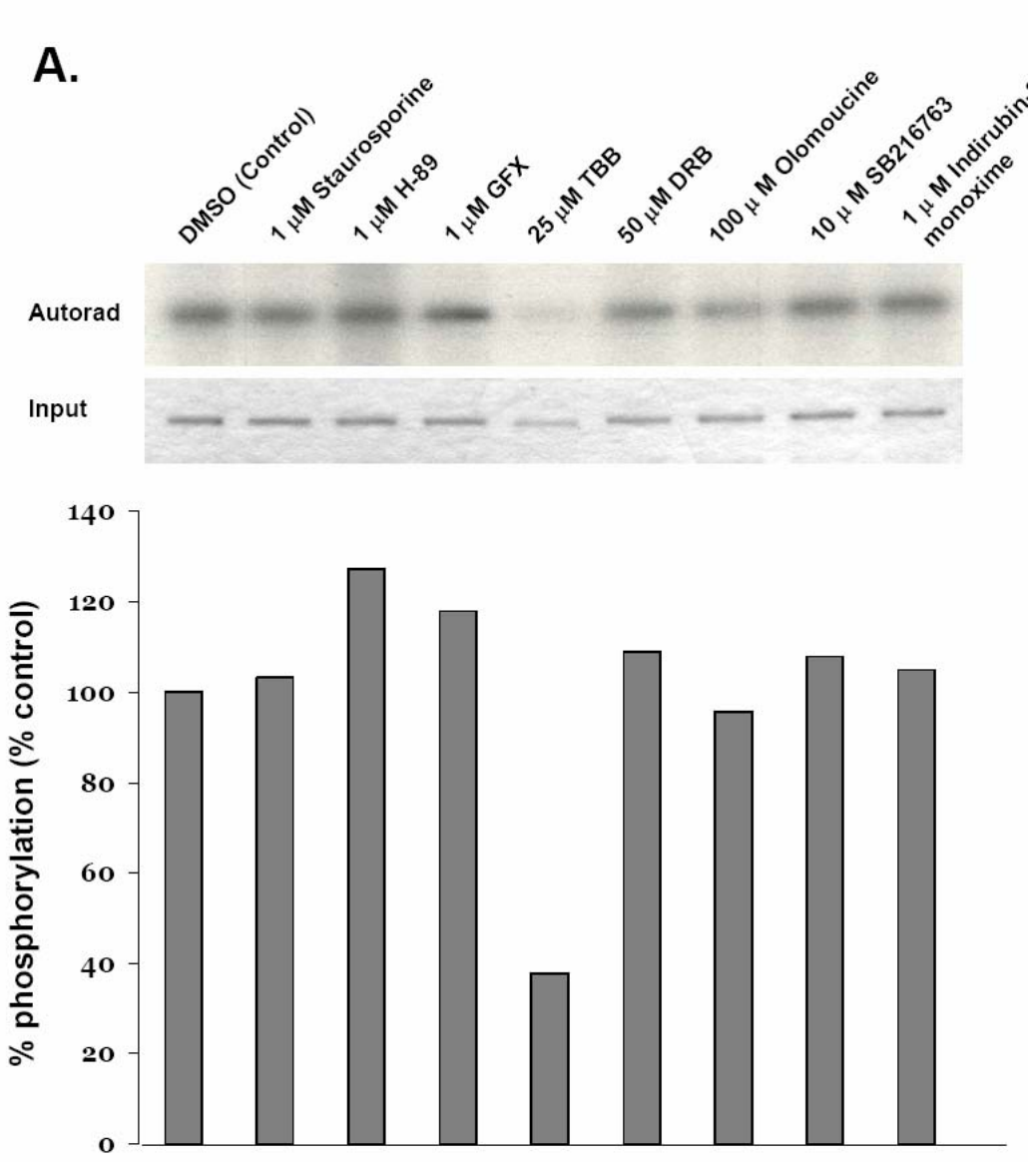


**Figure 9:** *In vivo* and *in vitro* phosphorylation of PAP7

(A) HEK 293T cells were transfected with myc-tagged PAP7 and labeled with $^{32}$P-orthophosphate in the presence or absence of various kinase inhibitors, revealing that PAP7 is phosphorylated by CK2. Inhibitors (Kinase): Staurosporine (general Ser/Thr kinase), H-89 (PKA), GFX (PKC), TBB (CK2 – strong inhibitor), DRB (CK2 – weak inhibitor), Olomoucine (CDK5), SB216763 (GSK3β) and Indirubin-3-monoxime (GSK3β, CDK1, CDK5). The ratio of the densities of bands of the autoradiograph signal to Commassie blue signal was calculated, then normalized to control.

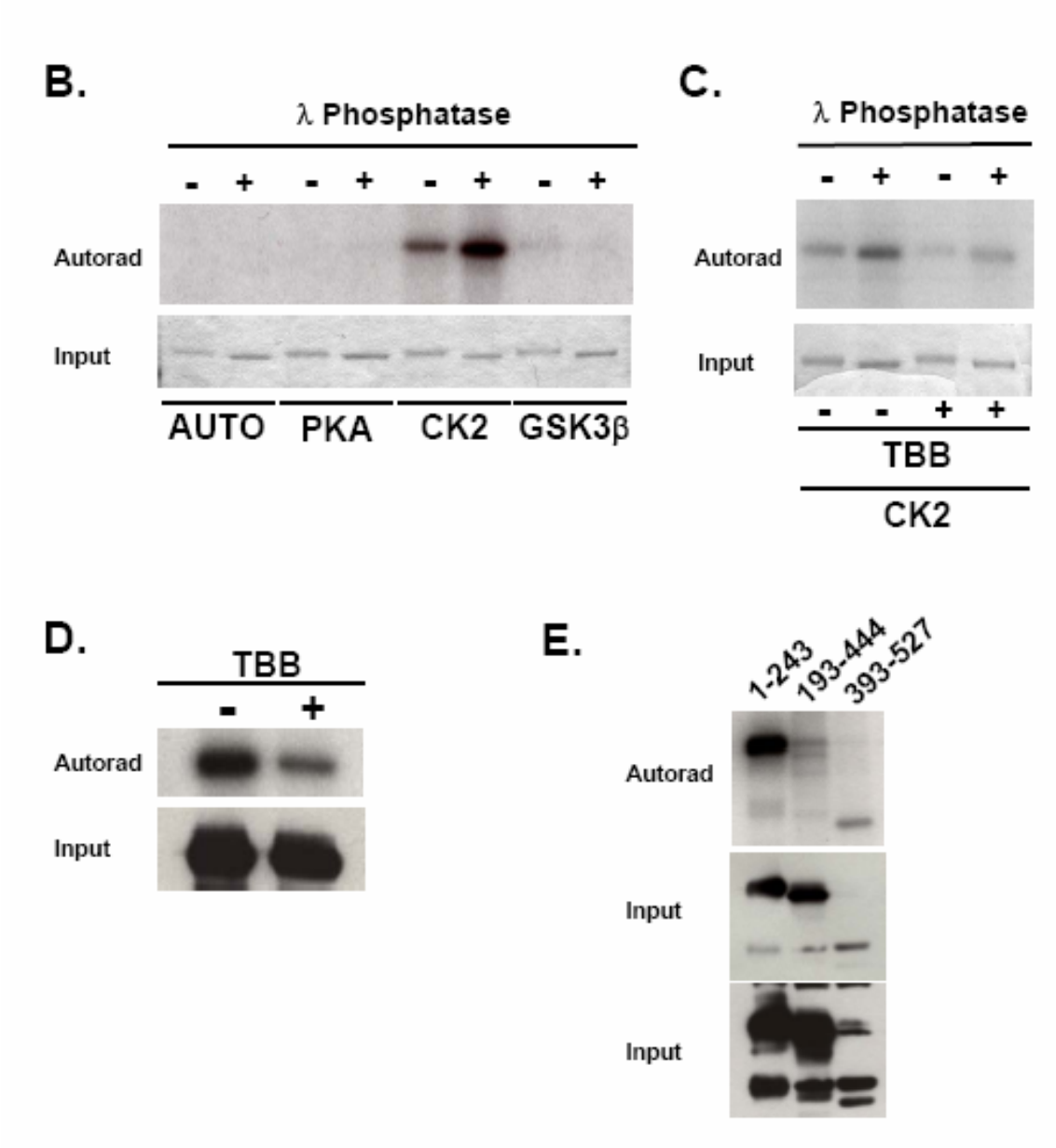


B) Myc-tagged PAP7 was immunoprecipitated from transfected HEK 293T cells, treated with lambda phosphatase, then phosphorylated with various kinases, showing that CK2 specifically and robustly phosphorylates PAP7. This phosphorylation was significantly reduced both *in vitro* (C) and *in vivo* (D) with treatment of the samples with TBB. (E) *In vivo* phosphorylation experiments show that PAP7 is phosphorylated at the N- and C-terminus, but not in the middle of the protein.

phosphorylated at both the N- and C-terminus, but not in the middle of the protein and not in the region that interacts with Dexras1 (Figure 9E). The specific site and consequence of this phosphorylation is still unknown.

*Part 1.2: Interaction of Dexras1 and PAP7*

From the yeast-two hybrid, Dexras1 interacts with PAP7 between amino acids 193-444, encompassing parts of the E-, Q- and N-rich domains, as well as the first part of the GOLD domain. We have confirmed the Dexras1-PAP7 interaction by transient transfections of GST-PAP7 and Dexras1-Myc in HEK 293T cells, which reveals selective binding of Dexras1 and PAP7 (Figure 10A). PAP7 also binds to a constitutively active form of Dexras1 (A178V)(Graham et al., 2001) at about the same level as while-type, indicating the activity status of Dexras1 is not important for protein interaction. In fact, Dexras1 has the ability to bind PAP7 even in the presence of 10 mM EDTA, which would chelate the $Mg^{2+}$ from Dexras1 and render it nucleotide free (Figure 10B).

We have narrowed down the binding region of Dexras1 on PAP7. Starting with the 193-444 region, which binds to Dexras1 (Figure 11A), we made deletion constructs of this region from both the N-terminus and the C-terminus (Figure

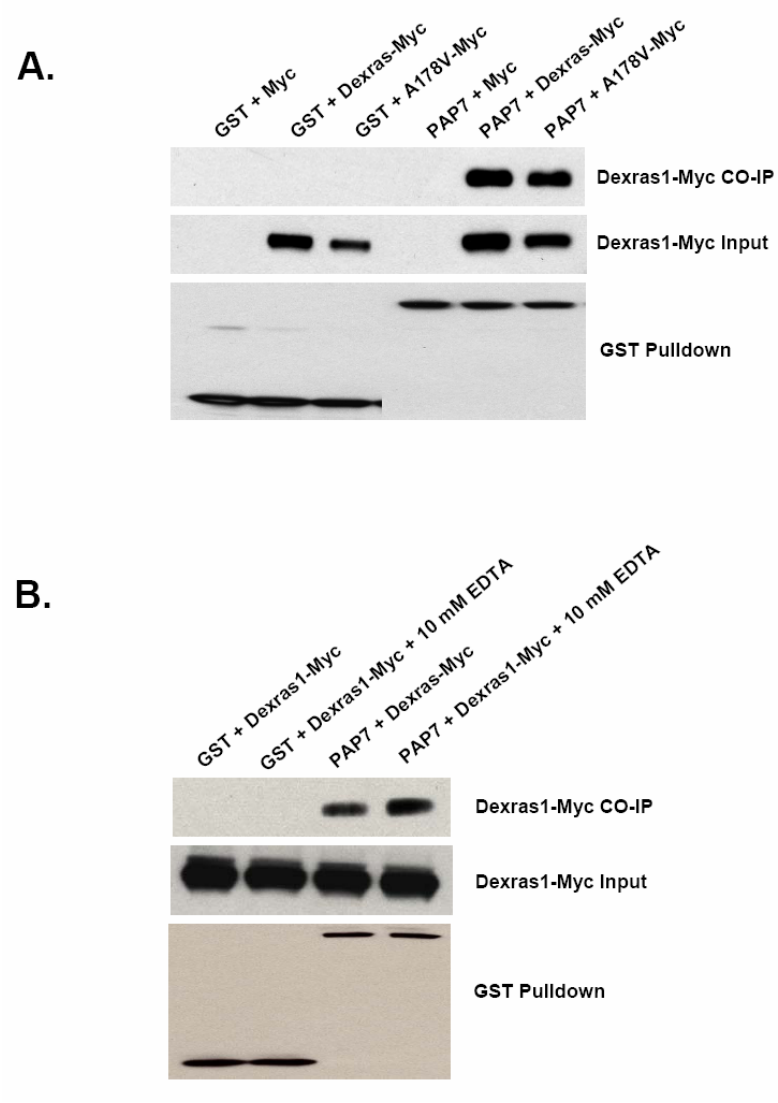


**Figure 10:** Dexras1 binds to PAP7 in transfected HEK 293T cells

(A) HEK 293T cells were transfected with GST or GST-PAP7 and either wild-type or constitutively active (A178V) Dexras1. GST pulldown experiments show that both wild-type and A178V Dexras1 specifically binds to PAP7, in about equal amounts, suggesting that the activity status of Dexras1 does not affect binding. (B) Dexras1 is still able to bind to PAP7 in the presence of 10 mM EDTA, which would render Dexras1 inactive.

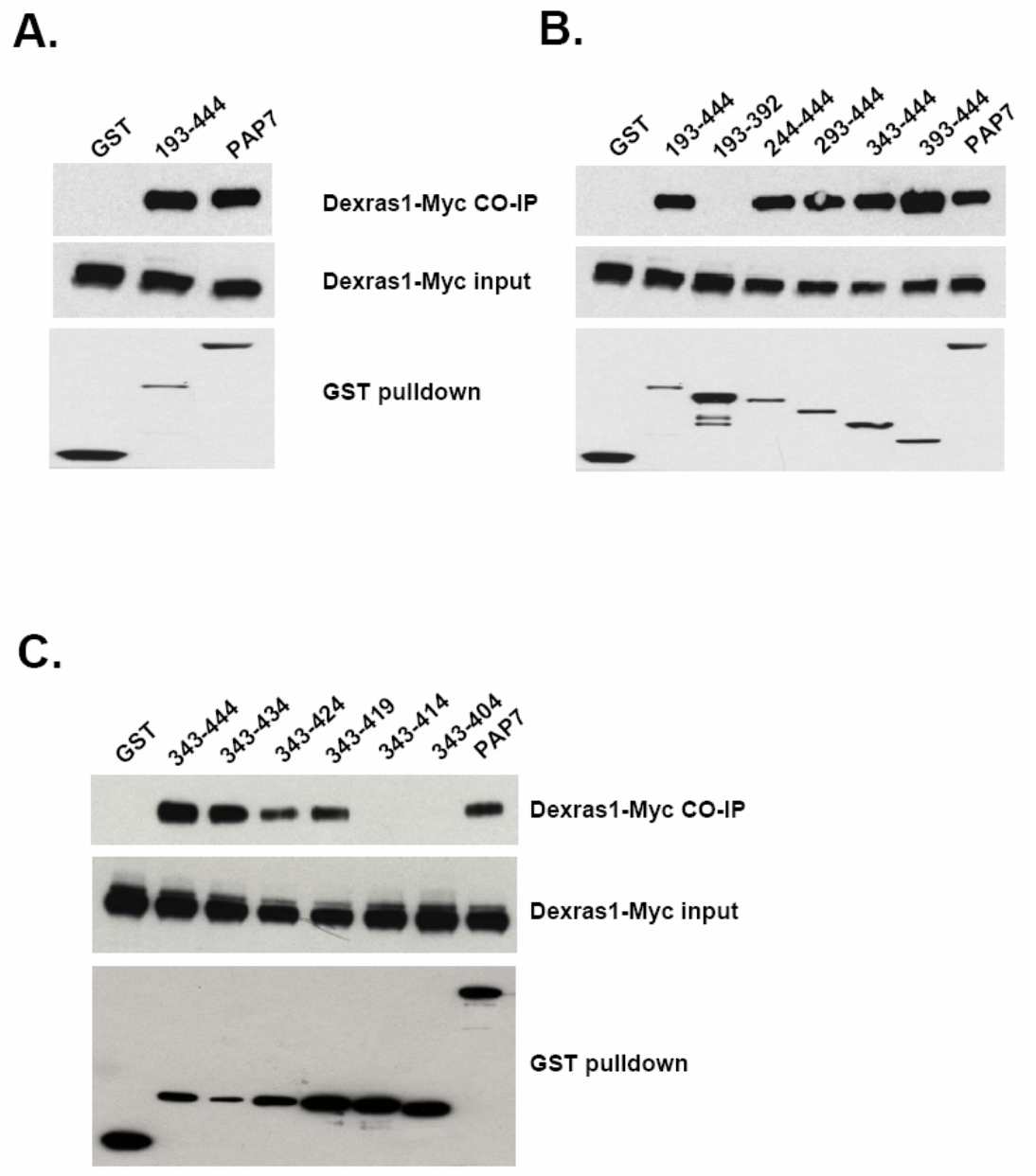


**Figure 11:** Narrowing down the Dexras1 binding region on PAP7

(A) Yeast-two hybrid analysis revealed the Dexras1 binding region on PAP7 to be between amino acids 193-444, which was confirmed by GST pulldown experiments in HEK 293T cells. Deletion constructs were made within this region and the binding was narrowed down to a 50 amino acid region (B) between amino acids 393–444, then further narrowed to a 5 amino acid region (C) between amino acids 414-419.

11B). Using this, we have determined that Dexras1 binds to PAP7 between amino acids 414-419 (Figure 11C). We have also narrowed down the binding region of PAP7 on Dexras1 to amino acids 96-101, close to the $Mg^{2+}$ loop of the G-protein (Figure 12).

Immunohistochemical staining of undifferentiated PC12 cells reveals PAP7 is localized to the Golgi apparatus and to the cytosol, while Dexras1 is cytosolic and plasma membrane associated, so Dexras1 and PAP7 co-localize in the cytosol (Figure 13).

*Part 1.3: Dexras1, PAP7 and DMT1 participate in iron trafficking*

To evaluate the interaction of endogenous Dexras1 and PAP7, we employed PC12 cells, which contain high levels of both PAP7 and Dexras1. Using an antibody to Dexras1, we observe specific co-immunoprecipitation of PAP7 (Figure 14A). An NCBI nucleotide sequence submission reported PAP7 as interacting with DMT1 (NCBI accession number NM_182843), though no data had yet been shown to prove this. Using PC12 cells and an antibody for DMT1, we have confirmed the binding of PAP7 and DMT1 by co-immunoprecipitation (Figure 14B). To examine a more physiological preparation, we conducted immunoprecipitation experiments in whole mouse

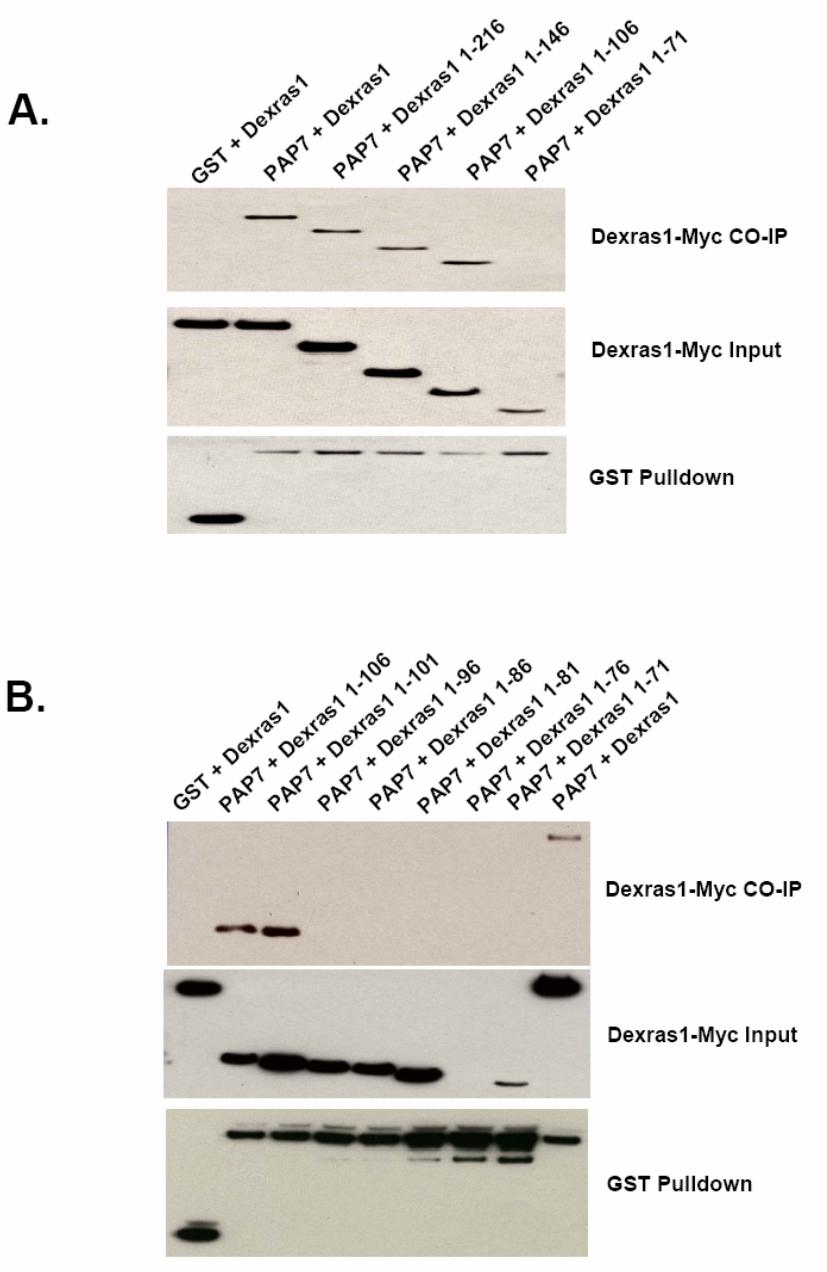


**Figure 12:** Narrowing down the PAP7 binding region on Dexras1

(A) Deletion constructs of Dexras1 were made such that they overlapped with identical regions of Rhes and GST pulldown experiments were performed in HEK 293T cells. Initial studies showed that PAP7 binds to Dexras1 between amino acids 71-106, and the binding region was further narrowed down to 5 amino acids (B) between amino acids 96-101.

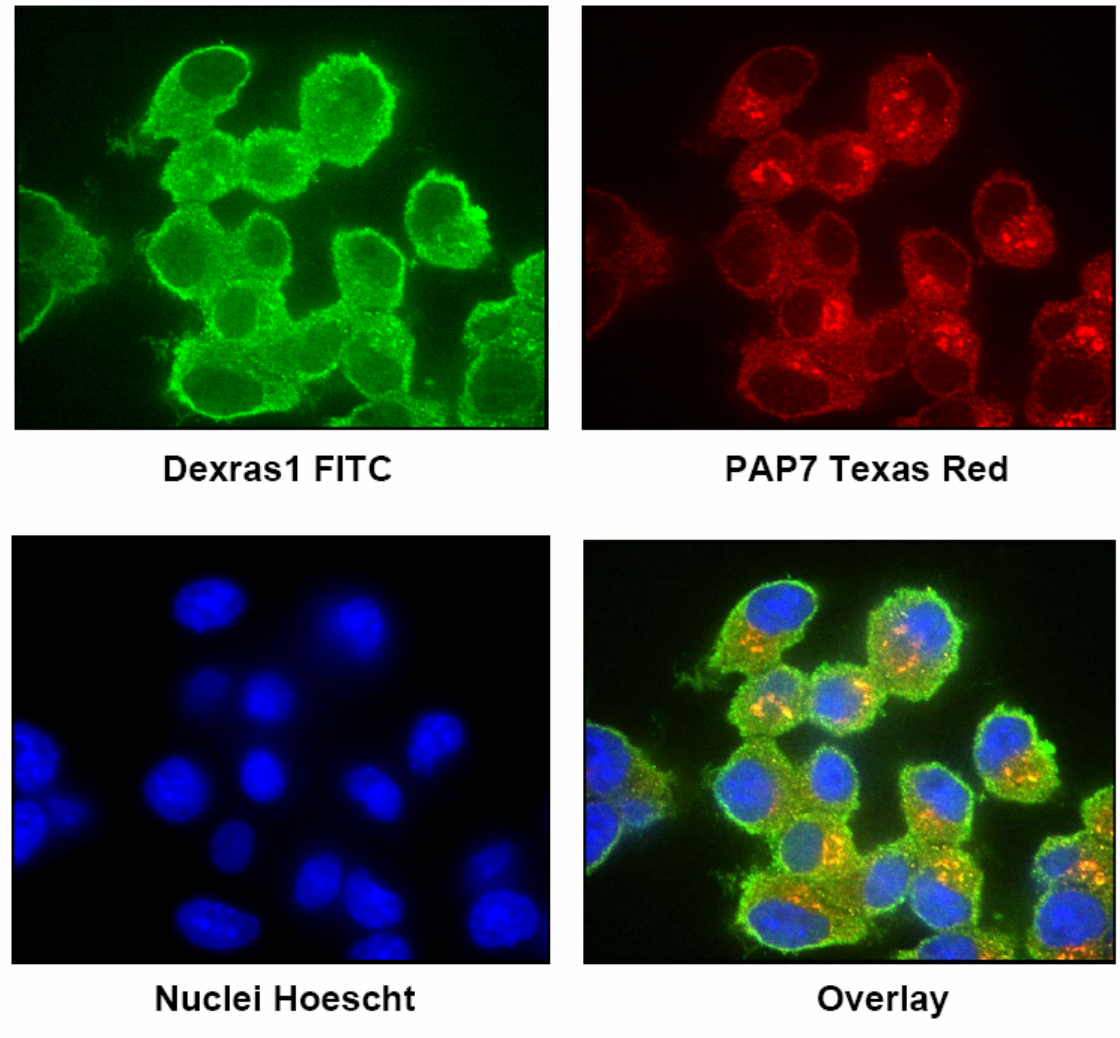


**Figure 13:** Immunohistochemical co-localization of Dexras1 and PAP7

Undifferentiated PC12 cells were fixed and stained for endogenous Dexras1 and PAP7. Dexras1 is localized to the cytosol and plasma membrane, while PAP7 is localized to the cytosol and Golgi apparatus.

brain and examined for the presence of a ternary complex. Using an antibody to PAP7, we observe simultaneous co-precipitation of both Dexras1 and DMT1 (Figure 14C). Thus, these three proteins appear to exist in a ternary complex in intact brain, suggesting that they may interact physiologically.

DMT1 is the only known iron importer in the cell, and since PAP7 and Dexras1 binds to DMT1, we wondered whether Dexras1 and PAP7 influence iron homeostasis. Using HEK 293T cells, which contain very low levels of PAP7, we show that over-expression of wild-type Dexras1 very modestly augments NTBI uptake, which is substantially enhanced by co-transfection with PAP7 (Figure 15). Thus, PAP7 is required for robust influence of Dexras1 on iron uptake. The action of Dexras1 on iron uptake derives from its GTPase actions, as a constitutively GTPase active form of Dexras1, with a mutation of alanine-178 to valine (A178V), increases iron uptake more than native Dexras1 in the presence or absence of PAP7.

As NO *S*-nitrosylates and activates Dexras1, we examined effects of NO donors on iron uptake. Treatment of undifferentiated PC12 cells with *S*-nitrosoglutathione (GSNO) results in *S*-nitrosylation of Dexras1 (Figure 16A) and enhances NTBI uptake in a concentration dependent

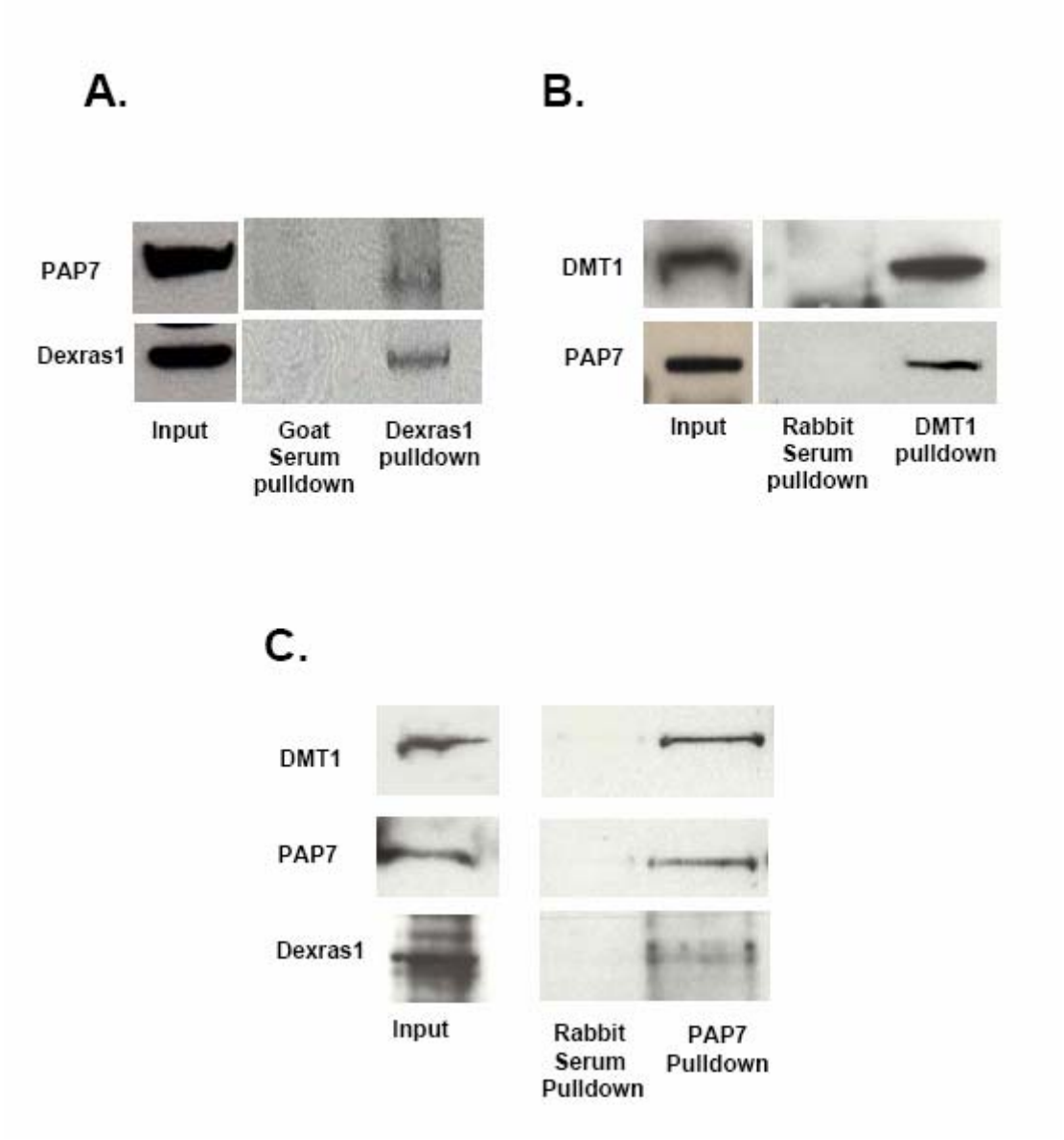


**Figure 14:** Endogenous interaction of Dexras1 and PAP7 and DMT1

(A) Immunoprecipitation experiments were performed using undifferentiated PC12 cells with a Dexras1 antibody, showing co-precipitation of PAP7. (B) Immunoprecipitation experiments were performed using undifferentiated PC12 cells with a DMT1 antibody, showing co-precipitation of PAP7. (C) Immunoprecipitation experiments were performed using mouse brain lysate with a PAP7 antibody, showing simultaneous immunoprecipitation of Dexras1 and DMT1, suggesting that the three proteins exist in a ternary complex in the cell.

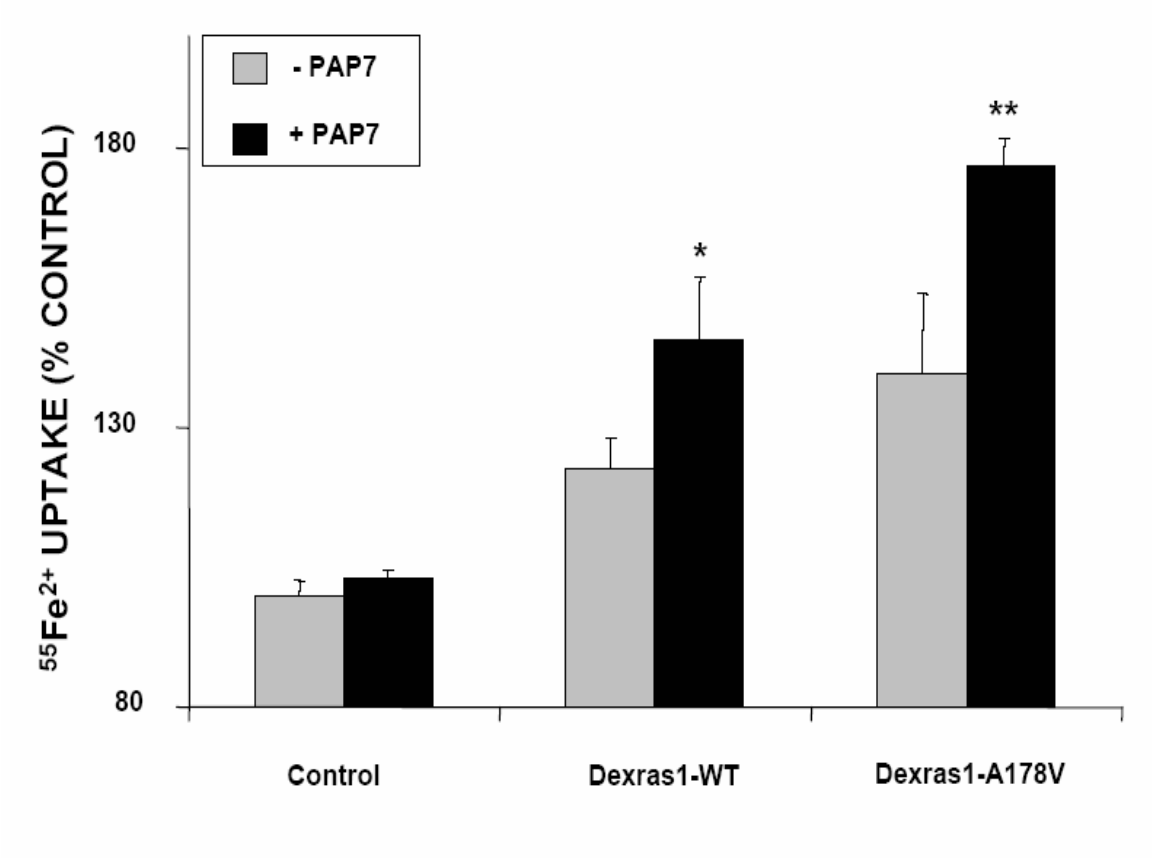


**Figure 15:** Over-expression of Dexras1 and PAP7 increases NTBI uptake

HEK 293T cells were transfected with Dexras1 or Dexras1-A178V in the presence or absence of PAP7. NTBI uptake was measured as described in the Materials and Methods. (*, $p<0.05$, **, $p<0.01$). Dexras1 and PAP7 together increase NTBI uptake, which is further augmented by the constitutively active Dexras1 mutant, A178V. (NTBI uptake experiments were repeated three times, each sample in triplicate. Comparison with two-tailed student's *t*-test; error bars represent SEM).

manner (Figure 16B). Other NO donors, sodium nitroprusside (SNP)(Figure 16C) and DETANONOate (Figure 16D), elicit similar effects. As Dexras1 activation by *S*-nitrosylation involves cysteine-11 (Jaffrey et al., 2002), we examined the effects of a Dexras1 cysteine mutant (C11S) on NO-mediated iron uptake. The C11S mutant still interacts with PAP7 (Figure 17A), however, in HEK 293T ells transfected with PAP7 and wild-type or C11S mutated Dexras1, the C11S mutation abolishes GSNO activation of NTBI uptake (Figure 17B).

To determine whether Dexras1 is required for NO-mediated iron uptake, we sought to deplete Dexras1. Since it is difficult to transfect primary cortical neurons, we employed undifferentiated PC12 cells, which contain endogenous Dexras1, PAP7 and DMT1. We successfully depleted Dexras1 in PC12 cells using vector-based RNA interference (Figure 18A). While GSNO augments NTBI uptake in control PC12 cells, it fails to increase uptake in the Dexras1-depleted cells (Figure 18B).

Previous work from our lab showed that Dexras1 is activated by glutamate-NMDA neurotransmission acting via nNOS and NO. We examined the influence of NMDA upon iron uptake in primary cortical neuronal cultures. These experiments were conducted in a media that contained about

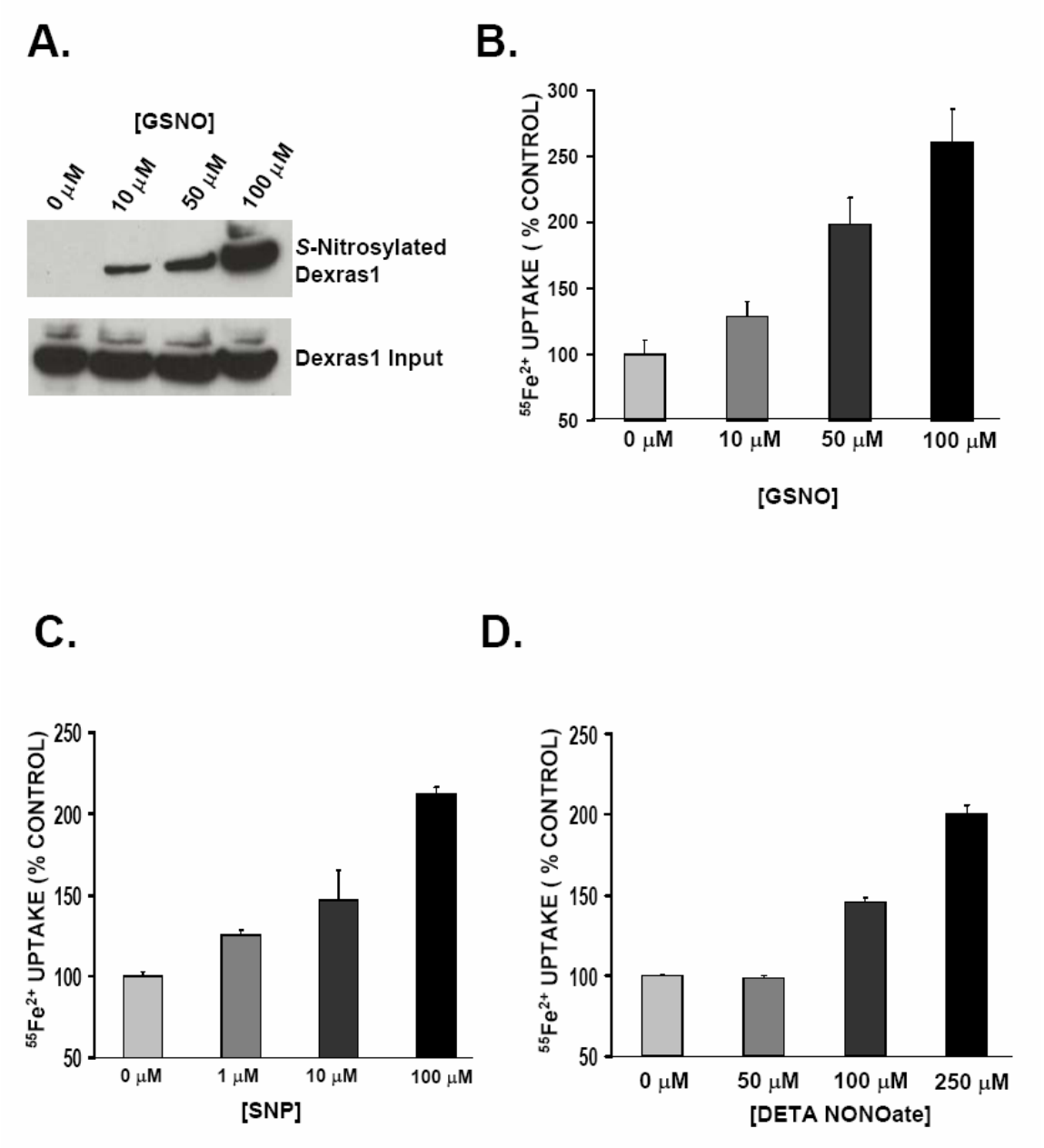


**Figure 16:** Dexras1 is *S*-nitrosylated and NTBI uptake is increased in PC12 cells after treatment with NO donors.

(A) Dexras1 in undifferentiated PC12 cells is S-nitrosylated by GSNO in a concentration-dependent manner (B) GSNO treatment for 3h leads to a concentration-dependent increase NTBI uptake in undifferentiated PC12 cells, as does (C) SNP for 1h and (D) DETA NONOate for 4h. (All NTBI uptake experiments were repeated three times, each sample in triplicate. Comparison with two-tailed student's *t*-test; error bars represent SEM).

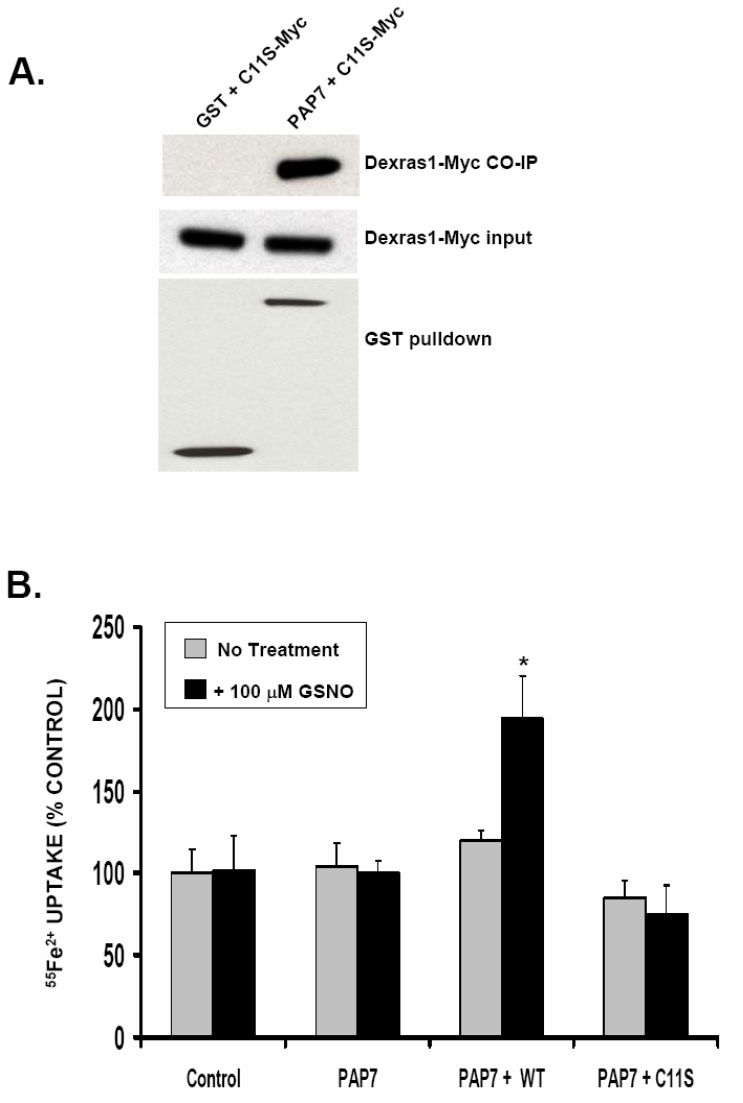


**Figure 17**: NO-mediated NTBI uptake is mediated by *S*-nitrosylation of Dexras1

(A) HEK 293T cells were transfected with GST or GST-PAP7 Dexras1-C11S-myc, a nitrosylation-dead mutant, which is able to bind specifically to PAP7. (B) HEK 293T cells were transfected with PAP7 and either wild-type Dexras1 or the C11S mutant. After transfection, the cells were treated with 100 μM GSNO for 3h and NTBI uptake was measured (*, $p<0.01$). GSNO treatment up-regulates NTBI uptake in cells containing wild-type Dexras1, but not the C11S mutant. (NTBI uptake experiments were repeated three times, each sample in triplicate. Comparison with two-tailed student's *t*-test; error bars represent SEM).

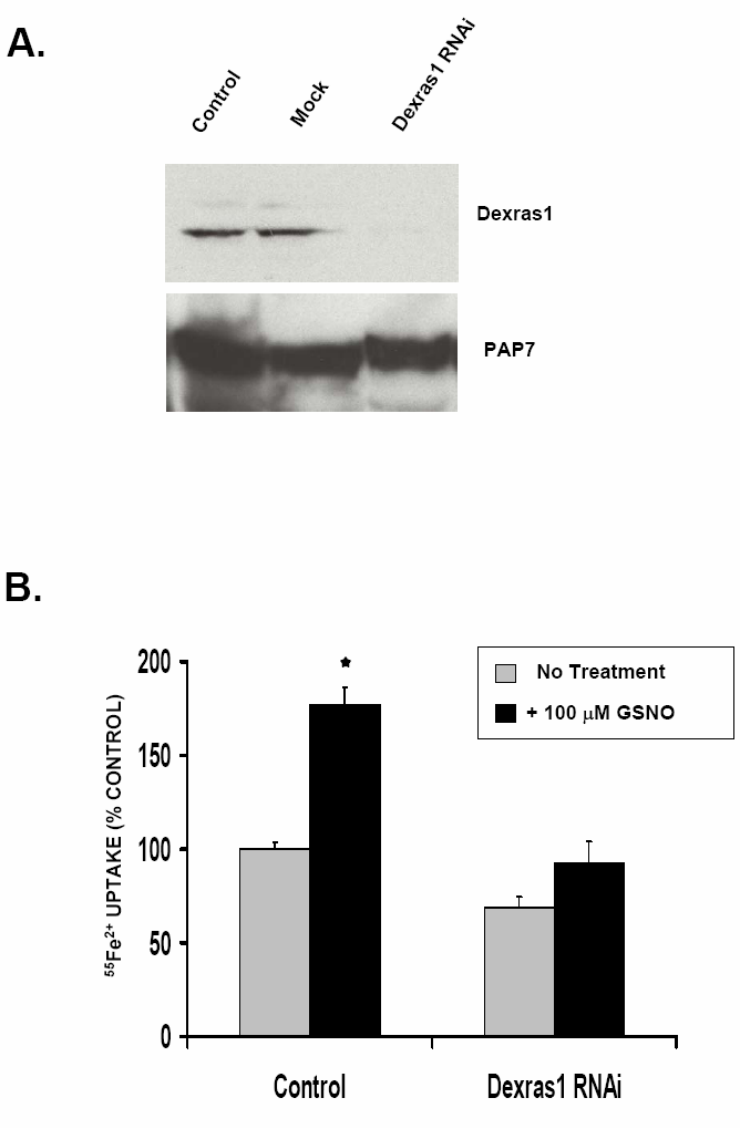


**Figure 18:** Depletion of Dexras1 in PC12 cells abolishes NO-mediated NTBI uptake

(A) Undifferentiated PC12 cells were transfected with either control RNAi or Dexras1 RNAi (mock is untransfected). Dexras1 protein levels was fully depleted after transfection with Dexras1 RNAi, but not in control or mock-transfected cells (B) Undifferentiated PC12 cells were transfected with either control RNAi or Dexras1 RNAi, treated with 100 μM GSNO for 3h and NTBI uptake was measured (*, $p<0.01$). GSNO treatment up-regulates NTBI uptake in control cells, but not in cells depleted of Dexras1. (All NTBI uptake experiments were repeated three times, each sample in triplicate. Comparison with two-tailed student's *t*-test; error bars represent SEM).

0.8 mM magnesium, a concentration which would be too low to impair NMDA neurotransmission and would not be expected to compete with iron uptake by DMT1 (Nowak et al., 1984; Picard et al., 2000). NMDA treatment increases NTBI uptake in a concentration-dependent manner (Figure 19A), with the effects blocked by pre-treatment with the NMDA antagonist MK801(+) (Figure 19C). NMDA fails to increase NTBI uptake in cultures from nNOS knockout mice, showing that nNOS and NO are required for NMDA-mediated NTBI uptake (Figure 19B and 19C). NMDA transmission augments calcium conductance though the NMDA receptor, which fits with the ability of the calcium ionophore, ionomycin, to stimulate NTBI uptake, and effect abolished in nNOS knockout cultures (Figure 19B).

*Part 1.4: Physiological and Pathophysiological Relevance of Dexras1 Regulation of Iron Uptake*

Iron taken up through the Tf-mediated iron uptake pathway is used for physiological processes, such as heme synthesis. We examined whether the effects seen on NTBI uptake were mimicked in the Tf-iron uptake pathway. Using cortical neurons, we observed a concentration dependent uptake in Tf-iron uptake after NMDA treatment (Figure 20A). Tf-mediated iron uptake is also augments by treatment with

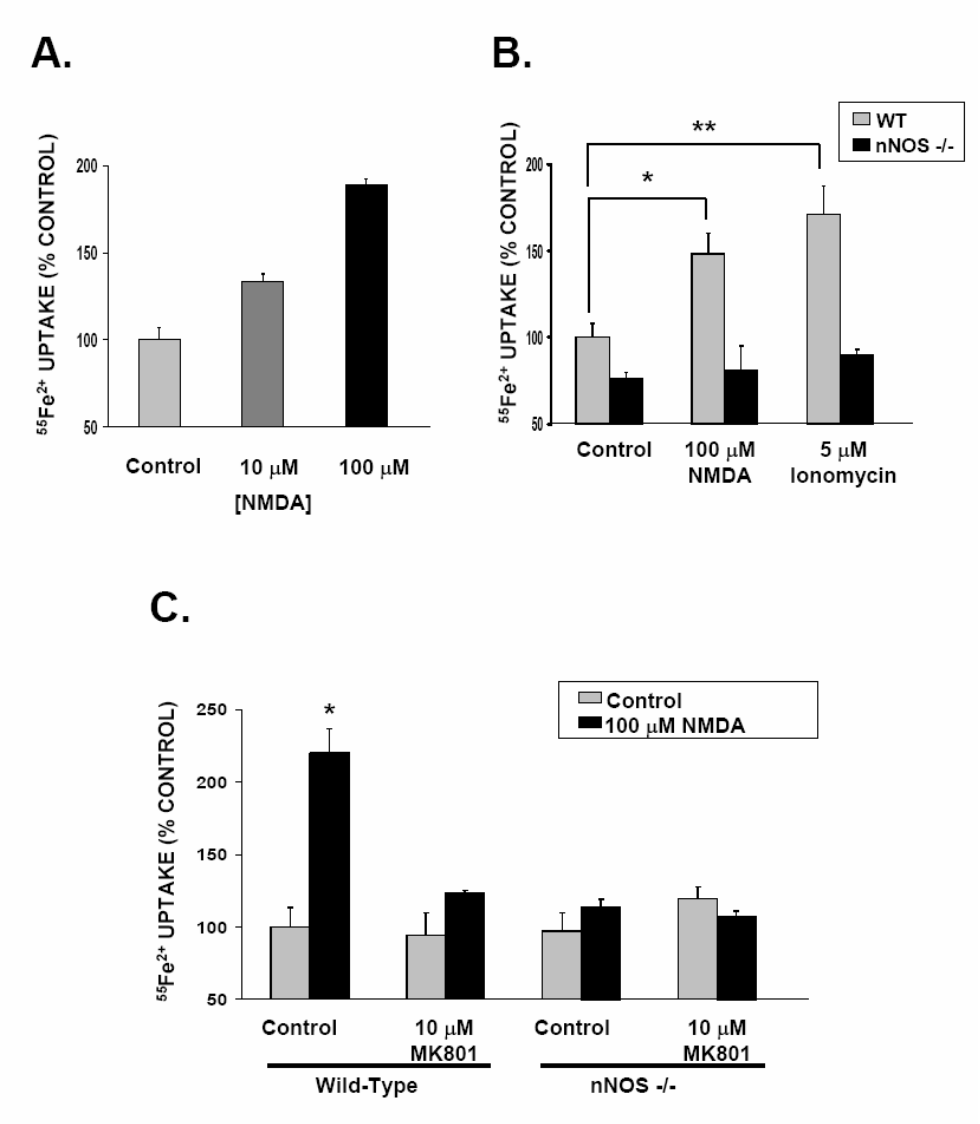


**Figure 19:** Glutamate-NMDA neurotransmission increases NTBI uptake, which is abolished in nNOS knockout mice

(A) NMDA stimulation increases NTBI uptake in primary cortical neurons in a concentration-dependent manner. (B) NTBI uptake in primary cortical neurons is increased by both NMDA stimulation and ionomycin treatment, a calcium ionophore. This up-regulation is not seen in primary cortical neurons from nNOS knockout mice (*, $p<0.05$, **, $p<0.01$) and (C) is abolished by pre-treatment with MK801, an NMDA receptor antagonist (*, $p<0.005$). (All NTBI uptake experiments were repeated three times, each sample in triplicate. Comparison with two-tailed student's *t*-test; error bars represent SEM).

ionomycin (Figure 20B), effects abolished by pre-treatment with MK801(+) or in nNOS knockout cultures (Figure 20B and 20C). To assess the physiological relevance of NMDA-stimulated iron uptake, we monitored $^{55}Fe$ incorporation into heme in cortical cultures treated with NMDA. NMDA stimulation markedly increases the rate of heme biosynthesis (Figure 21A). Interestingly, when we measure the total heme content in brains of either wild-type or nNOS knockout mice, the nNOS knockout mice had a 25% decrease in total heme as compared to their wild-type counterparts, regardless of the age of the mice (Figure 21B).

We wondered whether the stimulation of iron uptake by NMDA neurotransmission might have pathophysiological consequences, as over-activation of NMDA receptors leads to neurotoxicity which has been implicated in vascular stroke and neurodegenerative diseases (Choi, 1994). In cerebrocortical cultures, a concentration of 0.3 mM NMDA is well established to elicit neurotoxicity (Dawson et al., 1991; Koh and Choi, 1988). We have verified that this concentration of NMDA elicits a major augmentation in NTBI uptake (Figure 22A). As neurotoxicity is associated with a pronounced increase in reactive oxygen species (ROS), we monitored ROS formation utilizing a dye that selectively

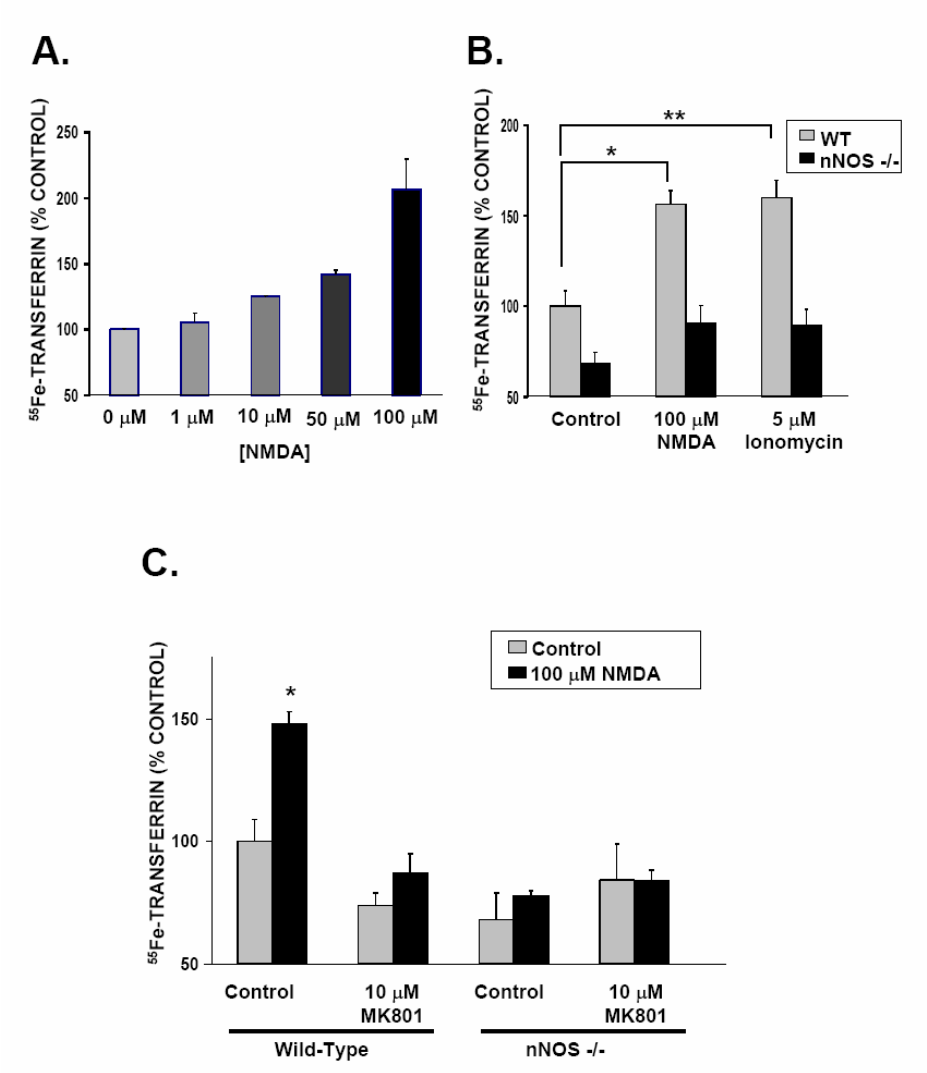


**Figure 20**: Glutamate-NMDA neurotransmission increases Tf-iron uptake, which is abolished in nNOS knockout mice

(A) Tf-mediated iron uptake is increased in a dose-dependent manner with NMDA treatment in primary cortical neurons. (B) Tf-mediated iron uptake is increased by both NMDA and ionomycin (*, $p<0.01$, **, $p<0.01$). This up-regulation is not seen in primary cortical neurons from nNOS knockout mice and (C) is abolished by pre-treatment with MK801 (*, $p<0.005$). No increase in uptake is seen in neurons from nNOS knockout mice. (All Tf uptake experiments were repeated three times, each sample in triplicate. Comparison with two-tailed student's *t*-test; error bars represent SEM).

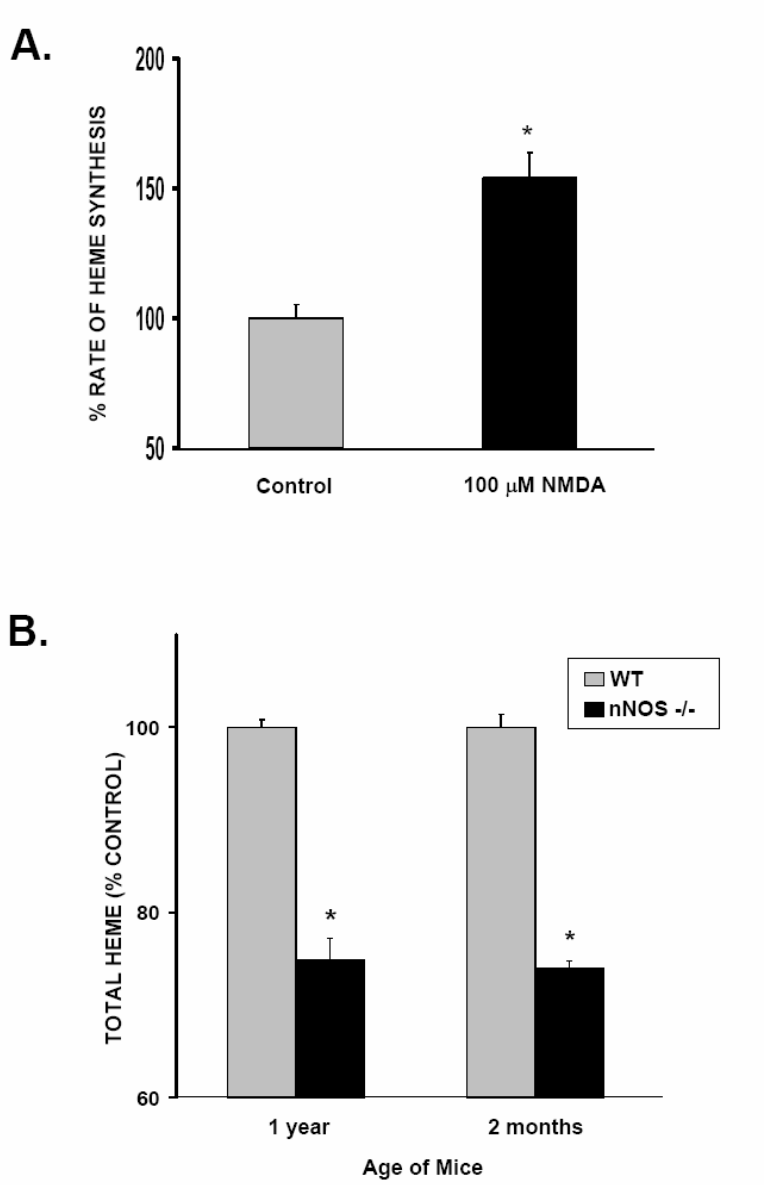


**Figure 21:** Physiological Relevance of Iron Uptake

(A) Rate of heme biosynthesis was measured using incorporation of $^{55}Fe$ into heme and was increased after NMDA treatment (*, $p<0.01$). (B) Total heme content of the brains of wild-type and nNOS knockout mice was measured using the HemoQuant assay, showing that there is a significant decrease in heme in the nNOS knockout mice, regardless of the age of the mice (*, $p<0.01$). (All experiments were repeated three times, each sample in triplicate. Comparison with two-tailed student's *t*-test; error bars represent SEM).

detects hydroxyl free radicals (Setsukinai et al., 2003). These radicals predominantly arise from the Fenton reaction that typically reflects iron interacting with hydrogen peroxide to form hydroxyl free radicals. Treatment with 0.3 mM NMDA elicits a 3.5 fold augmentation in hydroxyl free radical formation (Figure 22B). To determine whether this increase is caused by the Fenton reaction elicited by iron, we employed SIH (salicylaldehyde isonicotinoyl hydrazone), a selective cell permeable iron chelator. SIH treatment abolishes the increase in hydroxyl free radicals caused by NMDA, implying that the free radical formation arises from the iron whose influx is stimulated by NMDA (Figure 22B).

We also examined whether this influx of iron is involved in NMDA-mediated neurotoxicity. Preliminary experiments using primary hippocampal cultures show that 0.3 mM NMDA treatment leads to a significant amount of neuronal cell death after 24 hours. This phenomenon is attenuated by pre-treatment with either MK801(+), NOS inhibitors, SIH or DFO (desferroxamine), a cell non-permeable iron chelator (Figure 23). This suggests that iron could be the effector molecule of NMDA-induced cell death, working through nitric oxide.

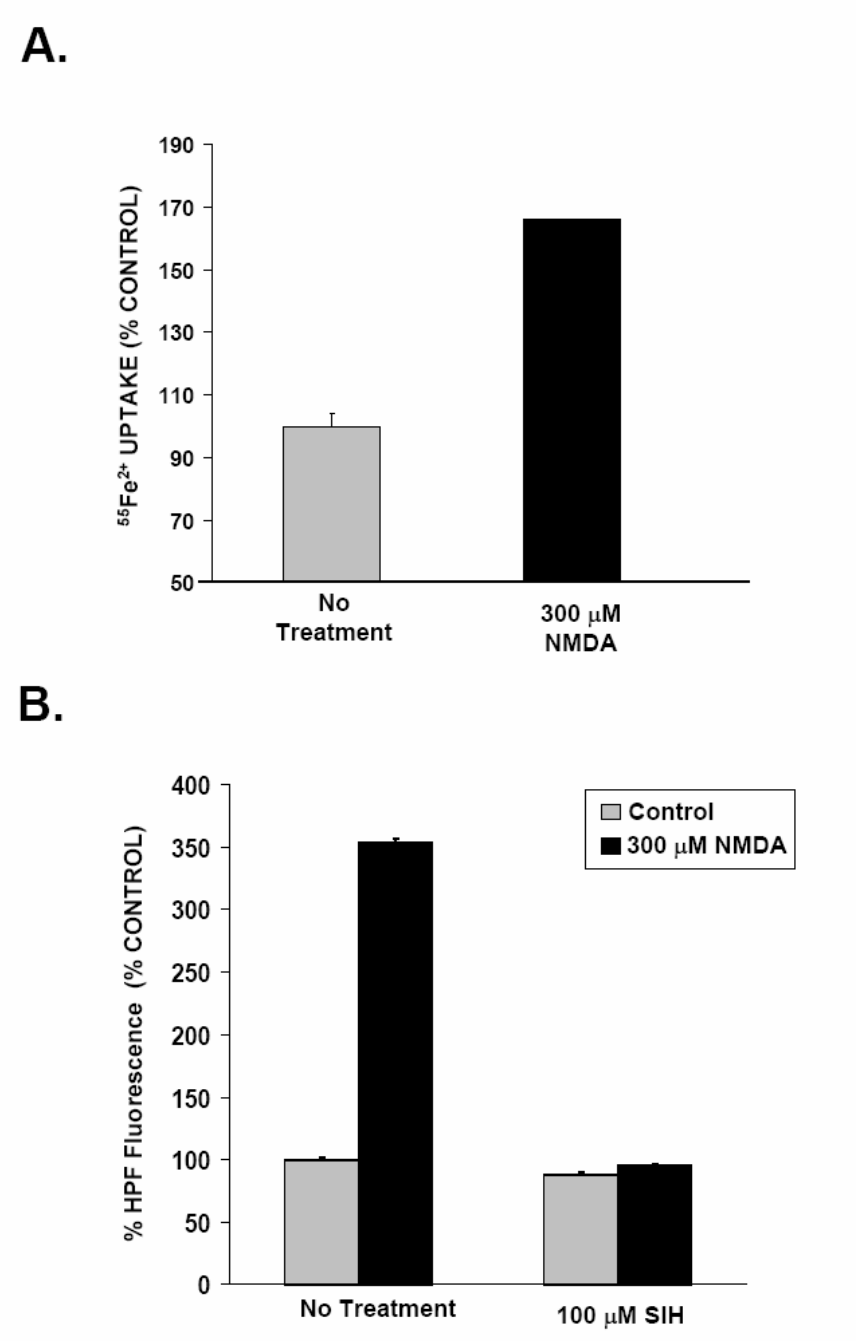


**Figure 22:** Excitotoxic concentration of NMDA stimulates iron uptake and formation of reactive oxygen species

(A) NTBI uptake is significantly increased after treatment with an excitotoxic concentration of NMDA. (B) An increase in HPF fluorescence was observed after treatment with NMDA, indicating an increase in ROS formation. This increase was abolished with pre-treatment of the neurons with SIH.

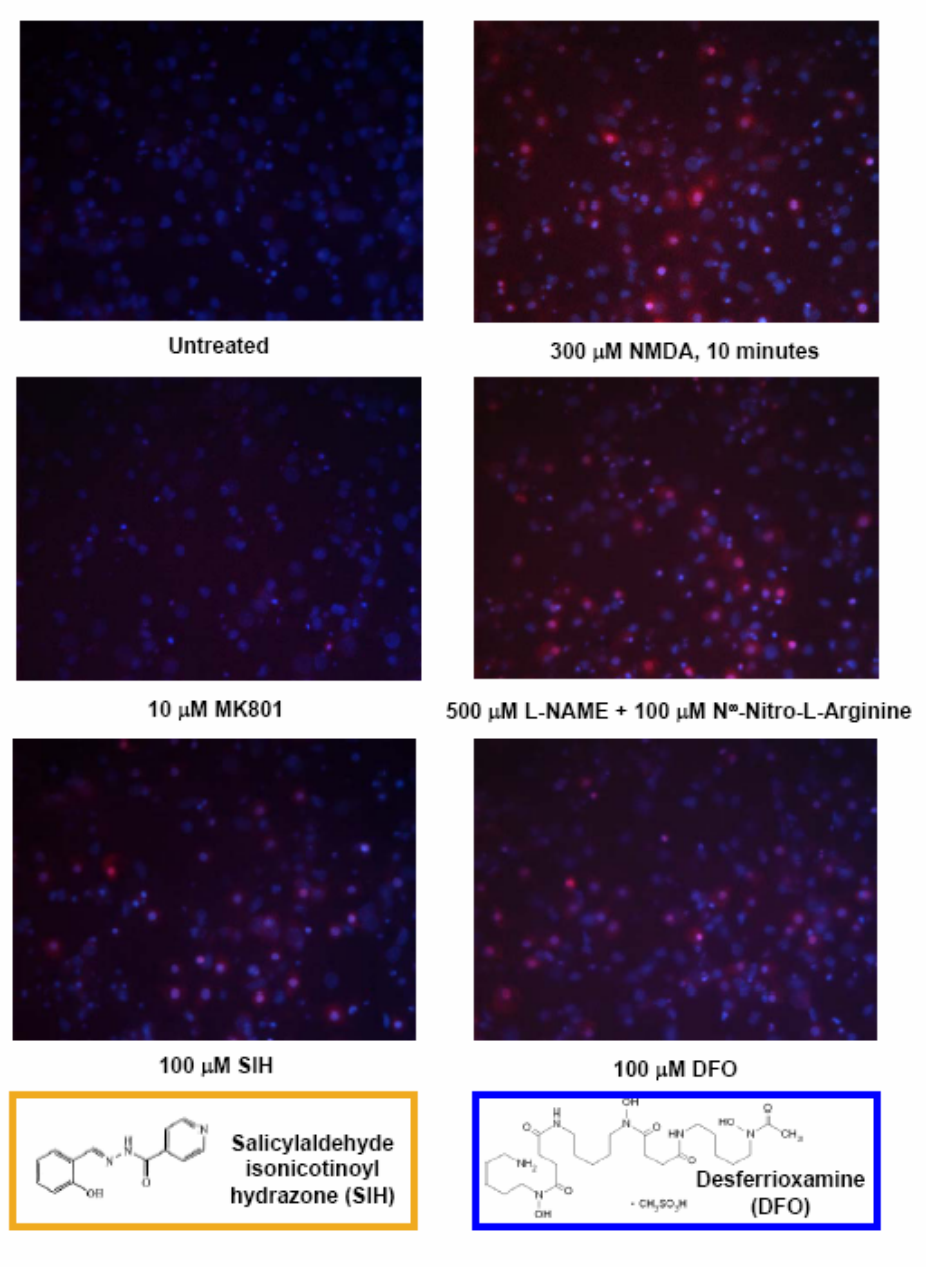


**Figure 23:** Iron chelators attenuate NMDA-induced cell death

Primary hippocampal neurons were pretreated for three hours with the following: 10 μM MK801(+), an NMDA receptor antagonist, 500 μM L-NAME + 100 μM $N^{\omega}$-Nitro-L-Arginine, nNOS inhibitors, 100 μM Salicylaldehyde isonicotinoyl hydrazone (SIH), a cell permeable iron chelator and 100 μM Desferrioxamine, a cell non-permeable iron chelator. The solutions were removed and the cells were treated with 300 μM NMDA for 10 minutes, then the cells were incubated for 24 hours before cell viability was assessed by propidium iodide staining. Pre-treatment of neurons with iron chelator significantly reduced cell death induced by NMDA.

We wondered whether the influx of iron was specific to NMDA and NO-induced cell death. Using undifferentiated PC12 cells, we treated them with 0.5 mM GSNO, 0.2 mM $H_2O_2$ or 1 μM staurosporine (STS) overnight and observed an increase in NTBI uptake only with GSNO treatment (Figure 24A), indicating that not all agonists of cell death stimulate iron uptake. To examine whether Dexras1, which we have already shown influences NO-mediated iron uptake, participates in NO-mediated cell death, we depleted Dexras1 from PC12 cells using RNA inteference, then treated with various cell death stimulants and measured cell viability. In cells depleted with Dexras1, GSNO-mediated cell death was attenuated, while cell death caused by $H_2O_2$ or STS was unaffected (Figure 24B).

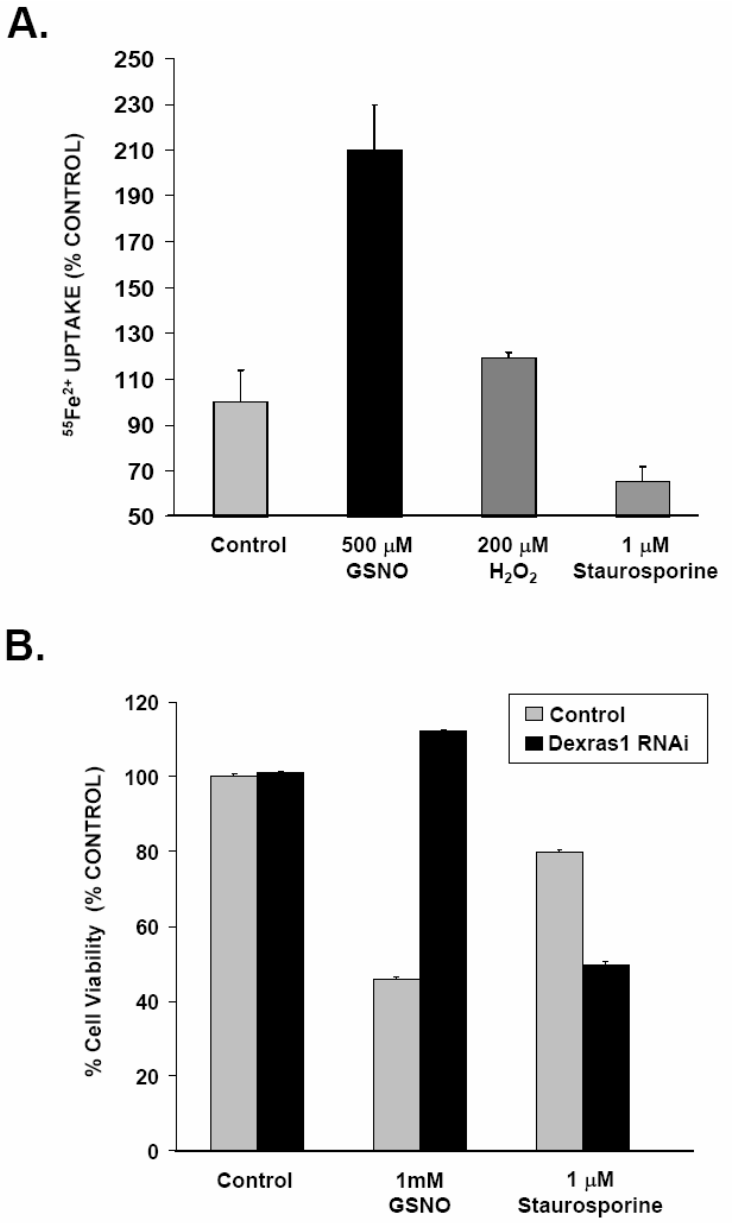


**Figure 24:** NO-induced cell death is mediated by Dexras1

(A) Undifferentiated PC12 cells were treated overnight with various stimulators of cell death and NTBI uptake measured. GSNO stimulated iron uptake, while $H_2O_2$ and staurosporine did not. (B) PC12 cells were double transfected with either control or Dexras1 RNAi, then treated overnight with GSNO or staurosporine. Cell viability was measured using the MTT assay and normalized to control. Depletion of Dexras1 rescued GSNO-mediated cell death, while staurosporine-induced cell death was unaffected.

*Part 2: Characterization of Rhes and its interaction with PAP7*

Little is known about Rhes, except that it is enriched in the striatum and that it is transcriptionally upregulated by thyroid hormone (Falk et al., 1999; Vargiu et al., 2001). Dexras1 is known to be regulated by NO, but no studies about NO regulation of Rhes have yet been undertaken. We have produced an antibody to Rhes and have examined its protein expression levels in the whole body and the brain. The antibody is specific to Rhes, and does not detect either GST or Dexras1 (Figure 25A). Rhes is localized to the brain, adrenal, lung, spleen and testis (Figure 25B) Within the brain, it is localized to the cerebellum, cortex, hippocampus and striatum (Figure 25C). Rhes is expressed at high levels in PC12 and COS7 cells, as well as the mouse M213-2O striatal cell line, and the two neuroblastoma cells lines N2a and N1E-11, but not in HEK 293T or HeLa cells (Figure 25D).

As Rhes and Dexras1 share about 68% homology, we wondered if it was also regulated in a similar manner by nitric oxide and *S*-nitrosylation. Using the biotin switch assay (Jaffrey and Snyder, 2001), we transfected HEK 29T cells with myc-tagged Rhes and examined for the increase in the biotin signal after treatment with GSNO. While a

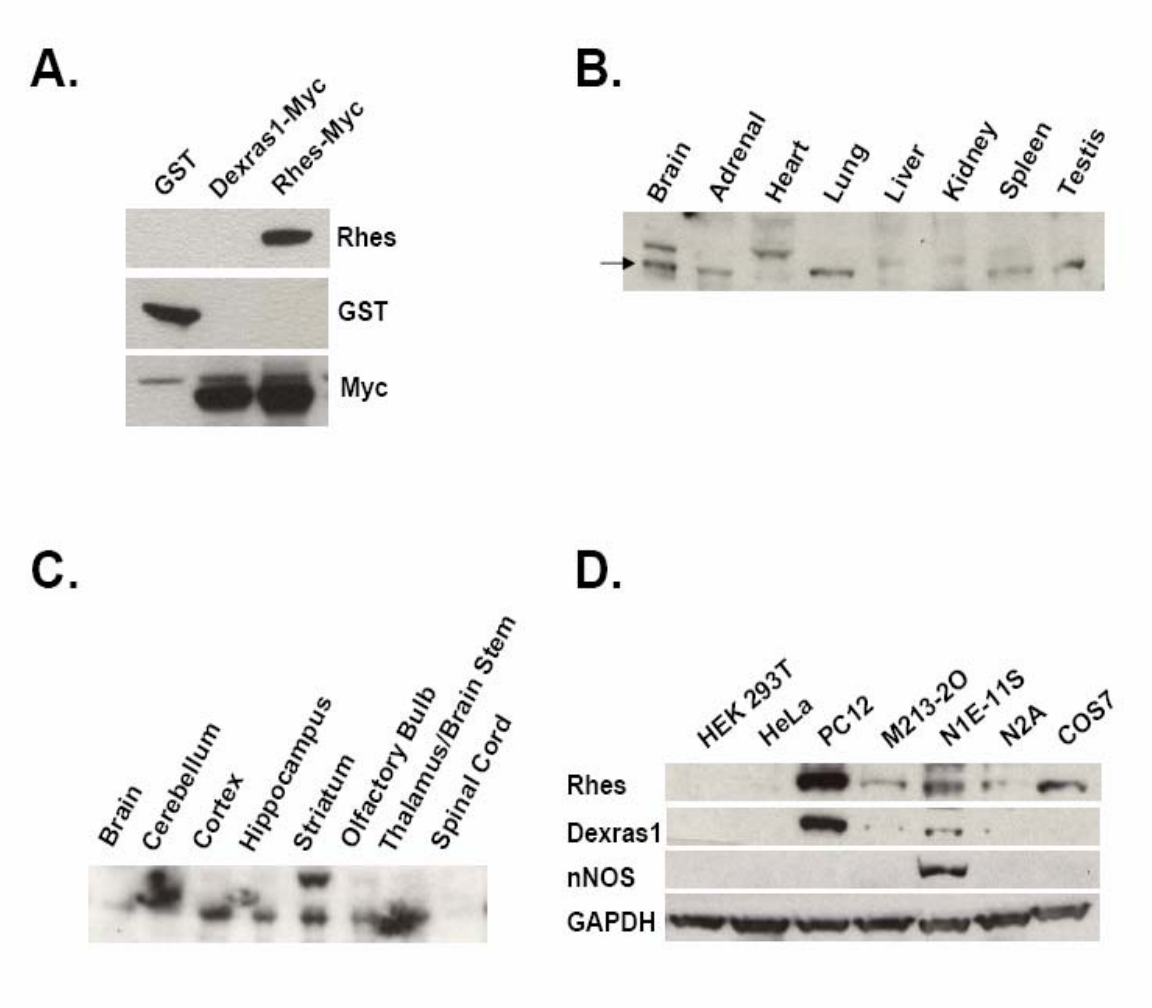


**Figure 25:** Localization of Rhes

(A) An antibody to Rhes was generated and was shown to be specific to Rhes using overexpressed protein in HEK 293T cells. (B) Using mouse tissue lysates, Rhes is shown to be localized to the brain, adrenal, lung, liver and testis. (C) Rhes is localized to various regions of the brain, including cerebellum, cortex, hippocampus, striatum and the olfactory bulb. (D) Rhes is localized to various cell lines, including PC12, N2a, N1E-11, COS7 and M213-2O cells, but not HEK 293T or HeLa cells, while Dexras1 is present in only PC12 and N2a cells and nNOS is only present in N1E-11 cells.

significant increase in biotin is seen after GSNO treatment of Dexras1, there is no increase in the biotin signal with Rhes, indicating that it is not nitrosylated (Figure 26).

We also examined whether Rhes can also bind to PAP7. We transiently transfected GST-PAP7 and Rhes-Myc in HEK 293T cells, pulled down with glutathione sepharose and reveal Rhes and PAP7 specifically interact with one another (Figure 27A), even in the presence of 10 mM EDTA (Figure 27B). Using deletion constructs of PAP7, we narrowed down the binding site of Rhes to amino acids 414-424 of PAP7, the same stretch of amino acids as Dexras1 (data not shown). We speculate, due to the high homology between Dexras1 and Rhes, that the binding region of PAP7 to Rhes will be the same as that of Dexras1, between amino acids 96-101.

We examined whether Rhes has a similar influence on iron uptake as that of Dexras1. Over expression of Rhes and PAP7 in HEK 293T cells significantly augments both NTBI (Figure 28A) and Tf-mediated iron uptake (Figure 28B). Though Rhes does not appear to be regulated by NO, perhaps it is involved in the regulation of iron uptake in other pathways or by thyroid hormone.

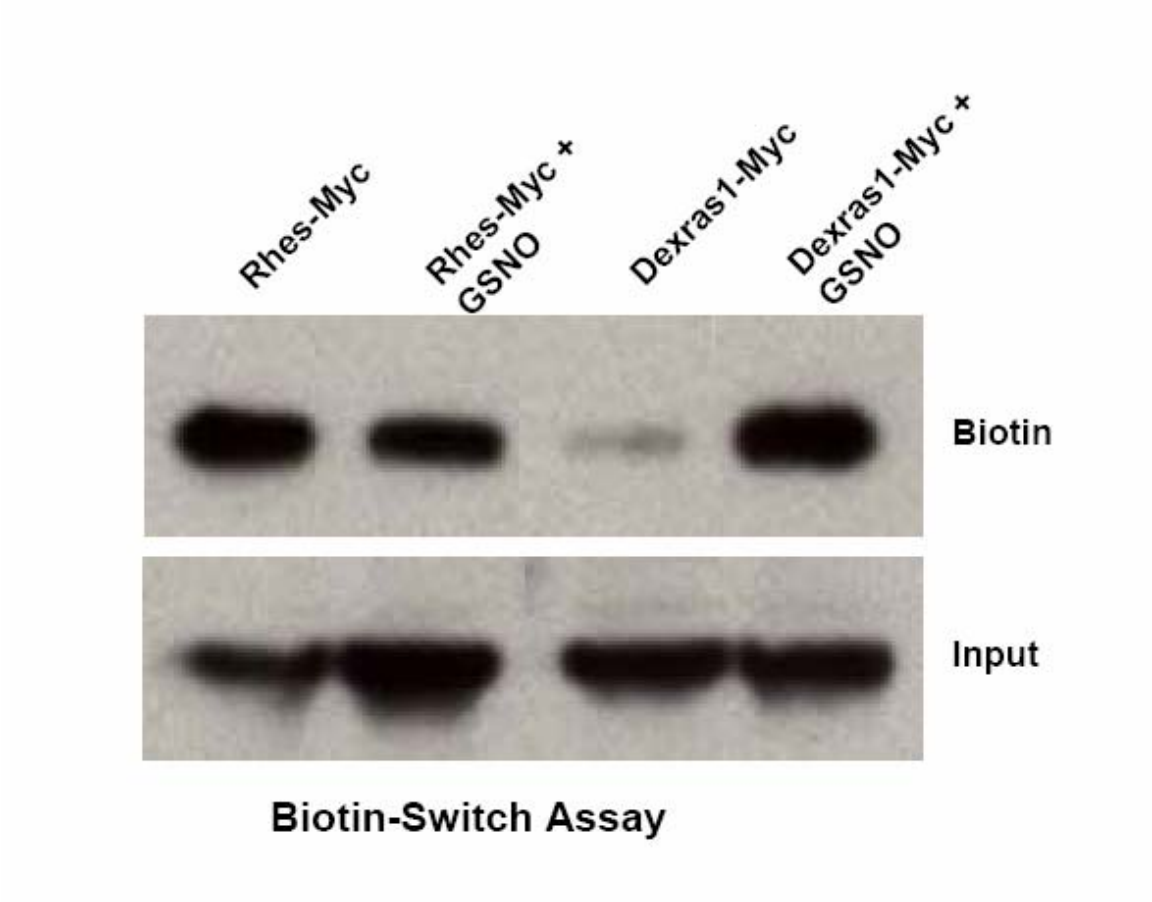


**Figure 26:** Rhes is not nitrosylated

Myc-tagged constructs of Rhes and Dexras1 were transfected into HEK 293T cells. After 48 hours, cells were treated with 100 μM GSNO for 3 hours, and the biotin switch assay was performed to assess the nitrosylation state of the protein. While there is an increase in the biotin signal after GSNO treatment of Dexras1, no increase in signal is seen in Rhes, indicating that Rhes is not nitrosylated.

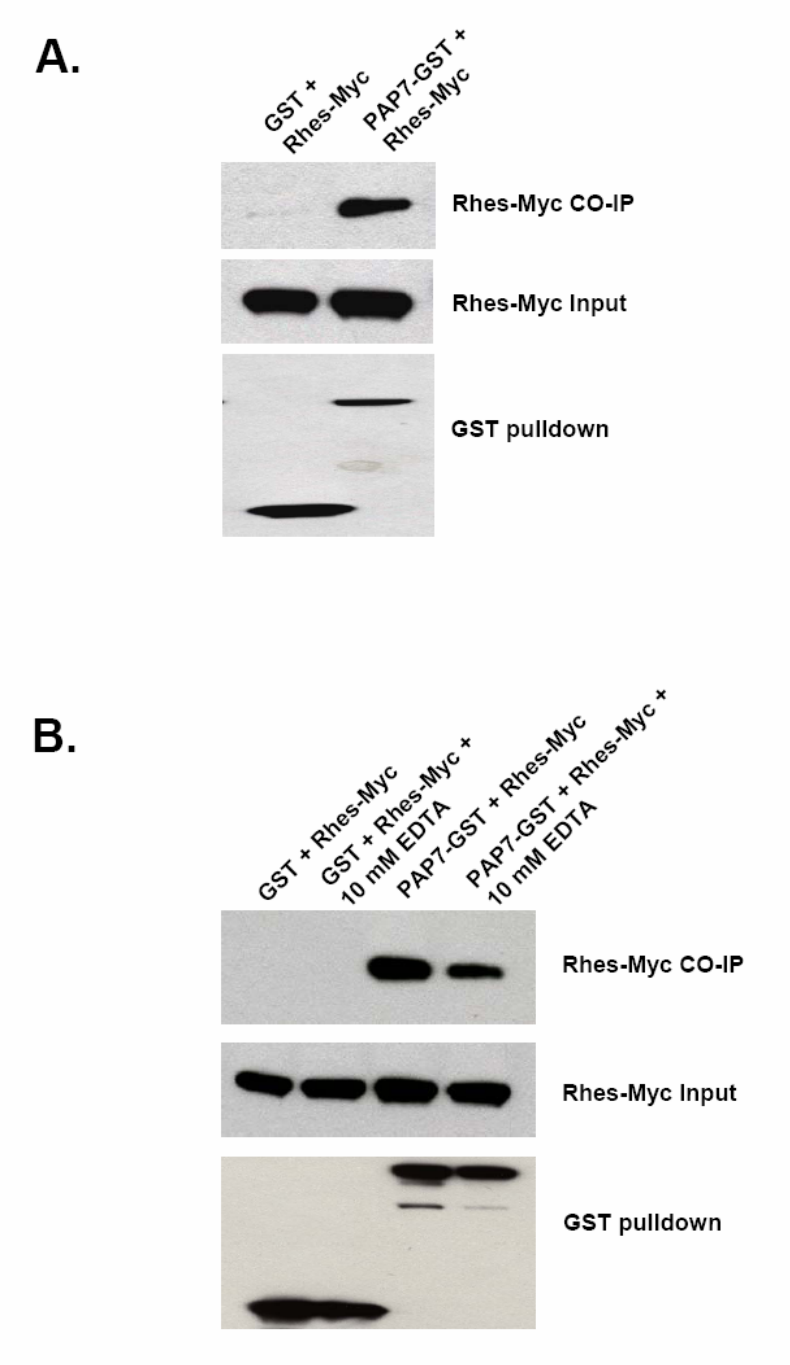


**Figure 27:** Rhes binds to PAP7

(A) HEK 293T cells were transfected with GST or GST-PAP7 and myc-tagged Rhes. GST pulldown experiments show that Rhes specifically binds to PAP7 and that (B) Rhes is still able to bind to PAP7 in the presence of 10 mM EDTA, which would render Rhes inactive.

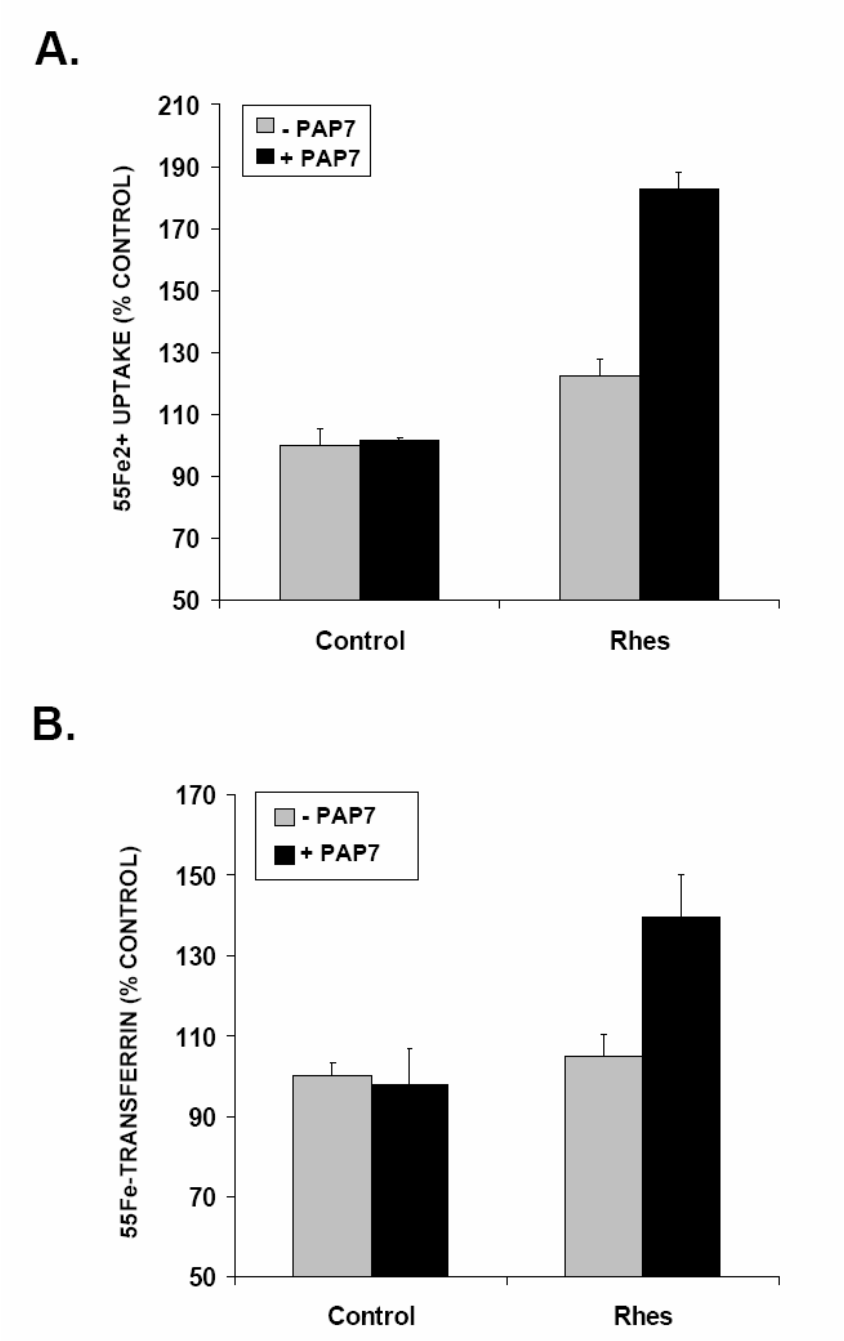


**Figure 28:** Rhes and PAP7 over-expression stimulates both NTBI and Tf-mediated iron uptake

(A) HEK 293T cells were transfected with Rhes in the presence or absence of PAP7. Rhes and PAP7 together increase NTBI uptake. (B) HEK 293T cells were transfected with Rhes in the presence or absence of PAP7. Rhes and PAP7 together increase Tf-mediated iron uptake.

*Part 3: Phosphorylation of Dexras1 and Rhes by PKA*

PAP7 was also identified to interact with the regulatory subunit of PKA (Li et al., 2001), though its effects on PKA are unknown. PAP7 itself is not phosphorylated by PKA, so we wondered whether PKA has any effects on Dexras1 and Rhes with PAP7 acting as a connector molecule between PKA and the two proteins. *In vitro* phosphorylation experiments show that both Dexras1 and Rhes are phosphorylated by PKA, an effect which is attenuated with treatment with H-89, a PKA inhibitor (Figure 29). Whether PAP7 plays a role in this phosphorylation, as well as the site of phosphorylation on both Dexras1 and Rhes, is currently unknown.

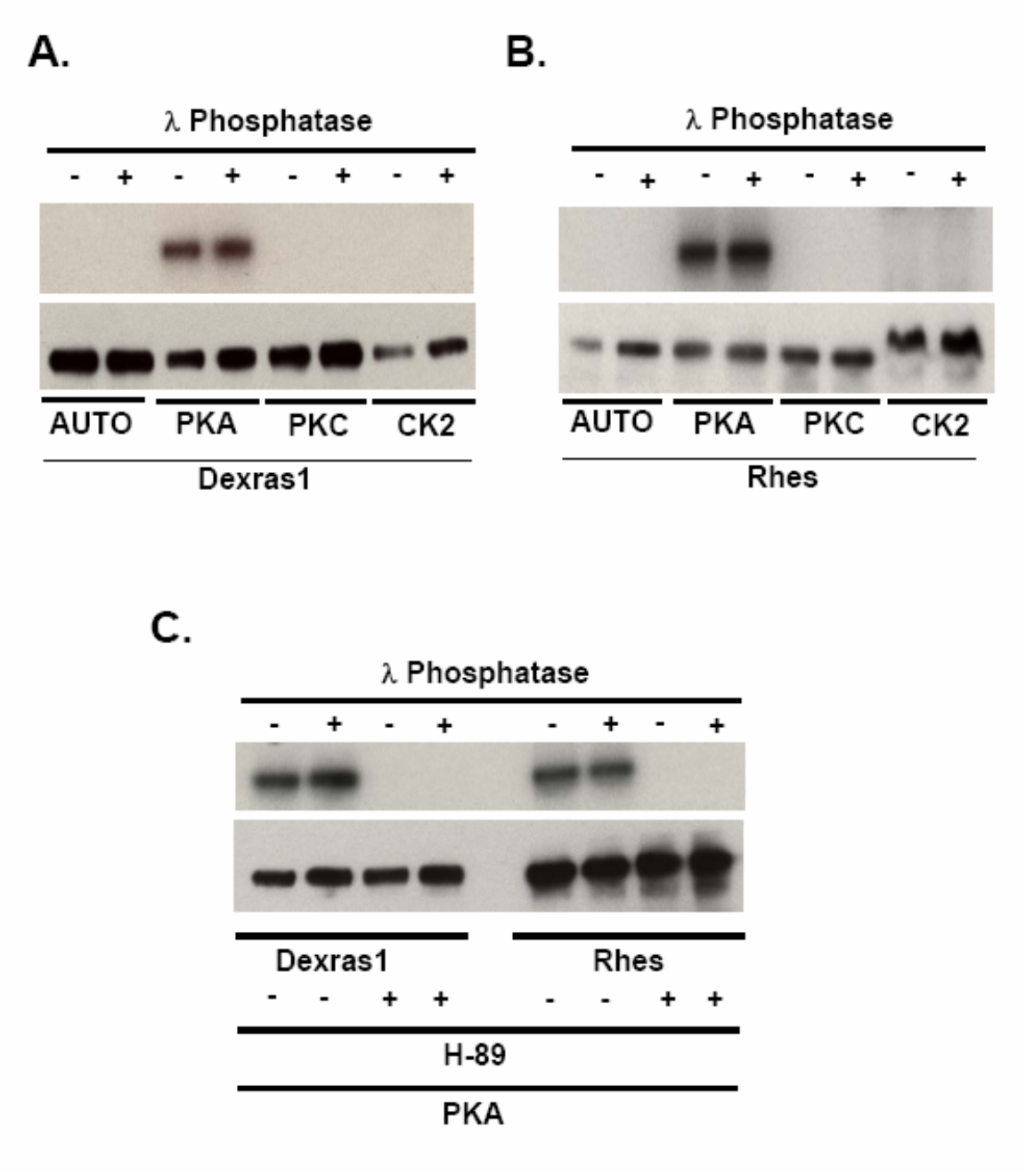


**Figure 29:** Dexras1 and Rhes are phosphorylated by PKA

(A) Myc-tagged Dexras1 and (B) Rhes was immunoprecipitated from transfected HEK 293T cells, treated with lambda phosphatase, then *in vitro* phosphorylated with various kinases, showing that PKA specifically and robustly phosphorylates PAP7. (C) This phosphorylation was significantly reduced with treatment of the samples with H-89, a PKA inhibitor.

*Part 4: Discussion*

In summary, we have identified a novel signaling cascade whereby neurotransmission regulates iron homeostasis (Figure 30). Glutamate, acting *via* NMDA receptors, activates nNOS to form NO, which leads to protein *S*-nitrosylation (Bredt and Snyder, 1994; Hess et al., 2005; Li et al., 2001). This modification activates Dexras1 which, by its link to PAP7, augments both Tf-mediated and NTBI uptake. PAP7 does not appear to have a direct influence on iron homeostasis, as its over-expression does not affect iron uptake, though it does potentiate Dexras1-induced enhancement of iron uptake. Instead, it presumably serves as a scaffold bringing Dexras1 into proximity to DMT1. Stimulation of iron uptake by Dexras1 reflects its GTPase activity, as constitutively active Dexras1 manifests enhanced activity in stimulating iron uptake. The influence of Dexras1 upon iron uptake is evidently the first example of a G-protein regulating an iron transporter.

The molecular mechanism whereby Dexras1 and its GTPase activity regulate signaling via PAP7 and DMT1 is unclear. We presume that Dexras1 influences DMT1 directly but cannot rule out some action upon PAP7. Conceivably, other reported activities of Dexras1 may participate. For instance, Dexras1 activates the ERK1,2 pathway in a pertussis toxin

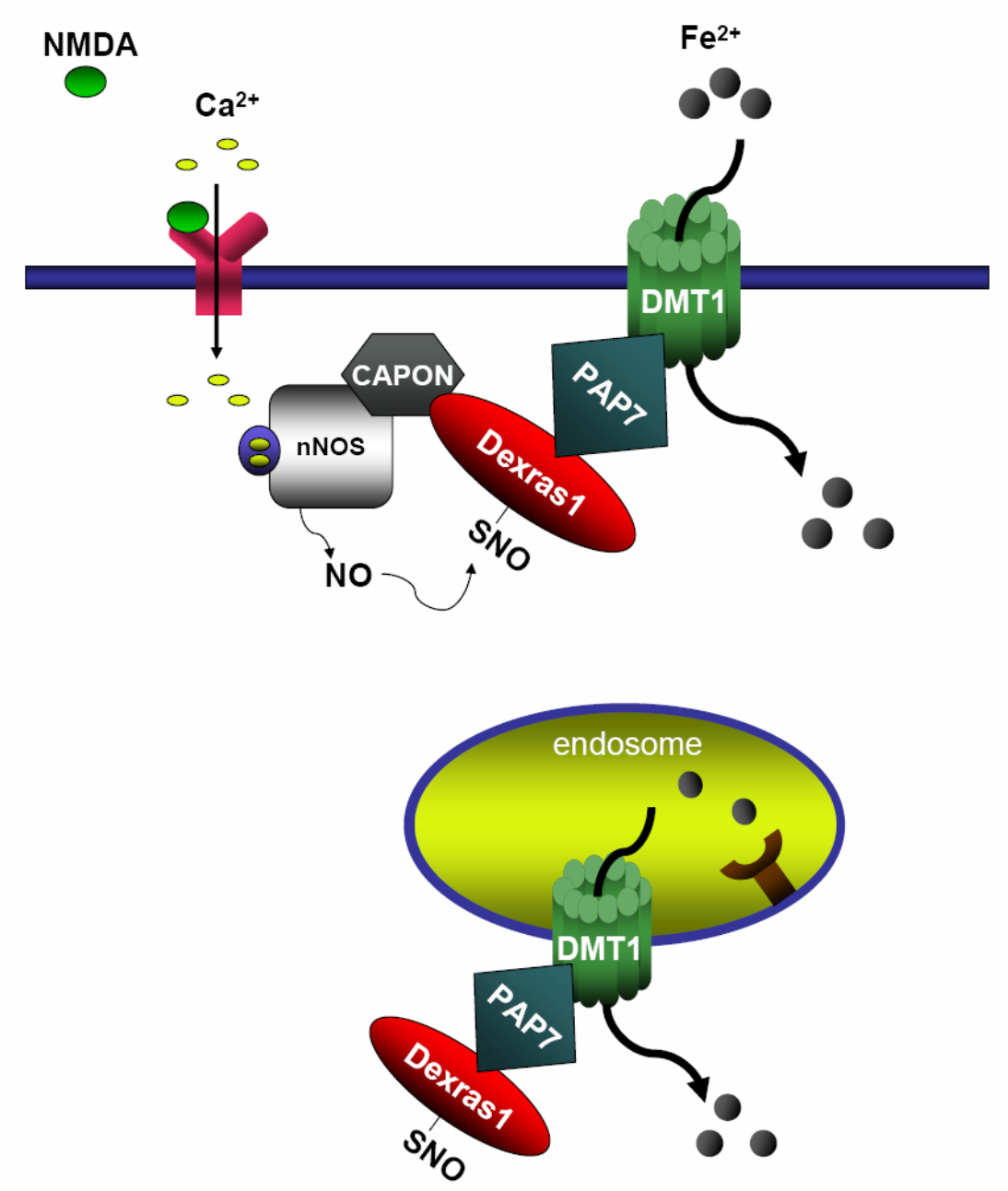


**Figure 30:** Dexras1, PAP7 and DMT1 mediate both NTBI and Tf-mediated iron uptake

A model of a signaling cascade whereby glutamate-NMDA neurotransmission regulates cellular iron homeostasis. Glutamate-NMDA stimulation leads to the activation of nNOS and, *via* the scaffolding protein CAPON, to *S*-nitrosylation of Dexras1, which interacts with PAP7 and DMT1 both at the endosome and the plasma membrane, thus influencing cellular iron uptake in the cell.

sensitive fashion (Cismowski et al., 2000). It impairs activation of G-protein coupled receptors that act via Gi, inhibiting adenylyl cylase (Graham et al., 2004). Functional relevance of those effects is suggested by its involvement in regulating circadian rhythm. Dexras1 expression cycles in a circadian fashion in the suprachiasmatic nucleus (Takahashi et al., 2003). Its genetic deletion reduces photic entrainment of circadian responses to glutamate-NMDA transmission (Cheng et al., 2004b). We have recently made a conditional Dexras1 knockout mouse and plan to examine whether it has any gross hematological defects. We postulate that the Dexras1 knockout mice will have defects in glutamate-NMDA induced iron uptake and wonder if neurons from these mice will be resistant to NMDA-induced excitotoxicity.

Rhes is a homologue of Dexras1 and is induced by thyroid hormone, an interesting contrast to the stimulation of Dexras1 by glucocorticoids (Falk et al., 1999; Vargiu et al., 2001). Rhes is selectively localized to the corpus striatum. It also binds to PAP7 and regulates iron uptake into the cell, but does not appear to be regulated by nNOS and NO in the same fashion as that of Dexras1. Perhaps Rhes regulates iron uptake stimulated through other yet unknown pathways.

Iron is required for many physiological processes, such as heme synthesis, mitochondrial oxidation reactions and DNA synthesis, but is toxic in excess, so that its cellular disposition is tightly regulated. Studies of iron in the brain have largely focused on its pathophysiological roles, with iron accumulation occurring in numerous neurodegenerative diseases. Heretofore, no influence of neurotransmission upon iron uptake has been reported. Our findings establish a physiologic role for glutamate neurotransmission is regulating iron uptake in the brain in a novel signaling cascade.

# REFERENCES


1. Abboud,S. and Haile,D.J. (2000). A novel mammalian iron-regulated protein involved in intracellular iron metabolism. J. Biol. Chem. *275*, 19906-19912.

2. Aisen,P. and Listowsky,I. (1980). Iron transport and storage proteins. Annu. Rev. Biochem. *49*, 357-393.

3. Anderson,B.F., Baker,H.M., Norris,G.E., Rice,D.W., and Baker,E.N. (1989). Structure of human lactoferrin: crystallographic structure analysis and refinement at 2.8 A resolution. J. Mol. Biol. *209*, 711-734.

4. Andrews,N.C. (1999). Disorders of iron metabolism. N. Engl. J. Med. *341*, 1986-1995.

5. Andrews,N.C. (2000). Iron homeostasis: insights from genetics and animal models. Nat. Rev. Genet. *1*, 208-217.

6. Bacon,B.R. and Britton,R.S. (1990). The pathology of hepatic iron overload: a free radical--mediated process? Hepatology *11*, 127-137.

7. Bailey,S., Evans,R.W., Garratt,R.C., Gorinsky,B., Hasnain,S., Horsburgh,C., Jhoti,H., Lindley,P.F., Mydin,A., Sarra,R., and . (1988). Molecular structure of serum transferrin at 3.3-A resolution. Biochemistry *27*, 5804-5812.

8. Baker,E.N. and Lindley,P.F. (1992). New perspectives on the structure and function of transferrins. J. Inorg. Biochem. *47*, 147-160.

9. Bredt,D.S., Hwang,P.M., and Snyder,S.H. (1990). Localization of nitric oxide synthase indicating a neural role for nitric oxide. Nature *347*, 768-770.

10. Bredt,D.S. and Snyder,S.H. (1989). Nitric oxide mediates glutamate-linked enhancement of cGMP levels in the cerebellum. Proc. Natl. Acad. Sci. U. S. A *86*, 9030-9033.

11. Bredt,D.S. and Snyder,S.H. (1990). Isolation of nitric oxide synthetase, a calmodulin-requiring enzyme. Proc. Natl. Acad. Sci. U. S. A *87*, 682-685.

12. Bredt,D.S. and Snyder,S.H. (1994). Nitric oxide: a physiologic messenger molecule. Annu. Rev. Biochem. *63*, 175-195.

13. Bridges,K.R. (1987). Ascorbic acid inhibits lysosomal autophagy of ferritin. J. Biol. Chem. *262*, 14773-14778.

14. Burdo,J.R. and Connor,J.R. (2003). Brain iron uptake and homeostatic mechanisms: an overview. Biometals *16*, 63-75.

15. Cellier,M., Prive,G., Belouchi,A., Kwan,T., Rodrigues,V., Chia,W., and Gros,P. (1995). Nramp defines a family of membrane proteins. Proc. Natl. Acad. Sci. U. S. A *92*, 10089-10093.

16. Cheng,H.Y., Obrietan,K., Cain,S.W., Lee,B.Y., Agostino,P.V., Joza,N.A., Harrington,M.E., Ralph,M.R., and Penninger,J.M. (2004a). Dexras1 potentiates photic and suppresses nonphotic responses of the circadian clock. Neuron *43*, 715-728.

17. Cheng,Y., Zak,O., Aisen,P., Harrison,S.C., and Walz,T. (2004b). Structure of the human transferrin receptor-transferrin complex. Cell *116*, 565-576.

18. Choi,D.W. (1994). Glutamate receptors and the induction of excitotoxic neuronal death. Prog. Brain Res. *100*, 47-51.

19. Cismowski,M.J., Ma,C., Ribas,C., Xie,X., Spruyt,M., Lizano,J.S., Lanier,S.M., and Duzic,E. (2000). Activation of heterotrimeric G-protein signaling by a ras-related protein. Implications for signal integration. J. Biol. Chem. *275*, 23421-23424.

20. Cismowski,M.J., Takesono,A., Bernard,M.L., Duzic,E., and Lanier,S.M. (2001). Receptor-independent activators of heterotrimeric G-proteins. Life Sci. *68*, 2301-2308.

21. Collawn,J.F., Lai,A., Domingo,D., Fitch,M., Hatton,S., and Trowbridge,I.S. (1993). YTRF is the conserved internalization signal of the transferrin receptor, and a second YTRF signal at position 31-34 enhances endocytosis. J. Biol. Chem. *268*, 21686-21692.

22. Conrad,M.E. and Umbreit,J.N. (1993). A concise review: iron absorption--the mucin-mobilferrin-integrin pathway. A competitive pathway for metal absorption. Am. J. Hematol. *42*, 67-73.

23. Dautry-Varsat,A., Ciechanover,A., and Lodish,H.F. (1983). pH and the recycling of transferrin during receptor-mediated endocytosis. Proc. Natl. Acad. Sci. U. S. A *80*, 2258-2262.

24. Dawson,V.L., Dawson,T.M., London,E.D., Bredt,D.S., and Snyder,S.H. (1991). Nitric oxide mediates glutamate neurotoxicity in primary cortical cultures. Proc. Natl. Acad. Sci. U. S. A *88*, 6368-6371.

25. Donovan,A. and Andrews,N.C. (2004). The molecular regulation of iron metabolism. Hematol. J. *5*, 373-380.

26. Donovan,A., Brownlie,A., Zhou,Y., Shepard,J., Pratt,S.J., Moynihan,J., Paw,B.H., Drejer,A., Barut,B., Zapata,A., Law,T.C., Brugnara,C., Lux,S.E., Pinkus,G.S., Pinkus,J.L., Kingsley,P.D., Palis,J., Fleming,M.D., Andrews,N.C., and Zon,L.I. (2000). Positional cloning of zebrafish ferroportin1 identifies a conserved vertebrate iron exporter. Nature *403*, 776-781.

27. Drysdale,J.W. (1988). Human ferritin gene expression. Prog. Nucleic Acid Res. Mol. Biol. *35*, 127-172.

28. Eisenstein,R.S. (2000). Iron regulatory proteins and the molecular control of mammalian iron metabolism. Annu. Rev. Nutr. *20*, 627-662.

29. Falk,J.D., Vargiu,P., Foye,P.E., Usui,H., Perez,J., Danielson,P.E., Lerner,D.L., Bernal,J., and Sutcliffe,J.G. (1999). Rhes: A striatal-specific Ras homolog related to Dexras1. J. Neurosci. Res. *57*, 782-788.

30. Fang,M., Jaffrey,S.R., Sawa,A., Ye,K., Luo,X., and Snyder,S.H. (2000). Dexras1: a G protein specifically coupled to neuronal nitric oxide synthase via CAPON. Neuron *28*, 183-193.

31. Farcich,E.A. and Morgan,E.H. (1992). Uptake of transferrin-bound and nontransferrin-bound iron by reticulocytes from the Belgrade laboratory rat:

comparison with Wistar rat transferrin and reticulocytes. Am. J. Hematol. *39*, 9-14.

32. Finch,C.A., Huebers,H., Eng,M., and Miller,L. (1982). Effect of transfused reticulocytes on iron exchange. Blood *59*, 364-369.

33. Fleming,M.D., Romano,M.A., Su,M.A., Garrick,L.M., Garrick,M.D., and Andrews,N.C. (1998). Nramp2 is mutated in the anemic Belgrade (b) rat: evidence of a role for Nramp2 in endosomal iron transport. Proc. Natl. Acad. Sci. U. S. A *95*, 1148-1153.

34. Fleming,M.D., Trenor,C.C., III, Su,M.A., Foernzler,D., Beier,D.R., Dietrich,W.F., and Andrews,N.C. (1997). Microcytic anaemia mice have a mutation in Nramp2, a candidate iron transporter gene. Nat. Genet. *16*, 383-386.

35. Furchgott,R.F. and Zawadzki,J.V. (1980). The obligatory role of endothelial cells in the relaxation of arterial smooth muscle by acetylcholine. Nature *288*, 373-376.

36. Garrick,L.M., Dolan,K.G., Romano,M.A., and Garrick,M.D. (1999). Non-transferrin-bound iron uptake in Belgrade and normal rat erythroid cells. J. Cell Physiol *178*, 349-358.

37. Girones,N., Alverez,E., Seth,A., Lin,I.M., Latour,D.A., and Davis,R.J. (1991). Mutational analysis of the cytoplasmic tail of the human transferrin receptor. Identification of a sub-domain that is required for rapid endocytosis. J. Biol. Chem. *266*, 19006-19012.

38. Graham,T.E., Key,T.A., Kilpatrick,K., and Dorin,R.I. (2001). Dexras1/AGS-1, a steroid hormone-induced guanosine triphosphate-binding protein, inhibits 3',5'-cyclic adenosine monophosphate-stimulated secretion in AtT-20 corticotroph cells. Endocrinology *142*, 2631-2640.

39. Graham,T.E., Prossnitz,E.R., and Dorin,R.I. (2002). Dexras1/AGS-1 inhibits signal transduction from the Gi-coupled formyl peptide receptor to Erk-1/2 MAP kinases. J. Biol. Chem. *277*, 10876-10882.

40. Graham,T.E., Qiao,Z., and Dorin,R.I. (2004). Dexras1 inhibits adenylyl cyclase. Biochem. Biophys. Res. Commun. *316*, 307-312.

41. Gray,N.K. and Hentze,M.W. (1994). Iron regulatory protein prevents binding of the 43S translation pre-initiation complex to ferritin and eALAS mRNAs. EMBO J. *13*, 3882-3891.

42. Gunshin,H., Allerson,C.R., Polycarpou-Schwarz,M., Rofts,A., Rogers,J.T., Kishi,F., Hentze,M.W., Rouault,T.A., Andrews,N.C., and Hediger,M.A. (2001). Iron-dependent regulation of the divalent metal ion transporter. FEBS Lett. *509*, 309-316.

43. Gunshin,H., Mackenzie,B., Berger,U.V., Gunshin,Y., Romero,M.F., Boron,W.F., Nussberger,S., Gollan,J.L., and Hediger,M.A. (1997). Cloning and characterization of a mammalian proton-coupled metal-ion transporter. Nature *388*, 482-488.

44. Gutteridge,J.M., Rowley,D.A., and Halliwell,B. (1981). Superoxide-dependent formation of hydroxyl radicals in the presence of iron salts. Detection of 'free' iron in biological systems by using bleomycin-dependent degradation of DNA. Biochem. J. *199*, 263-265.

45. Haile,D.J., Rouault,T.A., Tang,C.K., Chin,J., Harford,J.B., and Klausner,R.D. (1992). Reciprocal control of RNA-binding and aconitase activity in the regulation of the iron-responsive element binding protein: role of the iron-sulfur cluster. Proc. Natl. Acad. Sci. U. S. A *89*, 7536-7540.

46. Harford,J.B., Rouault,T.A., and Klausner,R.D. (1994). The Molecular Basis of Blood Diseases. (Philadelphia: WB Saunders Co.).

47. Harris,Z.L., Durley,A.P., Man,T.K., and Gitlin,J.D. (1999). Targeted gene disruption reveals an essential role for ceruloplasmin in cellular iron efflux. Proc. Natl. Acad. Sci. U. S. A *96*, 10812-10817.

48. Harrison,P.M. (1977). Ferritin: an iron-storage molecule. Semin. Hematol. *14*, 55-70.

49. Hayes,G.R., Enns,C.A., and Lucas,J.J. (1992). Identification of the O-linked glycosylation site of

the human transferrin receptor. Glycobiology *2*, 355-359.

50. Hentze,M.W. and Kuhn,L.C. (1996). Molecular control of vertebrate iron metabolism: mRNA-based regulatory circuits operated by iron, nitric oxide, and oxidative stress. Proc. Natl. Acad. Sci. U. S. A *93*, 8175-8182.

51. Hentze,M.W., Muckenthaler,M.U., and Andrews,N.C. (2004). Balancing acts: molecular control of mammalian iron metabolism. Cell *117*, 285-297.

52. Hess,D.T., Matsumoto,A., Kim,S.O., Marshall,H.E., and Stamler,J.S. (2005). Protein S-nitrosylation: purview and parameters. Nat. Rev. Mol. Cell Biol. *6*, 150-166.

53. Hibbs,J.B., Jr., Taintor,R.R., and Vavrin,Z. (1987). Macrophage cytotoxicity: role for L-arginine deiminase and imino nitrogen oxidation to nitrite. Science *235*, 473-476.

54. Hubert,N. and Hentze,M.W. (2002). Previously uncharacterized isoforms of divalent metal transporter (DMT)-1: implications for regulation and cellular function. Proc. Natl. Acad. Sci. U. S. A *99*, 12345-12350.

55. Huebers,H.A., Huebers,E., Csiba,E., and Finch,C.A. (1984). Heterogeneity of the plasma iron pool: explanation of the Fletcher-Huehns phenomenon. Am. J. Physiol *247*, R280-R283.

56. Iacopetta,B.J. and Morgan,E.H. (1983). The kinetics of transferrin endocytosis and iron uptake from transferrin in rabbit reticulocytes. J. Biol. Chem. *258*, 9108-9115.

57. Ignarro,L.J., Buga,G.M., Wood,K.S., Byrns,R.E., and Chaudhuri,G. (1987). Endothelium-derived relaxing factor produced and released from artery and vein is nitric oxide. Proc. Natl. Acad. Sci. U. S. A *84*, 9265-9269.

58. Jaffrey,S.R., Fang,M., and Snyder,S.H. (2002). Nitrosopeptide mapping: a novel methodology reveals s-nitrosylation of dexras1 on a single cysteine residue. Chem. Biol. *9*, 1329-1335.

59. Jaffrey,S.R., Snowman,A.M., Eliasson,M.J., Cohen,N.A., and Snyder,S.H. (1998). CAPON: a protein associated with neuronal nitric oxide synthase that regulates its interactions with PSD95. Neuron *20*, 115-124.

60. Jaffrey,S.R. and Snyder,S.H. (2001). The biotin switch method for the detection of S-nitrosylated proteins. Sci. STKE. *2001*, L1.

61. JANDL,J.H. and KATZ,J.H. (1963). The plasma-to-cell cycle of transferrin. J. Clin. Invest *42*, 314-326.

62. Kang,D.K., Jeong,J., Drake,S.K., Wehr,N.B., Rouault,T.A., and Levine,R.L. (2003). Iron regulatory protein 2 as iron sensor. Iron-dependent oxidative modification of cysteine. J. Biol. Chem. *278*, 14857-14864.

63. Kaptain,S., Downey,W.E., Tang,C., Philpott,C., Haile,D., Orloff,D.G., Harford,J.B., Rouault,T.A., and Klausner,R.D. (1991). A regulated RNA binding protein also possesses aconitase activity. Proc. Natl. Acad. Sci. U. S. A *88*, 10109-10113.

64. Karin,M. and Mintz,B. (1981). Receptor-mediated endocytosis of transferrin in developmentally totipotent mouse teratocarcinoma stem cells. J. Biol. Chem. *256*, 3245-3252.

65. Kemppainen,R.J. and Behrend,E.N. (1998). Dexamethasone rapidly induces a novel ras superfamily member-related gene in AtT-20 cells. J. Biol. Chem. *273*, 3129-3131.

66. Kim,S. and Ponka,P. (2002). Nitrogen monoxide-mediated control of ferritin synthesis: implications for macrophage iron homeostasis. Proc. Natl. Acad. Sci. U. S. A *99*, 12214-12219.

67. Klausner,R.D., Van,R.J., Ashwell,G., Kempf,C., Schechter,A.N., Dean,A., and Bridges,K.R. (1983). Receptor-mediated endocytosis of transferrin in K562 cells. J. Biol. Chem. *258*, 4715-4724.

68. Koh,J.Y. and Choi,D.W. (1988). Vulnerability of cultured cortical neurons to damage by excitotoxins: differential susceptibility of neurons containing NADPH-diaphorase. J. Neurosci. *8*, 2153-2163.

69. Krishnamurthy,P., Ross,D.D., Nakanishi,T., Bailey-Dell,K., Zhou,S., Mercer,K.E., Sarkadi,B., Sorrentino,B.P., and Schuetz,J.D. (2004). The stem cell marker Bcrp/ABCG2 enhances hypoxic cell survival through interactions with heme. J. Biol. Chem. *279*, 24218-24225.

70. LaVaute,T., Smith,S., Cooperman,S., Iwai,K., Land,W., Meyron-Holtz,E., Drake,S.K., Miller,G., bu-Asab,M., Tsokos,M., Switzer,R., III, Grinberg,A., Love,P., Tresser,N., and Rouault,T.A. (2001). Targeted deletion of the gene encoding iron regulatory protein-2 causes misregulation of iron metabolism and neurodegenerative disease in mice. Nat. Genet. *27*, 209-214.

71. Lawson,D.M., Artymiuk,P.J., Yewdall,S.J., Smith,J.M., Livingstone,J.C., Treffry,A., Luzzago,A., Levi,S., Arosio,P., Cesareni,G., and . (1991). Solving the structure of human H ferritin by genetically engineering intermolecular crystal contacts. Nature *349*, 541-544.

72. Levi,S., Luzzago,A., Cesareni,G., Cozzi,A., Franceschinelli,F., Albertini,A., and Arosio,P. (1988). Mechanism of ferritin iron uptake: activity of the H-chain and deletion mapping of the ferro-oxidase site. A study of iron uptake and ferro-oxidase activity of human liver, recombinant H-chain ferritins, and of two H-chain deletion mutants. J. Biol. Chem. *263*, 18086-18092.

73. Li,H., Degenhardt,B., Tobin,D., Yao,Z.X., Tasken,K., and Papadopoulos,V. (2001). Identification, localization, and function in steroidogenesis of PAP7: a peripheral-type benzodiazepine receptor- and PKA (RIalpha)-associated protein. Mol. Endocrinol. *15*, 2211-2228.

74. McCance,R.A. and Widdowson,E.M. (1938). The absorption and excretion of iron following oral and intravenous administration. J. Physiol *94*, 148.

75. McClarty,G.A., Chan,A.K., Choy,B.K., and Wright,J.A. (1990). Increased ferritin gene expression is associated with increased ribonucleotide reductase gene expression and the establishment of hydroxyurea resistance in mammalian cells. J. Biol. Chem. *265*, 7539-7547.

76. McGraw,T.E. and Maxfield,F.R. (1990). Human transferrin receptor internalization is partially dependent upon an aromatic amino acid on the cytoplasmic domain. Cell Regul. *1*, 369-377.

77. McKie,A.T., Marciani,P., Rolfs,A., Brennan,K., Wehr,K., Barrow,D., Miret,S., Bomford,A., Peters,T.J., Farzaneh,F., Hediger,M.A., Hentze,M.W., and Simpson,R.J. (2000). A novel duodenal iron-regulated transporter, IREG1, implicated in the basolateral transfer of iron to the circulation. Mol. Cell *5*, 299-309.

78. Moos,T. and Morgan,E.H. (1998). Evidence for low molecular weight, non-transferrin-bound iron in rat brain and cerebrospinal fluid. J. Neurosci. Res. *54*, 486-494.

79. Muir,A. and Hopfer,U. (1985). Regional specificity of iron uptake by small intestinal brush-border membranes from normal and iron-deficient mice. Am. J. Physiol *248*, G376-G379.

80. Nicolas,G., Chauvet,C., Viatte,L., Danan,J.L., Bigard,X., Devaux,I., Beaumont,C., Kahn,A., and Vaulont,S. (2002). The gene encoding the iron regulatory peptide hepcidin is regulated by anemia, hypoxia, and inflammation. J. Clin. Invest *110*, 1037-1044.

81. Nowak,L., Bregestovski,P., Ascher,P., Herbet,A., and Prochiantz,A. (1984). Magnesium gates glutamate-activated channels in mouse central neurones. Nature *307*, 462-465.

82. Palmer,R.M., Ferrige,A.G., and Moncada,S. (1987). Nitric oxide release accounts for the biological activity of endothelium-derived relaxing factor. Nature *327*, 524-526.

83. Paterson,S., Armstrong,N.J., Iacopetta,B.J., McArdle,H.J., and Morgan,E.H. (1984). Intravesicular pH and iron uptake by immature erythroid cells. J. Cell Physiol *120*, 225-232.

84. Pattanapanyasat,K., Hoy,T.G., and Jacobs,A. (1987). The response of intracellular and surface ferritin

after T-cell stimulation in vitro. Clin. Sci. (Lond) *73*, 605-611.

85. Picard,V., Govoni,G., Jabado,N., and Gros,P. (2000). Nramp 2 (DCT1/DMT1) expressed at the plasma membrane transports iron and other divalent cations into a calcein-accessible cytoplasmic pool. J. Biol. Chem. *275*, 35738-35745.

86. Ponka,P. (2004). Hereditary causes of disturbed iron homeostasis in the central nervous system. Ann. N. Y. Acad. Sci. *1012*, 267-281.

87. Quigley,J.G., Yang,Z., Worthington,M.T., Phillips,J.D., Sabo,K.M., Sabath,D.E., Berg,C.L., Sassa,S., Wood,B.L., and Abkowitz,J.L. (2004). Identification of a human heme exporter that is essential for erythropoiesis. Cell *118*, 757-766.

88. Raffin,S.B., Woo,C.H., Roost,K.T., Price,D.C., and Schmid,R. (1974). Intestinal absorption of hemoglobin iron-heme cleavage by mucosal heme oxygenase. J. Clin. Invest *54*, 1344-1352.

89. Richardson,D.R. and Ponka,P. (1997). The molecular mechanisms of the metabolism and transport of iron in normal and neoplastic cells. Biochim. Biophys. Acta *1331*, 1-40.

90. Riedel,H.D., Remus,A.J., Fitscher,B.A., and Stremmel,W. (1995). Characterization and partial purification of a ferrireductase from human duodenal microvillus membranes. Biochem. J. *309 ( Pt 3)*, 745-748.

91. Rothenberger,S., Iacopetta,B.J., and Kuhn,L.C. (1987). Endocytosis of the transferrin receptor requires the cytoplasmic domain but not its phosphorylation site. Cell *49*, 423-431.

92. Rouault,T.A. (2001). Systemic iron metabolism: a review and implications for brain iron metabolism. Pediatr. Neurol. *25*, 130-137.

93. Sawyer,S.T. and Krantz,S.B. (1986). Transferrin receptor number, synthesis, and endocytosis during erythropoietin-induced maturation of Friend virus-

infected erythroid cells. J. Biol. Chem. *261*, 9187-9195.

94. Schwartz,S., Dahl,J., Ellefson,M., and Ahlquist,D. (1983). The "HemoQuant" test: a specific and quantitative determination of heme (hemoglobin) in feces and other materials. Clin. Chem. *29*, 2061-2067.

95. Setsukinai,K., Urano,Y., Kakinuma,K., Majima,H.J., and Nagano,T. (2003). Development of novel fluorescence probes that can reliably detect reactive oxygen species and distinguish specific species. J. Biol. Chem. *278*, 3170-3175.

96. Shayeghi,M., Latunde-Dada,G.O., Oakhill,J.S., Laftah,A.H., Takeuchi,K., Halliday,N., Khan,Y., Warley,A., McCann,F.E., Hider,R.C., Frazer,D.M., Anderson,G.J., Vulpe,C.D., Simpson,R.J., and McKie,A.T. (2005). Identification of an intestinal heme transporter. Cell *122*, 789-801.

97. Shoham,S. and Youdim,M.B. (2000). Iron involvement in neural damage and microgliosis in models of neurodegenerative diseases. Cell Mol. Biol. (Noisy. -le-grand) *46*, 743-760.

98. Shongwe,M.S., Smith,C.A., Ainscough,E.W., Baker,H.M., Brodie,A.M., and Baker,E.N. (1992). Anion binding by human lactoferrin: results from crystallographic and physicochemical studies. Biochemistry *31*, 4451-4458.

99. Sohda,M., Misumi,Y., Yamamoto,A., Yano,A., Nakamura,N., and Ikehara,Y. (2001). Identification and characterization of a novel Golgi protein, GCP60, that interacts with the integral membrane protein giantin. J. Biol. Chem. *276*, 45298-45306.

100. Sorond,F.A. and Ratan,R.R. (2000). Ironing-out mechanisms of neuronal injury under hypoxic-ischemic conditions and potential role of iron chelators as neuroprotective agents. Antioxid. Redox. Signal. *2*, 421-436.

101. Spano,D., Branchi,I., Rosica,A., Pirro,M.T., Riccio,A., Mithbaokar,P., Affuso,A., Arra,C., Campolongo,P., Terracciano,D., Macchia,V., Bernal,J., Alleva,E., and Di,L.R. (2004). Rhes is involved in striatal function. Mol. Cell Biol. *24*, 5788-5796.

102. Stein,B.S. and Sussman,H.H. (1986). Demonstration of two distinct transferrin receptor recycling pathways and transferrin-independent receptor internalization in K562 cells. J. Biol. Chem. *261*, 10319-10331.

103. Stuehr,D.J. and Nathan,C.F. (1989). Nitric oxide. A macrophage product responsible for cytostasis and respiratory inhibition in tumor target cells. J. Exp. Med. *169*, 1543-1555.

104. Takahashi,H., Umeda,N., Tsutsumi,Y., Fukumura,R., Ohkaze,H., Sujino,M., van der,H.G., Yasui,A., Inouye,S.T., Fujimori,A., Ohhata,T., Araki,R., and Abe,M. (2003). Mouse dexamethasone-induced RAS protein 1 gene is expressed in a circadian rhythmic manner in the suprachiasmatic nucleus. Brain Res. Mol. Brain Res. *110*, 1-6.

105. Theil,E.C. (1987). Ferritin: structure, gene regulation, and cellular function in animals, plants, and microorganisms. Annu. Rev. Biochem. *56*, 289-315.

106. Thomas,M. and Jankovic,J. (2004). Neurodegenerative disease and iron storage in the brain. Curr. Opin. Neurol. *17*, 437-442.

107. Torti,F.M. and Torti,S.V. (2002). Regulation of ferritin genes and protein. Blood *99*, 3505-3516.

108. Van,R.J., Bridges,K.R., Harford,J.B., and Klausner,R.D. (1982). Receptor-mediated endocytosis of transferrin and the uptake of fe in K562 cells: identification of a nonlysosomal acidic compartment. Proc. Natl. Acad. Sci. U. S. A *79*, 6186-6190.

109. Vargiu,P., De,A.R., Garcia-Ranea,J.A., Valencia,A., Santisteban,P., Crespo,P., and Bernal,J. (2004). The small GTP-binding protein, Rhes, regulates signal transduction from G protein-coupled receptors. Oncogene *23*, 559-568.

110. Vargiu,P., Morte,B., Manzano,J., Perez,J., De,A.R., Gregor,S.J., and Bernal,J. (2001). Thyroid hormone regulation of rhes, a novel Ras homolog gene expressed in the striatum. Brain Res. Mol. Brain Res. *94*, 1-8.

111. Vulpe,C.D., Kuo,Y.M., Murphy,T.L., Cowley,L., Askwith,C., Libina,N., Gitschier,J., and Anderson,G.J.

(1999). Hephaestin, a ceruloplasmin homologue implicated in intestinal iron transport, is defective in the sla mouse. Nat. Genet. *21*, 195-199.

112. Weinstein,D.A., Roy,C.N., Fleming,M.D., Loda,M.F., Wolfsdorf,J.I., and Andrews,N.C. (2002). Inappropriate expression of hepcidin is associated with iron refractory anemia: implications for the anemia of chronic disease. Blood *100*, 3776-3781.

113. Williams,A.M. and Enns,C.A. (1991). A mutated transferrin receptor lacking asparagine-linked glycosylation sites shows reduced functionality and an association with binding immunoglobulin protein. J. Biol. Chem. *266*, 17648-17654.

114. Williams,A.M. and Enns,C.A. (1993). A region of the C-terminal portion of the human transferrin receptor contains an asparagine-linked glycosylation site critical for receptor structure and function. J. Biol. Chem. *268*, 12780-12786.

115. Xu,H., Jin,J., DeFelice,L.J., Andrews,N.C., and Clapham,D.E. (2004). A spontaneous, recurrent mutation in divalent metal transporter-1 exposes a calcium entry pathway. PLoS. Biol. *2*, E50.

116. Yamanaka,K., Ishikawa,H., Megumi,Y., Tokunaga,F., Kanie,M., Rouault,T.A., Morishima,I., Minato,N., Ishimori,K., and Iwai,K. (2003). Identification of the ubiquitin-protein ligase that recognizes oxidized IRP2. Nat. Cell Biol. *5*, 336-340.

117. Yamashiro,D.J., Tycko,B., Fluss,S.R., and Maxfield,F.R. (1984). Segregation of transferrin to a mildly acidic (pH 6.5) para-Golgi compartment in the recycling pathway. Cell *37*, 789-800.

118. Zak,O., Trinder,D., and Aisen,P. (1994). Primary receptor-recognition site of human transferrin is in the C-terminal lobe. J. Biol. Chem. *269*, 7110-7114.

119. Zecca,L., Youdim,M.B., Riederer,P., Connor,J.R., and Crichton,R.R. (2004). Iron, brain ageing and neurodegenerative disorders. Nat. Rev. Neurosci. *5*, 863-873.

120. Zerial,M., Melancon,P., Schneider,C., and Garoff,H. (1986). The transmembrane segment of the human transferrin receptor functions as a signal peptide. EMBO J. *5*, 1543-1550.

# JAIME H. CHEAH

## EDUCATION

1999 – present Johns Hopkins School of Medicine Baltimore, MD
Ph.D. Candidate in Biochemistry, Cellular and Molecular Biology, Concentration in Neuroscience

1995 – 1999 McGill University Montreal, Quebec
B.Sc. in Biochemistry

## RESEARCH EXPERIENCE

Sept 1999 – present Johns Hopkins School of Medicine
Supervisor: Dr. Solomon H. Snyder
"Behind the Iron Curtain: Dexras1 mediates Glutamate-NMDA induced neuronal iron uptake"

Jan 1998 – July 1999 McGill University
Supervisor: Dr. Alice Vrielink
"Crystallization and structural determination of L-Amino Acid Oxidase by X-ray crystallography"

Jan 1997 – August 1997 McGill University
Supervisor: Dr. Alice Vrielink
"Crystallization of Cut repeat-3 and homeodomain protein"

May 1996 – August 1996 Harvard Medical School
Supervisor: Dr. Tom Ellenberger
"Site-directed mutagenesis of AlkA and crystallization of EndoV"

## AWARDS

May 26, 2005 *Biochemical Journal* Young Investigators Award
First Congress of the International BioIron Society, Prague, Czech Republic, May 22-27, 2005

June, 2002 Outstanding Preceptor Award
Johns Hopkins University – Paul Lawrence Dunbar High School Partnership

237 W. LANVALE STREET, BALTIMORE, MD 21217
PHONE: 410-669-2968 ■ EMAIL: JCHEAH@JHMI.EDU

## PUBLICATIONS

1. **Cheah JH**, Kim SF, Hester LD, Clancy KW, Patterson SE, Papadopoulos V and Snyder SH: Glutamate-NMDA receptor-nitric oxide transmission mediates neuronal iron homeostasis via the GTPase Dexras1. Neuron. 2005 (in revision)

2. Hara MR, Agrawal N, Kim SF, Cascio MB, Fujimuro M, Ozeki Y, Takahashi M, **Cheah JH**, Tankou SK, Hester LD, Ferris CD, Hayward SD, Snyder SH and Sawa A: S-nitrosylated GAPDH initiates apoptotic cell death by nuclear translocation following Siah1 binding. Nat Cell Biol. 2005, Jul;7(7):665-74.

3. Huang Y, Man HY, Sekine-Aizawa Y, Han Y, Juluri K, Luo H, **Cheah J**, Lowenstein C, Huganir RL and Snyder SH: S-nitrosylation of N-ethylmaleimide sensitive factor mediates surface expression of AMPA receptors. Neuron. 2005 May 19;46(4):533-40

4. Pawelek PD, **Cheah J**, Coulombe R, Macheroux P, Ghisla S and Vrielink A: The structure of L-amino acid oxidase reveals the substrate trajectory into an enantiomerically conserved active site. EMBO J. 2000 Aug 15;19(16):4204-15.

## ABSTRACTS FOR ORAL PRESENTATIONS

1. Kim SF, **Cheah JH**, Hester LD, Clancy KW, Patterson SE, Papadopoulos V and Snyder SH: A novel mode of regulating brain iron homeostatis.
*First Congress of the International BioIron Society*. *Prague, Czech Republic* May 22-27, 2005

2. **Cheah J**, Luo X, Hanle LJ, Ha HC, Wellington CL, Igarashi S, Hester LD, Hayden MR, Ross CA, Snyder SH and Sawa A: Influence of Huntington toxicity by GAPDH
*Society for Neuroscience, New Orleans, LA* November 4-9, 2000

## ABSTRACTS FOR POSTER PRESENTATIONS

1. **Cheah JH**, Kim SF, Hester LD, Clancy KW, Patterson SE, Papadopoulos V and Snyder SH: Dexras1 regulates transferrin-mediated iron trafficking in the brain. *First Congress of the International BioIron Society*. *Prague, Czech Republic* May 22 - 27, 2005

2. **Cheah JH**, Kim SF, Hester LD, Clancy KW, Patterson SE, Papadopoulos V and Snyder SH: Dexras1 mediates iron trafficking. *Society for Neuroscience, San Diego, CA* October 23 - 27, 2004

3. **Cheah JH**, Rao M, Penzes P and Snyder SH: Kalirins as modulators of Dexras1 activity. *Society for Neuroscience, New Orleans, LA* November 8 – 12, 2003

4. Kim S, **Cheah J** and Snyder SH: Heme Oxygenase and Nitric Oxide Synthase interaction under stress conditions. *Society for Neuroscience, New Orleans, LA* November 8 – 12, 2003

## ABSTRACTS FOR POSTER PRESENTATIONS (CONTINUED)

5. Huang Y, Man H, Aizawa T, Luo H, **Cheah J**, Lowenstein C, Huganir R and Snyder SH: NMDA-induced relocalization of AMPA receptors into membrane raft domains is mediated by S-nitrysolation of NSF. *Society for Neuroscience, New Orleans, LA* November 8 – 12, 2003

6. Watkins CC, Kaplin AI, Rao M, **Cheah JH**, Boehning D, Benham CA, Ferris CD and Snyder SH: Differential roles of neuronal Nitric Oxide Synthase and Heme Oxygenase-2 in the proximal and distal gastrointestinal pathway correspond to distinct properties of CO and NO. *Society for Neuroscience, Orlando, FL* November 2 - 7, 20027.

Dinkova-Kostova AT, **Cheah J** and Talalay P: Amplification of cellular mechanisms for protection against electrophiles and oxidants by Michael reaction acceptors. *Proceedings of the American Association for Cancer Research* 43:478, 2002

8. **Cheah JH**, Hester LD, Blackshaw S, Sawa A and Snyder SH: Dexras1 and hippocampal atrophy. *Society for Neuroscience, San Diego, CA* November 10 - 15, 2001

## RELATED EXPERIENCES

| | |
|---|---|
| 2002 - present | The Restriction Digest<br>The Graduate Student Association Newsletter<br>2004-2005: Senior Editor<br>2002-present: Editor |
| 2000 | Biochemistry, Cellular and Molecular Biology Lecture Invited Speaker: 1995 Nobel Laureate, Dr. Eric Wieschaus, Princeton |
| 2000 | Biochemistry, Cellular and Molecular Biology Big Sib/Little Sib Program |

## REFERENCES


1. Dr. Solomon H. Snyder, Professor and Director
   Department of Neuroscience, Johns Hopkins School of Medicine
   725 N. Wolfe Street, WBS 813, Baltimore, MD 21205
   Phone: 410-955-3024
   Fax: 410-955-3623
   Email: ssnyder@jhmi.edu

2. Dr. Michael J. Caterina, Associate Professor
   Department of Biological Chemistry
   Johns Hopkins School of Medicine
   725 North Wolfe Street , Baltimore, MD 21205
   Phone: 410-502-5457
   Fax: 410-955-5759
   Email: caterina@jhmi.edu

3. Dr. Alice Vrielink, Associate Professor
   Departments of Biology and Chemistry,
   University of California-Santa Cruz
   Sinsheimer Labs, 1156 High Street, Santa Cruz, CA 95064
   Phone: 813-459-5126
   Fax: 813-459-3139
   Email: vrielink@biology.ucsc.edu

4. Dr. Tom Ellenberger, Wittcoff Professor and Head
   Biochemistry and Molecular Biophysics
   Washington University School of Medicine
   660 S. Euclid, Campus Box 8231, St. Louis, MO 63110
   Phone: 314-747-8893
   Fax: 314-747-1145
   Email: tome@wustl.edu